IJESG

International Journal of Energy and Smart Grid

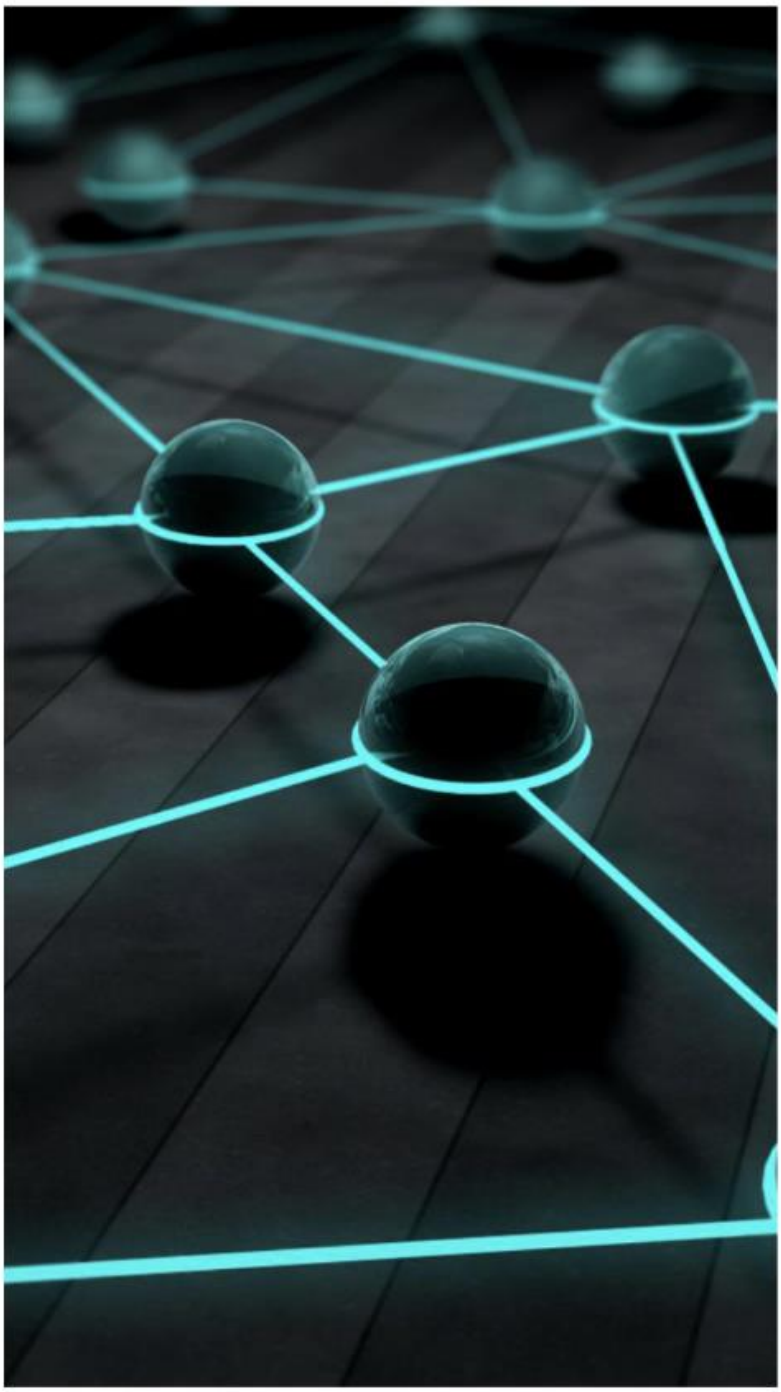

Volume 9
Issue 1
2024

e-ISSN:2636-7904

Email : ijesgrid@gmail.com
Visit our home page on www.dergipark.org.tr/ijesg

CONTENTS

Research Articles

Review Articles

IJESG
e-ISSN 2636-7904
International Journal of Energy and Smart Grid
Vol 9, Number 1, 2024
Doi: 10.55088/ijesg.1449194

Research Article

MODELLING AND EXERGETIC TECHNO-ECONOMIC ANALYSIS OF A SYSTEM FOR HYDROGEN PRODUCTION FROM EMPTY BANANA FRUIT BUNCH

Akpaduado Friday JOHN*[1], Joseph Oyekale OYETOLA[2]

[1]Department of Mechanical Engineering, Federal University of Petroleum Resources Effurun, PMB 1221 Effurun, Nigeria. Orcid[1]: https://orcid.org/ 0000-0002-8220-7093
[2]Department of Mechanical Engineering, Federal University of Petroleum Resources Effurun, PMB 1221 Effurun, Nigeria. https://orcid.org/ 0000-0003-4018-4660
* Corresponding author; afj223@lehigh.edu

Abstract: *One of the most effective and reliable methods for generating hydrogen fuel using biomass is the gasification method. However, using different biomass feedstock can withstand syngas production, which can be utilized for several applications. The study investigated the feasibility of hydrogen from Empty Banana Fruit Bunch (EBFB) biomass and the energetic techno-economic analyses of biomass gasification plants with a developed system simulation model, Aspen Plus simulator V11. Five chemical reactions were used in the production process and were simulated in ASPEN Plus simulator through biomass gasification method which aimed to remove C, CO, CO_2, CH_4, and H_2O to convert them into hydrogen gas. However, the total exergy-out divided by the total exergy-in gives exergy efficiency. Hence, total energy-out subtracted from total exergy-in depicts exergy destruction. The exergoeconomic method utilized in the exergoeconomic analyses is the Specific Cost method (SPECO). The results affirmed that 80.465 kg/h of H_2 can be produced from 2000 kg/h of empty banana fruit bunch at every 39.92 k mol/h mole flow of Empty Banana Fruit Bunch (EBFB). However, at a temperature below 900 degrees Celsius (^{o} C), CO decreases, and CO_2 increases. Above 1000 degrees Celsius (^{o} C), CO increases hence, decreasing CO_2 emission. The system total exergy in, total exergy out, percentage exergy efficiency, and exergy destruction are 4534.77 kJ/kg, 3857.295 kJ/kg, 0.8506 %, and 677.475 kJ/kg. Hence, system exergy stream cost rate, component-related cost rate, component-related cost difference, and component exergoeconomic factor are 407527.644 $/h, 1555.57 $/h, 0.5679 %, and 0.9089 % respectively. Further studies may concentrate on reducing CO through regulated temperature and pressure differences to increase the quantity of hydrogen production.*

Keywords: *Biomass; sensitivity analysis; empty banana fruit bunch; combustor; gasifier; separator; exergy; exergoeconomic*

Received: March 8, 2024 *Accepted: December 16, 2024*

1. Introduction

Hydrogen fuel has been recommended as an alternative to reduce the reliance on fossil fuels. Investigations confirmed that over 92.5 billion kilograms of hydrogen are being produced annually and that 76 % of hydrogen production globally is from reforming natural gas via steam methane reformer, 22 % from coal gasification (primarily from China), and only 2 % from water electrolysis, respectively [1-2]. It has been proven beyond a reasonable doubt that hydrogen fuel is a clean energy source that does not damage the environment and liberates only water as effluent when utilized in a fuel cell system. Hydrogen can however be obtained via various renewable energy raw materials [3-5]. Renewable energy sources like solar, hydro, wind, and biomass, along with domestic resources like nuclear power and natural gas. The above attributes and much more increase the importance of this fuel as a better and more reliable fuel, especially for industrial use, transportation, power generation, grid balancing, petrochemical, and refinery processing. Its usefulness can never be overemphasized, fueling cars, running generators in houses, for portable power, etc. Due to its nature, hydrogen can be used to move, store, and deliver energy produced from other sources [6]. Ping et al. analyzed the significant impact of

hydrogen on the economy in clean energy technologies [7]. Hence, a detailed description of a dehydrogenation route that applies to different non-food-related biomass waste. Most especially wheat straw, corn straw, rice straw, reed, bagasse, bamboo sawdust, and cardboard. His observation affirmed the possibility of H_2 yields up to 95 % from a one-pot, two-step reaction with a 69 ppm molecularly iridium catalyst, imidazoline moiety in formic acid, through a 1 v % dimethyl sulfoxide of biomass. Hydrogen does not exist alone. It is extracted from other elements in the molecule in which it occurs. Investigation proved that hydrogen exists in numerous sources hence, different methods of producing hydrogen [8]. Biomass is a renewable organic resource. This technology includes agriculture crop residues e.g., corn stove or wheat straw, forest residues, special crops grown specifically for energy consumption e.g., switch grass or willow trees, organic municipal solid waste, and animal wastes. Biomass produces hydrogen along with other by-products by gasification. Literature confirms that the combination of agricultural biomass, heat, steam, and oxygen at temperatures above 700 degrees Celsius, without combustion, liberates hydrogen [10-13]. This process is known as hydrogen production through biomass gasification (Figure 1).

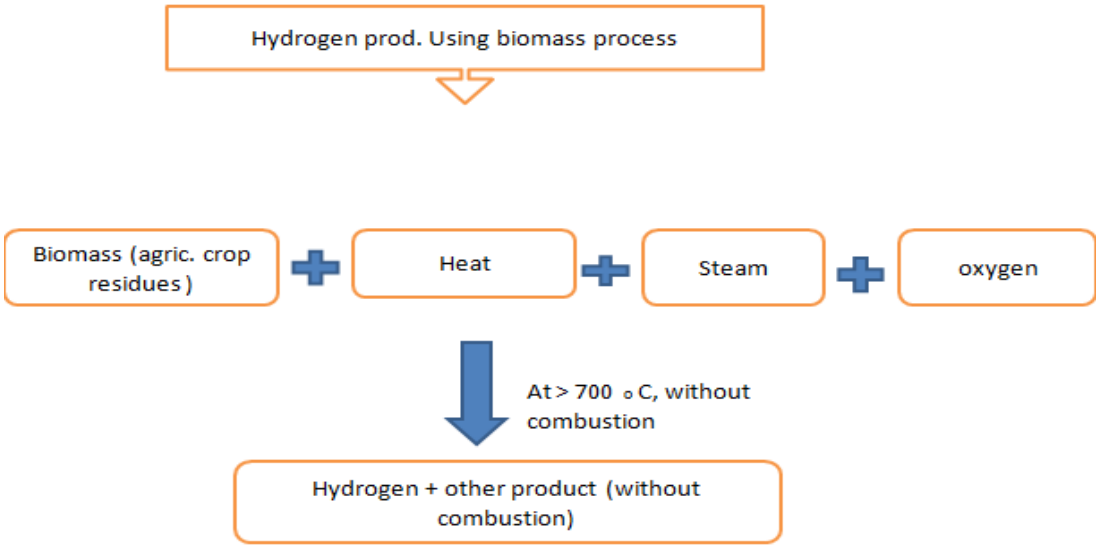

Figure 1. Hydrogen production through biomass gasification

Gasification is a key technology in hydrogen production, wherein biomass undergoes thermal decomposition in a low-oxygen environment rather than combustion. This process utilizes a controlled methodology to convert biomass into hydrogen and a variety of other gaseous by-products. By carefully managing temperature, pressure, and reactant flow, the gasification process optimizes the yield and purity of hydrogen, making it a viable option for sustainable energy solutions [14-15]. Chen et al. (2010) produced hydrogen using the biomass gasification method in supercritical water with the help of concentrated solar energy [9]. Agricultural residue like rice husks, cereal straws, coconut husks, maize cob, empty banana bunch, etc. is normally utilized for gasification through biomass. Others include charcoal, wood waste, peat, and wood. Marcantonio et al. (2019) considered biomass feedstock to generate syngas consisting of H_2, CO, and CH_4, which can also be utilized for several applications. Investigations have revealed that food waste valorization to hydrogen is a viable energy source with potential economic benefits [20-21]. The concept of exergy analysis elucidated and showcased causes for the inefficient performance of components. This concept allows accurate quality energy determination for the causes and reveals losses even when determining the residues in heat generation processes in a thermal plant. This deals with the performance of chemical processes. Exergy consists of

four elements: physical, chemical, kinetic, and potential energies. The combination of exergy analysis and economic principles, such as assisting in the verification of cost flow in a system and optimizing the system performance is termed exergoeconomic [22]. In upgraded exergoeconomic analysis, the specific capability of various industrial processes is utilized to find the exergy destruction hence, inversion cost rates to step up the sustainability of a plant. The exergoeconomic method adopted in the energy-economic analysis is the Specific Cost method (SPECO). Fuel and product of components are defined using direct capturing of a systematic value of all the stream exergy entering and subtracting from all the stream exergy leaving the component. The component-related cost difference and rate average cost per exergy unit production are calculated based on SPECO principles. Cabezas et al. (2020) affirmed that exergy efficiency gives more realistic specifications than the corresponding energy efficiency because exergy efficiency provides more understanding of performance. Results affirmed that exergy analysis methods of availability improve greater efficiency to define the second operational flow efficiency [8]. Xu et al. (2018) analyzed the exergy analysis of hydrogenation via gasification of steam through biomass as a renewable source. The steam biomass rate flow rate initially increases and finally decreases the efficiency due to exergy. Moreover, reaction catalysts may have positive, negative, or negligible efficiency issues due to exergy, whereas residence time generally has a slight efficiency issue due to the exergy [26-28]. Olusegun et al. (2023) investigated the generation of biodiesel from rubber seed oil by comparing the ethyl-based HCR and MSR. The Aspen Hysys engineering tool was utilized in the simulations to investigate the ethanolysis process for RSO in both HCRs and MSRs. The results affirmed that HCR can convert 99.01 % of RSO compared to the MSR's 94.85 % [25]. Chen et al. (2010) adopted a concentrated solar energy method with the help of superficial water in a gasification plant for hydrogen [9]. Arafat & Dincer, (2016) produced his hydrogen from oil palm biomass with the help of a water gas-shift gasification method [1]. Marcantonio et al. (2019) got their hydrogen from agricultural feedstock by adopting biomass gasification methods. Nevertheless, researchers have extensively addressed fossil fuel substitutes from both individual and institutional perspectives through their numerous works. Hence, despite their studies, the following main points are however pointed out as a base factor for Empty Banana Fruit Bunch (BEFB) consideration;

- Less attention has been given to Empty Banana Fruit Bunch (BEFB) for hydrogen production through a series of perceptions as to the levels of implementation of their research. During combustion, Empty Banana Fruit Bunch (BEFB) minimal carbon dioxide is emitted,
- Availability of Empty Banana Fruit Bunch (BEFB), less or no pollution of the immediate environment and the agricultural biomass is not in competition with human food,
- The use of renewable energy sources over fossil fuels reduces carbon emissions, promoting clean energy and protecting the ozone layer. Empty Banana Fruit Bunch (BEFB) can generate high energy efficiency due to its ability to emit low or no net CO2 during combustion [16-20].

To bridge this gap, this study aims to apply the Aspen Plus software to model and assess the feasibility of a system for hydrogen production from empty banana fruit bunch for electricity generation and to adopt a conventional exergy and exergoeconomic analyses calculator in solving thermal losses in the gasification power plant. The specific objectives are;

i. To model and simulate a hydrogen production system from an empty banana fruit bunch (EBFB) using Aspen plus simulator;
ii. To investigate the sensitivities of some system components such as gasifier, combustor, and separator to variations in thermodynamic properties such as temperature and pressure;
iii. To assess the operational technicality of the system hence, system components by utilization of a conventional exergy analysis approach;

iv. To assess the economic system performance using a classical energy-economic method.

Section two of the paper outlines the methodology used in this study. Results are presented and discussed in section three, and the main conclusions are summarized in section four.

2. Methodology

2.1. Simulation model

Assumption

The following depict assumptions were made in modeling the gasification process (Marcantonio et al., 2019), (Lim et al., 2018).

- Drying and pyrolysis did not occur instantaneously, and volatile products mainly consist of H_2, N_2, O_2, CO_2, CO, CH_4, and H_2O,
- The process is in steady-state and isothermal,
- No pressure drop and heat loss were considered during the simulation (all gases behave ideally). All considered components are in chemical equilibrium,
- Sulfur, nitrogen, and chlorine in the biomass flow into the gas phase of the process. The char/ash is a hundred percent carbon.

2.2. Process scheme

Figure 2 depicts the schematic of the gasification of biomass for the extraction of hydrogen in the study. The biomass feedstock adopted was Banana Empty Fruit Bunch (BEFB). The RSTOIC (drying) and the RYIELD stage simulate the first part of the gasification process and produce H_2, CH_4, H_2O, CO, CO_2, and ash.

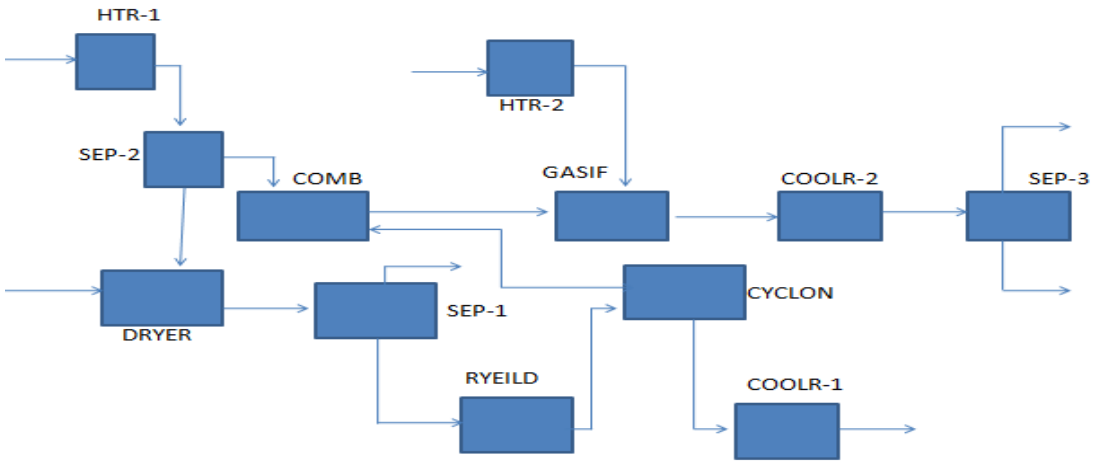

Figure 2. Schematic of biomass gasification of the hydrogen production process

Table 1. Aspen plus flow-sheet unit operations

Aspen plus name	Block ID	Function
RSTOIC	RSTOIC	Rstoic reactor (dryer) – simulates the biomass by drying the biomass before going into a separator (SEP-1).
SEP	SEP	Separator: SEP-1; separates the biomass into two streams before entering the Ryield reactor. N_2 + H_2O in a stream and dry biomass in another stream. SEP-2: separates the atmospheric air, delivers N_2 into the RSTOIC and O_2 into the COMBUSTOR. SEP-3; extracts pure hydrogen, and syngas with 75 % efficiency
HEATER	HEATER	Heater-1 increases atm air and delivers into SEP-2. Heater-2 increases atm air and delivers into the combustor.
R-YIELD	DECOMP	Yield reactor - converts the non-conventional stream dry-biomass from SEP-1 into its conventional components (C, H, O).
SSplit	CYCLONE	SSplit- removes ash from the pyrolysis before entering the COOLER-1 and delivers the conventional biomass into the COMBUSTOR.
COOLER	COOLER	Cooler-1 lowers the ash temperature; Cooler-2 lowers the gasifier product temperature.
RGIBB'S	COMBUSTOR GASIF	Combustor (Gibb's free energy reactor)-combines the conventional biomass from the SSplit with O_2 from SEP-2 at high temperature. Gibb's free energy reactor (simulates, partial oxidation, and gasification) at restricted chemical equilibrium of the specified reaction aligns the syngas composition in specifying a temperature approach for each reaction.

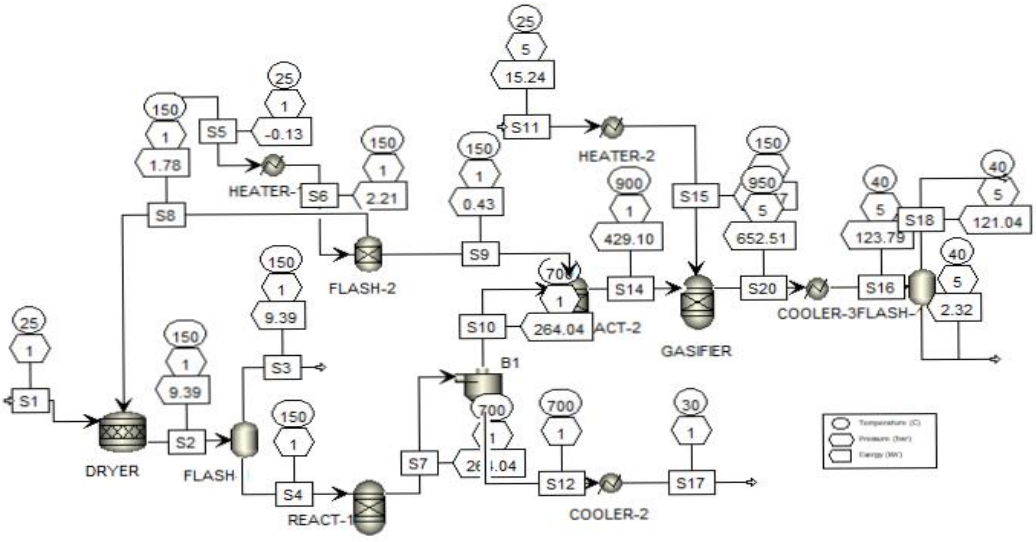

Figure 3. Investigated system components Flow-sheet

The simulation flow sheet developed through a sequence of stages with Aspen Plus is depicted in Figure 3. Table 1 depicts each unit of operational processes in the gasification plant. The atmospheric air at 25 degrees Celsius (°C) temperature and pressure of 1 bar flow at 400 kgh-1 flow rate into the heater block (HEATER-1), the heater increases the temperature to about 150 degrees Celsius (°C) at a constant pressure of 2 bar. Increase holding pressure constant at atmospheric temperature, heater-1 delivers the hot air containing nitrogen and oxygen gases into the separator (FLASH-2). At a Steady

flow rate of 2000 kghr-1, the biomass stream, constituted of Banana Empty Fruit Bunch (BEFB), goes into the Rstoic block (RSTOIC reactor) at 150 degrees Celsius (°C) and 1 bar. The RSTOIC reactor stimulates the biomass by drying (with nitrogen, N_2 from SEP-1) into dry biomass before entering into the separator-1 (SEP-1). The dry biomass from the stock is at 150 degrees Celsius (°C) and 1 bar enters the separator (FLASH). The separator of the same pressure and temperature splits the stream from the dryer into two streams. The first stream (stream 3) contains (N_2 + H_2O) nitrogen gas and the remaining quantity of water from the dry biomass because water is not completely removed from the dryer (stock). The second stream (stream 4) at the same pressure and temperature containing the dry biomass enters the DECOMP block (RYIELD reactor). The yield reactor, at 700 degrees Celsius (°C) and 1.5 bar converts the non-convectional dry biomass into conventional components (pyrolysis). The cyclone is an ash removal block. It removes all available ash from the pyrolysis (YIELD reactor) and delivers ash through the ash removal stream into a cooler-1 (Requil reactor) at the same temperature and pressure. The cooler-2 block drastically reduces the temperature to 400 degrees Celsius (°C) and pressure of 5 bar. Hence, the conventional elements (C, H, O), from the cyclone enter the combustor block at 900 degrees Celsius (°C) and 4 bar. Oxygen gas O_2 from the separator (FLASH -2) at 150 degrees Celsius (°C) and 1 bar for convectional elements from the cyclone in the combustor (COMB block). Combustor products at 900 degrees Celsius (°C) and 4 bar enter the gasifier (Gibb's free reactor). The dry-biomass conventional elements (C, H, O) are heated at a temperature above 700 degrees Celsius (°C) say degrees Celsius (°C) at 4 bars without combustion, and combustion products are made to enter into the Gibb's free reactor (gasifier). At 150 degrees Celsius (°C) and 2 bar, oxygen O_2 gas from atmospheric air from HEATER-2 into the gasifier for gasification. The heater-2 increases the atmospheric air to liberate O_2 at 150 degrees Celsius (°C) and 2 bar and delivers O_2 into the gasifier for the gasification process at 950 degrees Celsius (°C) and 5 bar. Proper process simulation occurs in Gibb's reactor for individual reactions at 950 degrees Celsius (°C) and 5 bar. This temperature is preferable in the simulation process because at temperatures higher than 1000 degrees Celsius (°C), there is an increase in the amount of carbon monoxide, and CO produced and a decrease in the amount of CO_2 produced. On the other hand, at a temperature below 900 degrees Celsius (°C), a higher amount of CO_2 is produced, hence, lessening the amount of CO_2, and CO produced (Zhenling et al., 2017). The gasifier product is discharged from the gasifier at 950 degrees Celsius (°C) and 5 bar then enters a cooler (COOLER-3). At constant pressure, the cooler reduces the temperature to about 40 degrees Celsius (°C) and 5 bar before entering a separator (SEP-3). This is done to reduce the temperature as a higher temperature can damage the separator or reduces the separator's efficiency. At the separation unit, a SEP ID block (FLASH-3) unit is required to gain high hydrogen purity at 40 degrees Celsius (°C) and 5 bar. Moreover, the characteristics and features of the apparatus used in the simulation were determined from the optimized values found in the literature for these membranes. The separator (FLASH -3) at 40 degrees Celsius (°C) and 5 bar split the gasifier product into two streams (stream 18 & stream 19). Stream 18 depicts the percentage of hydrogen H_2 and a minor fraction of other gases produced. The other stream (stream 19) reviews the amount of CO_2, CO, H_2O, and other gas released. The equilibrium reactions are restricted five consecutive equations are formed in combustion and gasifier Tables 4 & 5 [23, 24 & 28].

Physical and chemical properties of EBFB

Five chemical reactions were employed in combustion and gasification processes to produce highly purified hydrogen gas. Table 2 presents the ultimate and proximate analysis of simulated data for banana empty fruit bunch (BEFB) from kinds of literature (Sugumaram et al., 2012), (Marcantonio et al., 2019). These reactions were simulated using ASPEN Plus, to remove carbon (C), carbon monoxide (CO), carbon dioxide (CO_2), methane (CH_4), and water (H_2O) to convert them into hydrogen gas. The

combustion process consists of three chemical reactions, while the gasification process includes two reactions.

Table 2. General physical and chemical properties of empty banana fruit bunch **(**EBFB**)**

Properties	**Biomass value** **Empty fruit bunch (EFB)**
Ultimate analysis	
Carbon (%)	41.75
Oxygen (%)	51.73
Hydrogen (%)	5.10
Nitrogen (%)	1.23
Sulfur (%)	0.18
Proximate analysis	
Fixed carbon (%)	5.95
Moisture content (%)	5.21
Volatile matter (%)	78.83
Ash	15.73
Sulfanal analysis	
Organic % dry mass	0.18
Pyritic % dry mass	0
Sulfate % dry mass	0

Combustor

The three reactions considered in combustion with their stoichiometry reaction are listed in Table 3. Boundary condition was set in ASPEN Plus to carry out the reactions with the equations restricted to the chemical equilibrium specified temperature approach. The combustor operational condition was 900 degrees Celsius (^{o}C) and 4 bar. Nitrogen gas from SEP-2 (FLASH-2) at 200 kg hr-1 flow rate, 150 degrees Celsius (^{o}C), and 2 bar in the combustion process. The number of iterations considered is 30 with 0.0001 error tolerance.

Table 3. Combustion reactions

Specification Type	**Stoichiometry**	**Reaction name**
Temp. approach	$C + ½O_2 \Rightarrow CO$	Ash partial combustion
Temp. approach	$H2 + ½O_2 \Rightarrow H_2O$	H_2 partial combustion
Temp. approach	$CO + ½O_2 \Rightarrow CO_2$	CO shift

Gasifier

Two reactions considered in the gasification process are listed in Table 4**.** Oxygen gas O_2 from atmospheric air at 200 kg hr -1 flow rate, 150 degrees Celsius (^{o}C), and 1.1 bar in Gibb's reactor. The maximum accuracy is 30 with 0.0001 error tolerance. The temperature at 950 degrees Celsius (^{o}C) and pressure of 5 bar were set as a gasifier boundary condition. Oxygen from atmospheric air at 150 degrees Celsius (^{o}C) gas O_2 for process gasification 200 kg hr-1 flow rate. The composition of the stream exits the gasifier into the separator (HEATER-2).

Table 4. Gasifier reactions

Specification Type	Stoichiometry	Reaction name
Temp. approach	$C + H_2O \Rightarrow CO + H_2$	Water gas
Temp. approach	$CO + H_2O \Rightarrow CO + H_2$	CO shift

Separation units

SEP-1; The separator (FLASH-1) at 150 degrees Celsius (° C) and 2 bar separates the nonconventional biomass from the Rstoic into two streams: N_2 and H_2O into streams (stream 3) hence, dry-biomass into the second stream (stream 4) before entering into RYIELD reactor where the nonconventional dry biomass is broken down into smaller conventional unit (C, H, O).

SEP-2; A PSA unit at 150 degrees Celsius (° C) and 2 bar is required at an elevated temperature to gain high-purity delivery of N_2 and O_2. High-temperature atmospheric air from heater-1 is separated into nitrogen gas and oxygen gas through a separator (FLASH-2). The separator delivers nitrogen gas to the dryer (Rstoic) used for drying the biomass and delivers corresponding oxygen gas into Gibb's reactor for combustion.

SEP-3; The corresponding temperature and pressure values of SEP-3 utilized in the process concerning the efficiency were determined from the optimized values found in the literature. At 40 degrees Celsius (° C) and 5 bar, the separator separates the gasifier product from cooler-2 into two streams. In one stream carbon C and water H_2O in the other stream and a small fraction of CH_4, CO, CO_2, H_2O.

2.3. Sensitivity analysis

Components such as combustor, gasifier, and separator variation to present gases are examined through sensitivity analysis. This was performed with the Model Analysis Tools (MAT) in the Aspen Plus simulator. This is based on present gases in the components with 100 - 1000 manipulated variable limits starting and ending point limits and 50 division numbers of points. The Model Analysis Tools factor used for the block variable is 1.048113. The present gases for the sensitive modeling in the combustor block are: H_2, O_2, C, N_2, and S. For gasifier and separator (SEP-3) blocks, gases present are: H_2, O_2, N_2, H_2O, CO, CO_2, CH_4, NH_3, H_2S.

2.4. Concept of exergy

In the absence of the nuclear effect, magnetism, electricity, and surface tension exergy of a stream are segmented into distinct components: physical exergy, chemical exergy, kinetic exergy, and potential exergy (T.J. Kotas 1995, Exergy concepts).

Mathematically,

$$É = Ék + Ép + Éph + Ech \quad (1)$$

From where $\boldsymbol{\varepsilon k}$ is the kinetic exergy, $\boldsymbol{\varepsilon p}$ potential exergy, Eph exergy due to physical, and $\boldsymbol{\varepsilon ch}$ is the chemical exergy. Because the kinetic and potential exergies are accomplished under low and high-grade energy, they are usually negligible during calculation.

If ε equals the specific exergy of the system, then introducing the specific exergy from where

$$\boldsymbol{\varepsilon} = É/m \quad (2)$$

Hence,

$$\boldsymbol{\varepsilon} = \boldsymbol{\varepsilon k} + \boldsymbol{\varepsilon p} + \boldsymbol{\varepsilon ph} + \boldsymbol{\varepsilon ch} \quad (3)$$

Physical exergy of a perfect gas

This exergy is equal to the maximum amount of work obtainable when the stream of substance when brought from its initial state to the environmental state defined by environmental pressure $P_0$and environmental temperature T_0, by physical processes involving only thermal interaction with the environment is termed the physical exergy of the system. The physical exergy of perfect gas can be calculated using the expression below:

$$\mathcal{E}Ph = (h - h0) - T0\,(S - S0) \quad (4)$$

Putting enthalpy and entropy equations into the physical exergy equation, we have physical exergy expression given that the surrounding temperature equals 298.15 K and 1 atm,

However, the general formula for physical exergy is given by;

$$\mathcal{E}Ph = CP(T1 - T0 - T0\,InT1/T0) + RT0\,In\,(P1/P0) \quad (5)$$

Therefore, writing the general physical exergy equation concerning each block in the gasification power plant flow sheet with constant surrounding temperature T_0 and pressure P_0 (in 273.150K and 1bar), specific heat capacity C_P, and molar gas constant R (mean of C_P and R gases present per component, supplementary table 7 & supplementary table 8).

For DRYER: $\mathcal{E}PhDRYR$, SEP-1: $\mathcal{E}PhSEP - 1$, RYEILD: $\mathcal{E}PhRYD$, CYCLONE: $\mathcal{E}PhCYLN$, HEARTER-1:$\mathcal{E}PhHTR - 1$, SEP-2: $\mathcal{E}PhSEP - 2$, COOL-1: $\mathcal{E}PhCOOL - 1$, COMBUSTOR: $\mathcal{E}PhCOMB$, GASIFIER: $\mathcal{E}PhGASIF$, COOL-2: $\mathcal{E}PhCOOL - 2$, SEP-3: $\mathcal{E}PhSEP - 3$.

Standard molar chemical exergy for gas mixtures

A general formula for chemical exergy can be expressed as follows:

$$e\chi Ch - K = \sum i(\chi i * e\chi Ch) + RT0 \sum i(\chi i In\chi i) \quad (6)$$

where,

$$\sum i\chi i e\chi Ch = [(mole\ fraction\ of\ O2) * (standard\ chemical\ exergy\ of\ O2) + (mole\ fraction\ of\ CO2) * (standard\ chemical\ exergy\ of\ CO2) + (mole\ fraction\ of\ N2) * (standard\ chemical\ exergy\ of\ N2) + (mole\ fraction\ of\ H2O) * (standard\ chemical\ exergy\ of\ H2O)]$$

Hence,

$$e\chi Ch(i) = RT0In\,(P0/P(i)) \quad (7)$$

The partial pressure Pi and molar fraction of each substance air at a given relative humidity by Szargut et al. (1988). Mole fraction of combustion gases (Ibrahim Dincer and Marc. A. Rosen (Eds.) – Exergy, standard chemical exergy values for selected substances for air constituents adopted in the calculation of chemical exergies of various substances (boundary condition; T_0 = 298.15 K and P_0 = 1 atm), Kotas (1995), Bejan et al. (1996).

Assuming all gases behave ideally, the molar chemical exergy can then be fathomed using the below expression:

$$e\chi Ch - K = -RT0\,In(\chi iekP0\ /\ P0\ ) = -RT0\,In(\chi iek) \quad (8)$$

Thus, we need to write the general molar chemical exergy equation for the mixture of gases for each block in the biomass gasification power plant flow sheet.

DRYER: completely biomass, no chemical exergy formed: $e\chi Ch - K(DRYR)$ = Null

SEP-1: Constituent gases present are N_2 and H_2O: Standard molar chemical exergy with respect to SEP-1 equals:

$$e\chi Ch - K(SEP - 1) = \{(\chi N2 * e\chi ChN2) + (\chi H2O * e\chi ChH2O)\} + RT0\,\{(\chi N2 * In\chi N2) + (\chi H2O * In\chi H2O)\} \quad (9)$$

Where, $(e\chi Ch)N2, H2O = RT0In\,(P0/Pi, N2, H2O)$ (10)

RYEILD: Standard molar chemical exergy from the Ryeild reactor is null, as there are no constituent gases present

CYCLONE: H_2, O_2, N_2, C, and S - Therefore, standard molar chemical exergy due to cyclone

$$e\chi Ch - K(CYCL) = \{(\chi H2 * e\chi ChH2) + (\chi O2 * e\chi ChO2) + (\chi N2 * e\chi ChN2) + (\chi C * e\chi ChC) + (\chi S * e\chi Ch\,S)\} + RT0\,\{(\chi H2 * In\chi H2) + (\chi O2 * In\chi O2) + (\chi N2 * In\chi N2) + (\chi C * In\chi C) + (\chi S * In\chi S)\} \quad (11)$$

HEATER-1: Constituent gases present are O_2 and N_2:

$$e\chi Ch - K\,(HTR-1) = \{(\chi O2 * e\chi Ch\,O2) + (\chi N2 * e\chi ChN2)\} + RT0\,\{(\chi O2 * In\chi O2) + (\chi N2 * In\chi N2)\} \quad (12)$$

SEP-2: Constituent gases present are O_2 and N_2:

$$e\chi Ch - K\,(HTR-1) = (\chi O2 * e\chi Ch\,O2) + (\chi N2 * e\chi ChN2)\} + RT0\,\{(\chi O2 * In\chi O2) + (\chi N2 * In\chi N2)\} \quad (13)$$

COOLER -1: No constituent gas present. Therefore, $e\chi Ch - K\,(COOL-1) =$ null

COMBUSTOR: Constituent gases present are H_2, O_2, N_2, C, and S: Standard molar chemical exergy due combustor;

$$e\chi Ch - K\,(COMB) = \{(\chi H2 * e\chi Ch\,H2) + (\chi O2 * e\chi ChO2) + (\chi N2 * e\chi Ch\,N2) + (\chi C * e\chi Ch\,C) + (\chi S * e\chi Ch\,S)\} + RT0\,\{(\chi H2 * In\chi H2) + (\chi O2 * In\chi O2) + (\chi N2 * In\chi N2) + (\chi C * In\chi C) + (\chi S * In\chi S)\} \quad (14)$$

GASIFIER: Constituent gases present are H_2, O_2, N_2, H_2O, CO, CO_2, CH_4, NH_3, and H_2S :Standard molar chemical exergy due gasifier;

$$e\chi Ch - K\,(GASIF) = \{(\chi H2 * e\chi Ch\,H2) + (\chi O2 * e\chi ChO2) + (\chi N2 * e\chi Ch\,N2) + (\chi H2O * e\chi Ch\,H2O)\,(\chi CO * e\chi Ch\,CO) + (\chi CO2 * e\chi Ch\,CO2) + (\chi CH4 * e\chi Ch\,CH4) + (\chi NH3 * e\chi ChNH3) + (\chi H2S * e\chi Ch\,H2S)\} + RT0\,\{(\chi H2 * In\chi H2) + (\chi O2 * In\chi O2) + (\chi N2 * In\chi N2) + (\chi H2O * In\chi H2O) + (\chi SCO * In\chi CO) + (\chi CO2 * In\chi CO2) + (\chi CH4 * In\chi CH4) + (\chi NH3 * In\chi NH3) + (\chi H2S * In\chi H2S)\} \quad (15)$$

HEATER- 2: Constituent gases present are O_2 and N_2: Standard molar chemical exergy with respect to heater- 2 reactor;

$$e\chi Ch - K\,(HTR-2) = \{(\chi O2 * e\chi Ch\,O2) + (\chi N2 * e\chi ChN2)\} + RT0\,\{(\chi O2 * In\chi O2) + (\chi N2 * In\chi N2)\} \quad (16)$$

COOLER-2: Constituent gases present are H_2, O_2, N_2, H_2O, CO, CO_2, CH_4, NH_3, and H_2S:

$$e\chi Ch - K\,(COOL-2) = \{(\chi H2 * e\chi Ch\,H2) + (\chi O2 * e\chi ChO2) + (\chi N2 * e\chi Ch\,N2) + (\chi H2O * e\chi Ch\,H2O)\,(\chi CO * e\chi Ch\,CO) + (\chi CO2 * e\chi Ch\,CO2) + (\chi CH4 * e\chi Ch\,CH4) + (\chi NH3 * e\chi ChNH3) + (\chi H2S * e\chi Ch\,H2S)\} + RT0\,\{(\chi H2 * In\chi H2) + (\chi O2 * In\chi O2) + (\chi N2 * In\chi N2) + (\chi H2O * In\chi H2O) + (\chi SCO * In\chi CO) + (\chi CO2 * In\chi CO2) + (\chi CH4 * In\chi CH4) + (\chi NH3 * In\chi NH3) + (\chi H2S * In\chi H2S)\} \quad (17)$$

SEP- 3: Constituent gases present are H_2, O_2, N_2, H_2O, CO, CO_2, CH_4, NH_3, and H_2S :

$$e\chi Ch - K\,(SEP-3) = \{(\chi H2 * e\chi Ch\,H2) + (\chi O2 * e\chi ChO2) + (\chi N2 * e\chi Ch\,N2) + (\chi H2O * e\chi Ch\,H2O)\,(\chi CO * e\chi Ch\,CO) + (\chi CO2 * e\chi Ch\,CO2) + (\chi CH4 * e\chi Ch\,CH4) + (\chi NH3 * e\chi ChNH3) + (\chi H2S * e\chi Ch\,H2S)\} + RT0\,\{(\chi H2 * In\chi H2) + (\chi O2 * In\chi O2) + (\chi N2 * In\chi N2) + (\chi H2O * In\chi H2O) + (\chi SCO * In\chi CO) + (\chi CO2 * In\chi CO2) + (\chi CH4 * In\chi CH4) + (\chi NH3 * In\chi NH3) + (\chi H2S * In\chi H2S)\} \quad (18)$$

Percentage exergy efficiency

Total exergy in of a system to the total exergy out of the same system defines the percentage exergy efficiency of that particular system. Hence, the total exergy is the sum total of exergies of all streams that enter the system. The total of exergies of all streams that flow out of the system refers to the total exergy out of a system.

$\%\ exergy\ eff\ =\ (Total\ exergy\ Out)\ /\ (Total\ exergy\ In)$

That is, $\eta ex\ =\ \sum Exergy\ Out\ /\ \sum Exergy\ In$ (19)

Exergy destruction analysis

The difference between the total exergy in and the total exergy out of a system dictates the exergy destruction of the system. Hence, exergy destruction is expressed mathematically as:

$Exergy\ destruction\ =\ Total\ exergy\ In\ -\ Total\ exergy\ Out$

$\dot{E}DESTRUCTION\ =\ \sum Exergy\ In\ -\sum Exergy\ Out$ (20)

2.5. Exergoeconomic analysis

The exergoeconomic method utilized in the energy-economic analysis is the Specific Cost method (SPECO). Fuel and products of components are defined by directly capturing the systematic value of all the stream exergy entering and subtracting the stream exergy leaving the component.

2.6. Component exergoeconomic factor analysis

Evaluating component performance, we are interested in the relative significance in terms of the cost-efficiency profitability of the entire system at a given period for each category in the gasification through biomass power plant. However, this is provided by the energy-economic factor f_K defined for component K as follows:

$fK\ =\ \dot{Z}K\ /(\dot{Z}K\ +\ Cf,k\ *\ (\dot{E}D,K)$ (21)

$\dot{Z}K\ =\ \dot{Z}K\ Cl\ +\ \dot{Z}K\ OM$ (22)

$\dot{Z}K\ Cl\ =\ CFR\ (i,n)\ *\ TCI$ OR $\dot{Z}K\ Cl\ =\ (CFR\ /top)\ *\ PEC$ (23a&b)

$\dot{Z}K\ OM\ =\ FOM*\ TCI$ OR $\dot{Z}K\ OM\ =\ \dot{Z}Cl*\ \varphi$ (24a&b)

Hence, $TCI\ =\ \varphi\ =\ PEC$

$CFR\ =\ \{i(1+i)\ n\}/\ (1+i)\ n-1$ (25)

However, the cost rate associated with capital, ŻK OM = operating maintenance expenses, ŻK = summation of ŻK OM and ŻK Cl, CFR (i,n) = cost rated with capital in respect to interest rate 'i' and payment period 'n', TCI = total cost investment, FOM = maintain cost factor, PEC = purchase investment cost, φ = factor of operating and maintaining expenses, top = time of operation, $\dot{E}D_K$ = exergy destruction with to the component under consideration and f_K= exergoeconomic factor. For this study, FOM = 1.06 for each piece of equipment, i = 6 %, top = 1hr, n = 25years, maintenance cost factor FOM, interest rate 'i' and the average cost 'Cf, k' values based on U.S. Department of Energy Federal Management Program, 15 Sept 2016, i = 0.06, n = 25yrs, FOM = 1.06, top = 1hr, Cf, k = $0.8(U.S. Department of Energy Federal Management Program (FEMP), 15 Sept 2016), (ATMACA et al., 2018). Note that the assumption was made on the total cost investment of the gasification of biomass components from Google.com as of 2022/23.

3. Result and Discussion

3.1. Modeling of a system for hydrogen production from the empty banana fruit bunch

Syngas, hydrogen production from empty banana fruit bunch (EBFB)

The separator (SEP-3) containing Stream 18 and Stream 19 revealed the syngas quantity produced from EBFB. The amount of syngas produced in stream 19 is presented in **Table 5**. Results affirmed that 80.465kg/h of hydrogen gas can be generated by 2000 kg/h of empty banana fruit bunch at every 39.916 km/h mole flows (Stream 18). It is also noted that the total volume of purified syngas generated during the gasification is 571.894 cum/h from stream 18, separator outlet. Hence, the total volume of lost syngas generated in stream 19, separator outlet is 0.118 cum/h volume of hydrogen gas. The gasification process of empty banana fruit bunches produces a significant amount of carbon monoxide, specifically 1,522.69 kg/h. The quality of this carbon monoxide has a direct impact on hydrogen gas production. In other words, as the quantity of carbon monoxide increases, the amount of hydrogen gas produced decreases. Hence, the relationship is influenced by the high temperatures in both the combustor and gasifier components.

Table 5. Stream 18 and 19 (S_{18} & S_{19}) separator outlet of syngas composition from Aspen Plus

	Units	S18	S19
Mass Flows	**kg/hr**	**2055.96**	**114.746**
H2	kg/hr	80.465	0.00161246
O2	kg/hr	5.16925e-05	1.64433e-08
N2	kg/hr	330.058	0.0858868
H2O	kg/hr	29.1057	113.908
CO	kg/hr	1522.64	0.424152
CO2	kg/hr	90.0953	0.290451
C	kg/hr	0	0
BIOMASS	kg/hr	0	0
ASH	kg/hr	0	0
CH4	kg/hr	0.000163313	1.07621e-07
NH3	kg/hr	0.00925685	0.000172678
S	kg/hr	0	0
H2S	kg/hr	3.5907	0.036269

	Units	S18	S19
Mass Fractions			
H2		0.0391374	1.40524e-05
O2		2.51427e-08	1.43301e-10
N2		0.160537	0.000748493
H2O		0.0141567	0.992692
CO		0.740597	0.00369643
CO2		0.0438214	0.00253125
C		0	0
BIOMASS		0	0
ASH		0	0
CH4		7.94336e-08	9.37906e-10
NH3		4.50244e-06	1.50487e-06
S		0	0
H2S		0.00174648	0.000316081
Volume Flow	cum/sec	0.158859	3.26705e-05

	Units	S18	S19
Mole Flows	**kmol/hr**	**109.826**	**6.34952**
H2	kmol/hr	39.9156	0.000799878
O2	kmol/hr	1.61545e-06	5.13872e-10
N2	kmol/hr	11.7821	0.00306591
H2O	kmol/hr	1.61561	6.32283
CO	kmol/hr	54.3598	0.0151426
CO2	kmol/hr	2.04716	0.00659969
C	kmol/hr	0	0
CH4	kmol/hr	1.01798e-05	6.7084e-09
NH3	kmol/hr	0.000543544	1.01393e-05
S	kmol/hr	0	0
H2S	kmol/hr	0.105355	0.00106417

	Units	S18	S19
Mole Fractions			
H2		0.363443	0.000125975
O2		1.47092e-08	8.09309e-11
N2		0.10728	0.000482857
H2O		0.0147106	0.995798
CO		0.494962	0.00238485
CO2		0.01864	0.0010394
C		0	0
CH4		9.26904e-08	1.05652e-09
NH3		4.94913e-06	1.59686e-06
S		0	0
H2S		0.000959289	0.000167599

3.2. Sensitivity analysis results

Effect of temperature and pressure on gasification (combustor, gasifier, and separator units)

A sensitivity analysis was performed for the combustor, gasifier, and separator (SEP-3) as regards temperature and pressure. Figure 4 affirmed that in the combustor, all the present gases (H_2, O_2, N_2, C, S) increase in a sinusoidal form except sulfur which exists as a solid at room temperature. However, for the gasifier, Figure 5 shows that the rate at which H_2, CO_2, NH_3, and CH_4 flow decreases drastically

hence, the rate at which O_2, N_2, CO, and H_2O flow produced inside the gasifier increases. However, the corresponding H_2S maintains a linear path between 3.60 kg/h and 3.65 kg/h. Figure 6 (SEP-3) shows that the rate at which H_2 is produced and flows increases from 3.525 kg/h to 3.62 kg/h and maintains a linear path. Hence, H_2O 3.64 kg/h decreases and maintains a linear path at 3.52 kg/h. Whereas, O_2 and CH_4 keep a constant linear path. Results show that corresponding effects occur in syngas concerning an increase in pressure. This implies that, at every instant of increase in temperature and pressure, there is a significant change in the flow rate of some gases at a certain kg/h in the combustor and gasifier and in the separator.

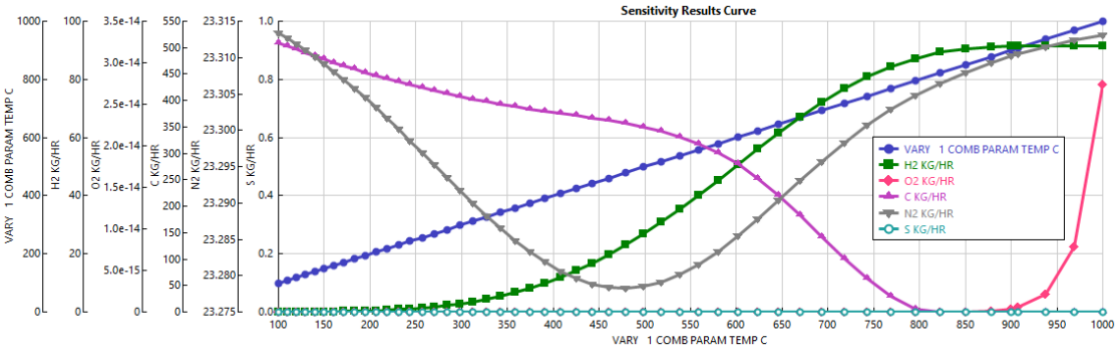

Figure 4. Gasification temperature effect on syngas out of combustor

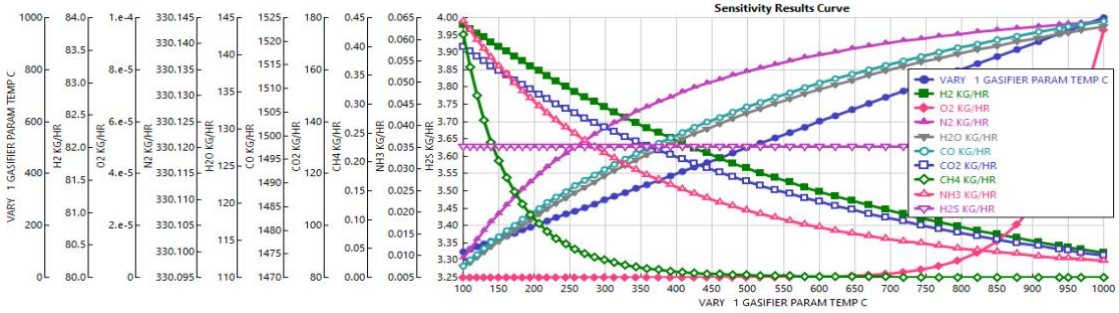

Figure 5. Gasification temperature effect on syngas out of gasifier

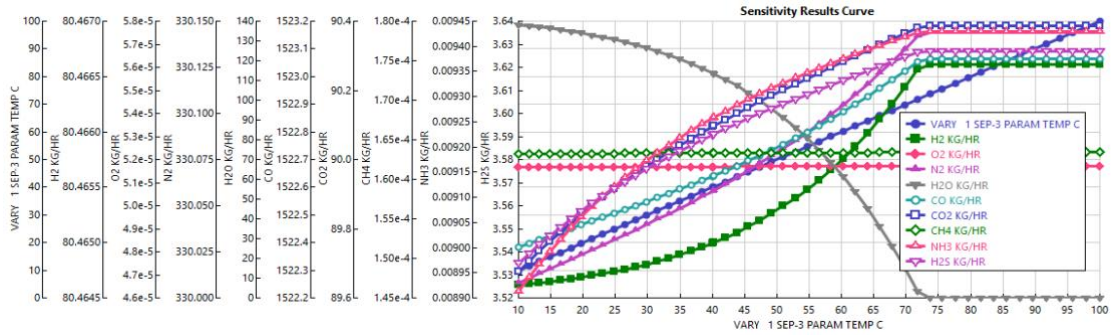

Figure 6. Gasification temperature effect on syngas out of the separator

3.3. Biomass gasification exergy results

Table 6 shows the system total exergy in, total exergy out, overall percentage exergy efficiency and exergy destruction are 4534.77 kJ /kg, 3857.295 kJ/kg, 0.8506 %, and 677.475 kJ/kg respectively. This indicates that a significant amount of energy is released during the gasification process, thereby

enhancing the sustainability of the biomass gasification system. However, high exergy destruction implies a loss of work in the system. Hence, the real processes are irreversible which measures the system degradation. Table 7 shows the components physical and chemical exergy of the system. The system's physical and chemical exergy is 36960.31 KJ/kg, 185.64 kJ/mol.

Table 6. Streams exergy, exergy efficiency, and exergy destruction table

COMPONENT	S. EXGY IN	S. EXGY OUT	% Ex eff (η)	$\dot{E}_{DESTRUCTION}$
DRYER	S_1, S_8 = 81.67	S_2 = 80.41	0.985	1.256
HEATER- 1	S_5 = 31.34	S_6 = 28.11	0.897	3.237
SEP- 1	S_2 = 180.41	S_3, S_4 = 155.22	0.860	25.198
SEP- 2	S_6 = 128.11	S_8, S_9 = 153.61	0.817	34.497
RYEILD	S_4 = 0	S7 = 563.55	0.00	0.00
CYCLONE	S_7 = 617,12	S_{10}, S_{12} = 609.12	0.987	0.800
COMBUSTOR	S_{10}, S_9 = 881.06	S_{14} = 872.40	0.990	8.656
GASIFIER	S_{14}, S_{15} = 1090.44	S_{20} = 1082.15	0.992	8.290
COOLER- 1	S_{12} = 0	S_{17} = 0	0.00	0.00
HEATER- 2	S_{11} = 137,16	S_{15} = 28.035	0.204	109.123
COOLER-2	S_{20} = 1082.15	S_{16} = 205.30	0.189	876.848
SEP- 3	S_{16} = 305.31	S_{18}, S_{19} = 284.69	0.932	20.612

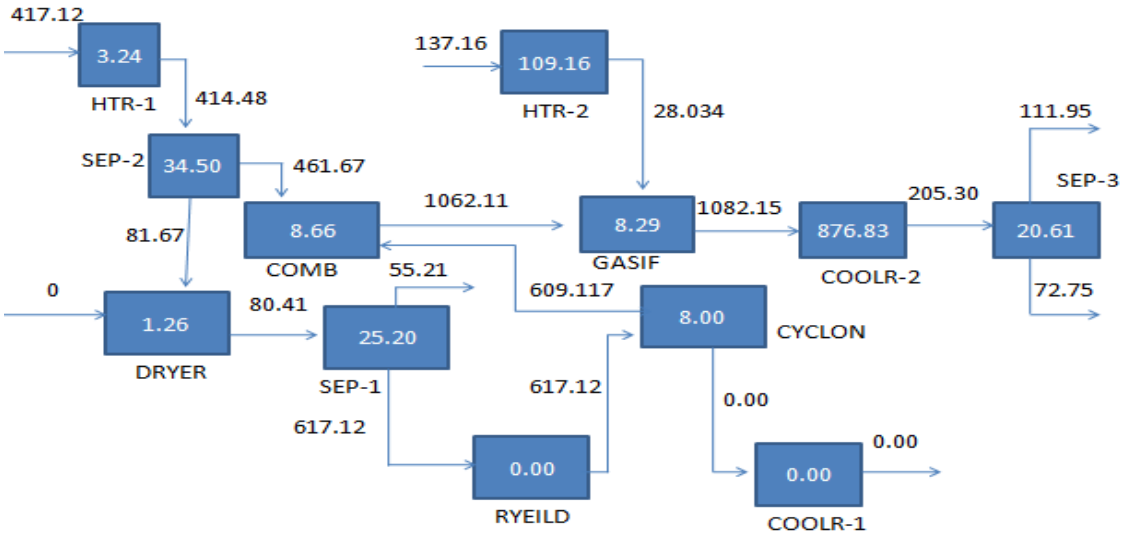

Figure 7. Block diagram for exergy flow in the biomass gasification plant (kW)

Figure 7 illustrates the gasification exergy process flow within the system. Exergy destruction of each component, subtracted from the total exergy of all incoming streams, must be equal to the total exergy of all outgoing streams from that component. Therefore, the block exergy flow diagram for the gasification of the biomass system is balanced.

3.4. Exergoeconomic analysis results

Table 7 and Table 8 present the Block physical and chemical exergy, rate due investment, and exergoeconomic evaluation results. The system exergy stream cost rate, component-related cost rate,

component-related cost difference, component exergoeconomic factor, and cost rate exergy destruction concerning fuel exergy destruction, cost rate exergy destruction concerning fixed product exergy destruction are 407527.644 $/h, 1555.57 $/h, 0.5679 %, 0.9089 %, 353.22 $/h, 73.135 $/h. The results from the evaluation show the necessity to improve the exergy utilization in some components such as cyclone, combustor, gasifier cooler-2, and SEP-3.

Table 7. Block physical and chemical exergy, rate due investment, and exergoeconomic factor results

COMPONENT	$\mathcal{E}_{Ph}$ (KJ/kg)	$e\chi_{Ch}^{-K}$(KJ/mol)	$\dot{Z}_{K,\,nth}$	f_K (%)
DRYER	80.84	0	2162.62	0.9993
HEATER- 1	78.47	19.36	1138.22	0.3862
SEP- 1	109.66	0.472	1707.33	0.9880
SEP- 2	78.47	19.41	1707.33	0.9841
RYEILD	364.03	0	1707.33	1.0000
CYCLONE	1204.40	0.660	1707.33	0.9963
COMBUSTOR	2002.70	374.66	1707.33	0.9960
GASIFIER	1874.3	717.02	1707.33	0.9961
COOLER- 1	58.51	0	1138.22	1.0000
HEATER- 2	78.47	16.85	1138.22	0.9514
COOLER-2	362.30	539.62	1138.22	0.6187
SEP- 3	362.30	539.62	1707.33	0.9904

Table 8. Results of exergoeconomic analysis of the study

COMPONENT	$C_{p,\,k}$	r_k%	$\dot{C}$ j	$\dot{C}_{D,k}\dot{E}_{p,k}$ fixed	$\dot{C}_{D,k}\dot{E}_{f,k}$ fixed
DRYER	0.812	0.0153	6602.20	2.056	1.0201
HEATER- 1	0.892	0.115	3065.99	2.589	2.887
SEP- 1	0.930	0.163	8855.71	20.158	23.434
SEP- 2	0.979	0.224	10052.79	27.598	33.773
RYEILD	0.000	-1.000	0	0	0
CYCLONE	0.811	0.0132	743666.63	6.400	6.488
COMBUSTOR	0.808	0.0101	192708.80	6.925	6.995
GASIFIER	0.807	0.00807	2825678.98	6.632	6.686
COOLER- 1	0.000	-1.000	0	0	0
HEATER- 2	3.922	3.902	13074.09	87.298	427.980
COOLER-2	4.233	4.291	976012.73	701.478	3711.698
SEP- 3	0.858	0.0729	110613.81	16.489	17.693

Table 9 shows comparative hydrogen production techniques and results from some reviewed works of literature. Results affirmed that an optimal peak operating efficiency can easily be achieved when considering the average unit cost of fuel $\dot{C}_{D,k}\dot{E}_{f,k}$ fixed with the product fixed as the main working fluid. However, this may not be beneficial for a component dryer, although its impact could be negligible since only one component is involved. Finally, the cycle performance curve drawing according to exergoeconomic multi-objective optimization results and its utilization are suggested.

Table 9. Comparative hydrogen production techniques and results from some reviewed works of literature

Reference	Work	Method (s)	Materials	Result (s)	Recommendation
Arzate et al [3]	Efficiency of an Au/TiO_2 photocatalyst for H_2 production and organic pollutant	Compound Parabolic Collector (CPC) at the Plataforma Solar de Almería (PSA)	Au/TiO2 photocatalyst, Wastewater as sacrificial agent	The energy efficiency of the process was 1.8%, and optimal catalyst loading was 0.2 g/L	Develop efficient photocatalysts, reuse catalysts, and test cheaper metals like Ni, and Cu.
Bing et al [4]	H_2 production from agricultural solid residue in Malaysia	ASPEN Plus to simulate the gasification process of palm oil biomass, Dual-fluidized bed reactor with NiO catalyst	ASPEN Plus software, palm oil biomass	The gasification process can produce H_2 with 95% purity.	Improving the efficiency of the gasification process and exploring the use of other catalysts
Boudries [5]	Techno-economic assessment of H_2 production in Algeria.	CPV-electrolysis system used for H_2 cost-effectiveness analysis	CPV-electrolysis system, PV-electrolysis.	A CPV-electrolysis system is an efficient and economical method of H_2.	Investigate CPV-electrolysis system parameters' effects and propose African-European collaboration to advance this technology.
Brynjarsdottir et al [7]	Effect of culture parameters on H_2 production	BM medium for culturing the strain GHL_{15}	Strain Thermo-anaerobacter GHL15	Thermoanaerobacter GHL15 yields 3.1 mol H_2/mol glucose at low H_2 pressure	Strain's sensitivity to initial substrate concentration and acetate accumulation
Jingwei et al [15]	H_2 production from biomass in supercritical water	Gasification in supercritical water (SCWG) and the use of concentrated solar energy	ASPEN Plus, glucose, corn meal, and wheat stalk, CSP power	Technical feasibility of the system and its advantages for H_2	Designing efficient reactors, continuous gasification of biomass with high dry matter
Hossain et al [12]	H_2 production from oil palm biomass by thermochemical process	Pyrolysis, gasification, and gasification in supercritical water.	Oil palm biomass,	Oil palm biomass is promising for H_2 due to high calorific value	Analysis of residual bio-char during H_2
Kalinci et al [13]	Life cycle assessment of H_2 production from biomass gasification systems	LCA to evaluate H_2 from biomass	Aspen plus, Life Cycle Assessment (LCA),	Downdraft Gasifier has lower fossil energy consumption and emissions compared to CFBG.	Combination of biomass and solar energy for H_2

Table 9 Continued.

Reference	Work	Method (s)	Materials	Result (s)	Recommendation
Kumar et al [24]	Comparative analysis of H_2 production from the thermochemical conversion of algal biomass	Techno-economic models, modeling, equipment sizing, and cost estimation	Algae biomass through thermal and supercritical water gasification	Supercritical water gasification is more cost-effective than thermal gasification	Improve algae biomass production, optimize processes, boost hydrogen yield, cut costs
Stefan et al [18]	H_2 production from biomass using a dual fluidized bed steam gasification system	IPSEpro to model the process, mass, and energy balance analysis	IPSEpro software, biomass as feedstock	61 MW of H_2 can be produced from 100 MW of wood chips and 6 MW of electricity	Improving the efficiency and cost-effectiveness of H_2 from biomass
Yaser et al [28]	Techno-economic analyses and life cycle assessments (LCA) of fluidized bed (FB) and entrained flow (EF)	Simulations and techno-economic analyses	Apen plus, fluidized bed (FB), and entrained flow (EF)	EF has 11% higher thermal efficiency than FB, and FB has a lower minimum H_2 selling price	Research needed to enhance efficiency and cut costs of biomass gasification
This study	Techno-economic analysis of a system for H_2 production from an empty banana fruit bunch	Aspen plus simulation, Biomass gasification	Empty banana fruit bunch, Aspen plus software	80.465 kg/h of H_2 from 2000 kg/h of EBFB at every instant of 39.92 km/h is feasible	Aligning temperature and pressure with CO_2 to boost H_2 production and reduce CO emissions

4. Conclusion

The research study was designed to simulate the production of hydrogen gas from an agricultural biomass residue, a quantified amount of empty banana fruit bunch, (EBFB) through biomass gasification for electricity generation. Aspen Plus version 11 was adopted for the simulation, the convectional exergy approach method for exergy analysis, and the Specific Cost method (SPECO) for exergoeconomic analyses. The following are the main study highlights:

- It has been observed that 80.465 kg/h of H_2 can be extracted from 2000 kg/h of empty banana fruit bunch at a constant mole flow rate of 39.92 km/h.
- The flow rates of H_2, O_2, N_2, and C in the combustor increase in a sinusoidal pattern at room temperature, while sulfur (S), in solid form, maintains a constant flow rate of 0.00 kg per hour. In the gasifier, the flow rates of H_2, CO_2, NH_3, and CH_4 decrease. In contrast, O_2, N_2, CO, and H_2O show an increase in flow content within the gasifier, while H_2S follows a linear trend.

- In the separator (SEP-3), the flow rate of H_2 increases from 3.525 kg/h to 3.62 kg/h, maintaining a linear trajectory. However, at a flow rate of 3.64 kg/h, H_2O decreases and settles at a linear rate of 3.52 kg/h. Consequently, both O_2 and CH_4 continue to follow a constant linear path.
- Carbon monoxide (CO) decreases and carbon dioxide (CO2) increases below 900 degrees Celsius. At temperatures of 1000 degrees Celsius and above, CO increases, which reduces CO2 emissions.
- The total exergy in, total exergy out, overall percentage exergy efficiency, and corresponding exergy destruction are 4534.77 kJ /kg, 3857.295 kJ /kg, 0.8506 %, and 677.475 kJ /kg respectively. The system exergy stream cost rate, component-related cost rate, component-related cost difference, and component exergoeconomic factor are: 407527.644 $/h, 1555.57 $/h, 0.5679 %, and 0.9089 %.

The author suggests that further research should be conducted under appropriate temperature and pressure conditions when working with CO_2. This approach aims to increase the production of H_2 while decreasing the emission of CO, thereby enhancing the overall CO_2 utilization. Additionally, it is essential to improve the exergy efficiency in specific components, including the cyclone, combustor, gasifier cooler-2, and SEP-3. Better performance can be achieved by adopting improved insulation and operational methods and reducing costs associated with investment and energy loss, specifically targeting low exergy destruction values.

Acknowledgment

I extend my sincere gratitude to the Federal University of Petroleum Resources for providing a conducive laboratory environment that greatly facilitated this research project.

Conflict of interest

There were no conflicts of interest during or after the course of this project. All research and findings were conducted independently and without any external influence.

Authors' Contributions

A. John: Conceptualization, Literature review, Methodology, Resources, Formal analysis, Writing - Original draft preparation (75 %)

J. Oyekale: Conceptualization, Supervision, Investigation (25 %).

All authors read and approved the final manuscript.

References

[1] AlZahrani, A. A., & Dincer, I. Integrated solar-based hydrogen extraction analysis. *International Journal of Hydrogen Energy*, *41*(19), 8042–8056. 2016. https://doi.org/10.1016/j.ijhydene.2015.12.103

[2] Amao, Y., Sakai, Y., &Takahara, S. Hydrogen Extraction from Solar via a cellulose biomass with an enzymatic system. *Chemical Research Intermediates*, *42*(11), 7753–7759. 2016. https://doi.org/10.1007/s11164-016-26602

[3] Arzate Salgado, S. Y., Ramírez Zamora, R. M., Zanella, R., Peral, J., Malato, S., & Maldonado, M. I. Photocatalytic Hydrogen Production. Foreign Energy Journal,*41*(28), 11933–11940. 2016. https://doi.org/10.1016/j.ijhydene.2016.05.039

[4] Bing, L. B., Chandrasekaran, P., Francis Xavier, V. D. C. S., Rajput, H. W., Ann, C. L., Mubarak, N. M., & Lau, S. Y. Hydrogen Extraction through Agricultural Solid Residue in Malaysia utilizing Aspen Plus Engineering Tool. Waste *and Biomass Valorization*, *11*(4), 1403–1419. 2020. https://doi.org/10.1007/s12649-018-0470-z

[5] Boudries, R. Techno-economic Assessment of Solar Hydrogen Production Using CPV-electrolysis Systems. *Energy Procedia*, *93*, 96–101. 2016. https://doi.org/10.1016/j.egypro.2016.07.155

[6] Boualati, Y., &Saouli, S. Experimental Study of Hydrogen Production Using Solar Energy in Ouargla (South East Algeria). *Journal of Solar Energy Engineering, Transactions of the ASME*, *140*(3). 2018. https://doi.org/10.1115/1.4039332

[7] Brynjarsdottir, H., Scully, S. M., &Orlygsson, J. Hydrogen Extraction through biohydrogen and lignocellulosic biomass. *International Journal of Hydrogen Energy*, *38*(34), 14467–14475. 2013. https://doi.org/10.1016/j.ijhydene.2013.09.005

[8] Cabezas, M. D., Franco, J. I., &Fasoli, H. J. Optimization of self-regulated hydrogen production from photovoltaic energy. *International Journal of Hydrogen Energy*, *45*(17), 10391–10397. 2020. https://doi.org/10.1016/j.ijhydene.2018.10.203

[9] Dimroth, F., Peharz, G., Wittstadt, U., Hacker, B., & Bett, A. W. (n.d.). *A PV concentrator using iii-v multi-junction solar cells for hydrogen.*

[10] Demirbas, A. Hydrogen through water gasification. *Part A: Recovery, Utilization and Environmental Effects*, *32*(14), 1342–1354. 2010. https://doi.org/10.1080/15567030802654038

[11] Ganeshan, I. S., Manikandan, V. V. S., Ram Sundhar, V., Sajiv, R., Shanthi, C., Kottayil, S. K., & Ramachandran, T.Regulated hydrogen production using a solar-powered electrolyzer. *International Journal of Hydrogen Energy*,*41(*24), 10322–10326. 2016. https://doi.org/10.1016/j.ijhydene.2015.05.048

[12] Hossain, M. A., Jewaratnam, J., & Ganesan, P. The prospect of hydrogen production through oil palm biomass – A review. In *International Journal of Hydrogen Energy* (Vol. 41, Issue 38, pp. 16637–16655. 2016. Elsevier Ltd. https://doi.org/10.1016/j.ijhydene.2016.07.104

[13] Kalinci, Y., Hepbasli, A., & Dincer, I. Hydrogen Life Cycle Assessment through Biomass. *International Journal of Hydrogen Energy*, *37*(19), 14026–14039. 2012. https://doi.org/10.1016/j.ijhydene.2012.06.015

[14] khanmohammadi, S., & Saadat-Targhi, M. Integrated system solar energy through waste food. *Energy*, *171*, 1066–1076. 2019. https://doi.org/10.1016/j.energy.2019.01.096

[15] Chen, J., Lu, Y., Guo, L., Zhang, X., & Xiao, P.Supercritical Hydrogen Extraction via Biomass.*International Journal of Hydrogen Energy*, *35*(13), 7134–7141. 2010. https://doi.org/10.1016/j.ijhydene.2010.02.023

[16] Marcantonio, V., de Falco, M., Capocelli, M., Bocci, E., Colantoni, A., &Villarini, M. Fluidized bed reactor with different separation systems. Foreign *Energy*, *44*(21), 10350–10360. 2019. https://doi.org/10.1016/j.ijhydene.2019.02.121

[17] Ma, Z., Zhang, S. P., Xie, D. Y., & Yan, Y. J.Novel hydrogen extraction via biomass energy. *International Journal of Hydrogen Energy*, *39*(3), 1274–1279. 2014. https://doi.org/10.1016/j.ijhydene.2013.10.146

[18] Müller, S., Stidl, M., Pröll, T., Rauch, R., &Hofbauer, H. Biomass hydrogen: Large-scale hydrogen production based on a dual fluidized bed steam gasification system. *Biorefinery*, *1*(1), 55–61. 2011. https://doi.org/10.1007/s13399-011-0004-4

[19] Xu, C., Chen, S., Soomro, A., Sun, Z., & Xiang, W.Hydrogen-rich syngas production through gasification of biomass. *Journal of the Energy Institute*, *91*(6), 805–816. 2018. https://doi.org/10.1016/j.joei.2017.10.014

[20] Zamfirescu, C., & Dincer, I. Assessment of a new integrated solar energy system for hydrogen production. *Solar Energy*, *107*, 700–713. 2014. https://doi.org/10.1016/j.solener.2014.05.036

[21] Zhang, L., Li, F., Sun, B., & Zhang, C. Intensified optimization design, and coupled power system. *Energies*, *12*(4). 2019. https://doi.org/10.3390/en12040687

[22] Samuel, O. D., Aigba, P. A., Tran, T. K., Fayaz, H., Pastore, C., Der, O., Erçetin, A., Enweremadu, C. C., & Mustafa, A. Comparison of the Techno-Economic and Environmental Assessment of Hydrodynamic Cavitation and Mechanical Stirring Reactors for the Production of Sustainable Hevea brasiliensis Ethyl Ester. *Sustainability*, *15*(23), 16287. 2023. https://doi.org/10.3390/su152316287

[23] Kitegi, M. S. P., Lare, Y., & Coulibaly, O. Potential for Green Hydrogen Production from Biomass, Solar, and Wind in Togo. *Smart Grid and Renewable Energy*, *13*(02), 17–27. 2022. https://doi.org/10.4236/sgre.2022.132002

[24] Kumar, M., Oyedun, A. O., & Kumar, A. A comparative analysis of hydrogen production from the thermochemical conversion of algal biomass. *International Journal of Hydrogen Energy*, *44*(21), 10384–10397. 2019. https://doi.org/10.1016/j.ijhydene.2019.02.220

[25] Li, D., Ishikawa, C., Koike, M., Wang, L., Nakagawa, Y., &Tomishige, K. Renewable Hydrogen-supported Co catalysts. *International Journal of Hydrogen Energy*, *38*(9),3572–3581. 2013. https://doi.org/10.1016/j.ijhydene.2013.01.057

[26] Liu, Q., Bai, Z., Wang, X., Lei, J., &Jin, H. Investigation of thermodynamic performances for two solar-biomass hybrid combined cycle power generation systems. *Energy Conversion and Management*, *122*, 252–262. 2016. https://doi.org/10.1016/j.enconman.2016.05.080

[27] Sakr, I. M., Abdelsalam, A. M., & El-Askary, W. A. Electrode demerit on hydrogen extraction via solar. *Energy*, *140*, 625–632. 2017. https://doi.org/10.1016/j.energy.2017.09.019

[28] Salkuyeh, Y. K., Saville, B. A., & MacLean, H. L.Techno-economic analysis and life cycle assessment hydrogen through biomass. *International Journal of Hydrogen Energy*, *43*(20), 9514–9528. 2018. https://doi.org/10.1016/j.ijhydene.2018.04.024

IJESG
e-ISSN 2636-7904
International Journal of Energy and Smart Grid
Vol 9, Number 1, 2024
Doi: 10.55088/ijesg.1569947

Research Article

TRIPLE-OBJECTIVE OPTIMIZATION OF SUPERCRITICAL CO_2 RECOMPRESSION BRAYTON CYCLE IN SOLAR TOWER SYSTEMS WITH ENERGY, EXERGY AND EXERGOECONOMIC ANALYSIS

Ahmet ELBİR*[1]

[1]Süleyman Demirel University, Isparta, Türkiye Orcid[1]:https://orcid.org/0000-0001-8934-7665
* Corresponding author; ahmetelbir@sdu.edu.tr

Abstract: *This study addresses the energy, exergy and exergoeconomic analyses of the supercritical CO_2 recompression Brayton cycle used in solar tower systems. In the study, a three-objective optimization model was developed using artificial neural networks (ANN) to optimize the system performance. The model provides information for the development of sustainable solar energy systems by providing analyses on key factors such as energy efficiency, environmental impact and economic viability. The results show that the supercritical CO_2 cycle provides higher thermal efficiency compared to conventional systems and offers cost advantages by reducing the size of system components. In addition, the analyses show that energy and exergy losses can be minimized and the cost effectiveness of the system can be increased, providing important findings in terms of the efficiency and economic viability of solar energy systems.*

Keywords*: Energy Analysis, Exergy Analysis, Multi-Objective Optimization, Artificial Neural Networks (ANN), Innovative Energy Solutions*

Received: October 18, 2024 *Accepted: December 16, 2024*

1. Introduction

Solar energy stands out as an important resource in response to the global energy crisis and environmental problems. Solar tower systems are one of the most promising ways to take advantage of these resources, thanks to their high efficiency and scalability. Supercritical CO_2 has many advantages over conventional fluids; such as higher thermal efficiency, smaller system size, and improved heat transfer properties.

Some studies in the literature: Abdelghafar et al. [1] conducted an energy, exergy, and exergoeconomic analysis of combined power cycles powered by sCO_2-based concentrated solar energy. Abid et al. [2] compared the solar-powered supercritical CO_2 power and hydrogen production cycle in terms of energy, exergy and exergoeconomic aspects. Adibhatla and Kaushik. [3] conducted an energy, exergy and economic analysis for a combined cycle power plant powered by an integrated solar steam generator. Almutairi et al. [4] presented a review examining the use of solar energy in power plants for preheating purposes. Al-Sulaiman and Atif. [5] compared performance by integrating different supercritical CO_2 Brayton cycles with the solar tower system. Atif and Al-Sulaiman. [6] performed energy and exergy analyses of solar tower-powered supercritical CO_2 recompression cycles at six different locations. Bai et al. [7] analyzed the use of CO_2-SF_6 mixing fluid in solar power plants in the supercritical Brayton cycle from a thermodynamic point of view. Bashan and Gümüş. [8] performed the energy and exergy analysis according to the optimal design parameters for the recovered supercritical CO_2 power cycle. Bejan et al. [9] presented a wide range of resources on thermal design and optimization. Cengel and Boles. [10] discussed gas-steam mixtures and air conditioning systems with a thermodynamic approach. Citaristi. [11] provides information on the International Energy Agency (IEA). Dincer and Rosen. [12] discussed the relationship between energy, environment and sustainable development. Ehsan et al. [13] evaluated the commercial potential and research status of supercritical

CO_2 power cycles. Guelpa and Verda. [14] conducted an exergoeconomic analysis on the supercritical CO_2 cycle design for concentrated solar power plants. Guo et al. [15] presented a comprehensive review on the use of supercritical CO2 cycles in energy industries. Heller et al. [16] analysed the technical and economic selection of supercritical CO_2 cycles for concentrated solar plants based on particle technology. Hinkley et al. [17] provide a roadmap on concentrated solar fuels. Kalogirou. [18] studied the development of solar collectors and their applications. Khan et al. [19] compared the recovery and exergoeconomic analysis of waste heat for two solar-powered supercritical CO_2 Brayton cycles. Kulhanek and Dostal. [20] conducted thermodynamic analysis and comparison on supercritical CO_2 cycles. Li et al. [21] examined the applications of supercritical CO_2 power cycles in nuclear power, solar power, and other energy industries. Liang et al. [22] performed simultaneous optimization of supercritical CO_2 Brayton and organic Rankine cycles integrated with a concentrated solar power plant. Liu et al. [23] compared the integration of coal-fired power plants with supercritical CO_2 Brayton cycles with steam Rankine cycles. Mehos et al. [24] presented a roadmap for concentrated solar power. Mohammadi et al. [25] performed advanced exergy analyses for recompression supercritical CO_2 cycles. Montes et al. [26] evaluated recent developments on pressurized central receivers and solar power plants operating with supercritical power cycles. Okonkwo et al. [27] conducted a second-law analysis and exergoeconomic optimization of solar tower-powered combined-cycle power plants. Osorio et al. [28] performed dynamic analysis of supercritical CO_2-based closed cycles powered by concentrated solar energy. Shah. [29] provides information on advanced power generation systems and thermal resources. Sun et al. [30] analyzed two supercritical CO_2 cycles in terms of recovery of gas turbine waste heat. Xin et al. [31] performed a thermodynamic analysis on a novel supercritical CO_2 Brayton cycle based on the thermal cycle division analysis method.

This study aims to explore the potential of supercritical CO_2 recompression Brayton cycles in solar tower systems that concentrate solar energy. With the integration of energy, exergy, and exergoeconomic analyses, this study provides valuable insights into optimizing the performance and economic viability of solar tower systems.

2. Materials and Methods

2.1. Solar Tower Systems and the Supercritical CO_2 Brayton Cycle

Solar tower systems generate high-temperature thermal energy by concentrating sunlight into a receiver using mirrors or heliostats. This energy can be converted into electricity through various thermodynamic cycles. The supercritical CO_2 cycle operates above the critical temperature and pressure of CO_2; In this way, a fluid that combines liquid and gas properties is obtained. This feature is important to improve thermal efficiency and make the system more compact. Figure 1 shows the general configuration of the solar tower system.

IJESG
e-ISSN 2636-7904
International Journal of Energy and Smart Grid
Vol 9, Number 1, 2024
Doi: 10.55088/ijesg.1569947

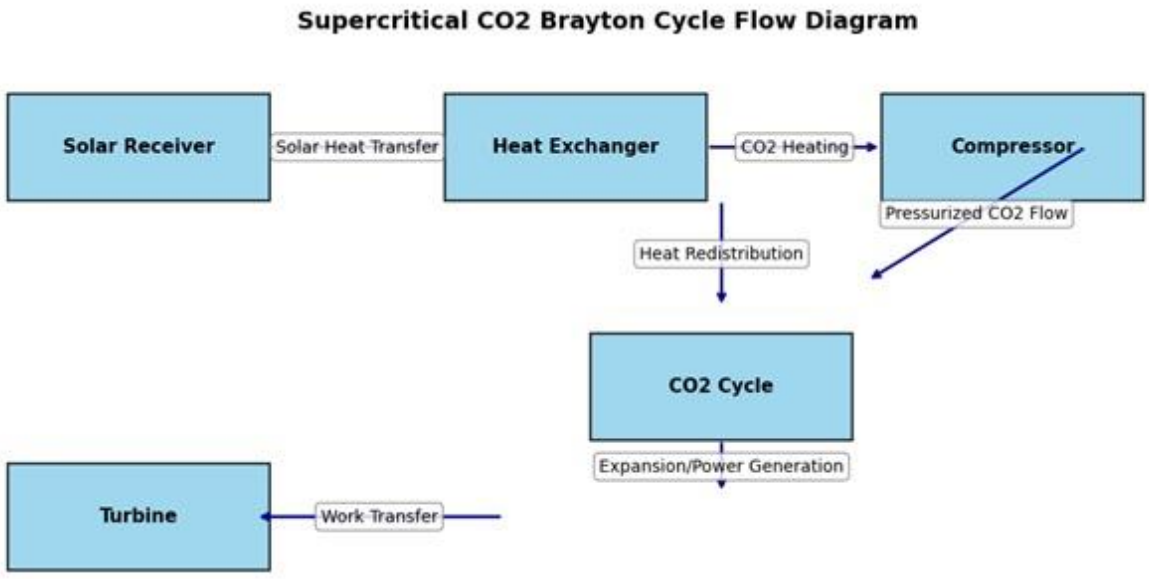

Figure 1. Solar Tower System Configuration

This graph shows the flow diagram of the supercritical CO_2 Brayton cycle. The diagram clearly reveals the energy flow and processes between the main components of the system. Solar Receiver: It is the first component that collects energy from the sun and transfers it to the CO_2 fluid. This is where the transfer of energy begins. Heat Exchanger: Increases the efficiency of the system by further heating the hot CO_2 fluid from the solar receiver. Heat transfer takes place here. Compressor: The heated CO_2 is pressurized here. This pressure increase is critical to improving the energy efficiency of the system. Turbine: Pressurized CO2 is expanded here to produce mechanical work. This process ensures the energy output of the system. CO_2 Cycle: The CO_2 coming out of the turbine completes the cycle in the system. At the end of the process, the CO_2 returns to the solar receiver and the cycle starts over. The graph has arrows that show the flow of energy between the components. Each arrow represents a specific process: Energy Transfer: From solar receiver to heat exchanger, Heating CO_2: Heat exchanger to compressor, Heat Transfer: Compressor to turbine, Pressurization: Turbine to CO_2 cycle, Work Production: Reconversion from CO_2 cycle to solar receiver. The diagram provides a visual representation of the operation of the system, providing an important reference for the energy efficiency and performance analysis of the supercritical CO_2 Brayton cycle.

2.2. Energy Analysis

Energy analysis evaluates energy efficiency by calculating energy flows, inputs, outputs and losses in the system. In this analysis, the energy equations in each component of the system, such as compressors, turbines, heat exchangers, etc., should be written in detail. In addition:

Energy equations: Energy equations should be written in each component where energy conservation is achieved.

Energy efficiency: Energy efficiency is defined as the ratio of the output energy of the system to the energy entering the system. By calculating this ratio on each component, the overall energy efficiency of the system can be achieved.

$$\eta_{energy}=\frac{E_{output}}{E_{input}} \quad (1)$$

In equation 1, E_{output} is the output energy and E_{input} is the input energy.

2.3. Exergy Analysis

Exergy analysis more comprehensively evaluates a system's efficiency, energy quality, and environmental impact. This analysis is important for a better understanding of energy losses and offers more in-depth information when compared to energy efficiency. Exergy is calculated by taking into account environmental energy losses and entropy. Exergy loss is associated with the fact that heat energy becomes less efficient in a given environment.

Exergy loss: Exergy loss can be calculated by considering the entropy changes for each component.

Exergy efficiency: Exergy efficiency, like energy efficiency, is defined as the ratio of output exergy to input exergy.

$$\eta_{exergy}=\frac{Ex_{output}}{Ex_{input}} \quad (2)$$

In equation 2, Ex_{output} is the output exergy and Ex_{input} is the input exergy.

2.4. Exergoeconomic Analysis

Exergoeconomic analysis evaluates the economic performance of an energy system by relating it to exergy losses. In this analysis, the costs of each component in the system are combined with the efficiency analyses. That is, the points where energy and exergy losses are linked to their costs should be detailed.

Cost calculations: The investment cost, operating costs and maintenance costs of each component, e.g. heat exchanger or turbine, can be calculated.

Exergoeconomic efficiency: This efficiency is often defined as a parameter that evaluates the ratio between exergy loss and costs. In this way, it can be optimized for cost minimization.

$$\eta_{exergoeconomic}= \frac{C_{exergy}}{C_{total}} \quad (3)$$

In Equation 3, C_{exergy} is the cost for exergy loss and C_{total} is the total cost.

2.5. Advanced Technical Details

Temperature and pressure dependence: Exergy and energy calculations often vary depending on the temperature and pressure in the system. It is necessary to calculate these parameters for components and study their effect on each component.

$$Ex=(h-h_0)-T_0\cdot(s-s_0) \quad (4)$$

In equation 4, h is enthalpy, s is entropy, T_0 is ambient temperature, and h_0 and s_0 are the reference enthalpy and entropy at environmental conditions.

Dynamic simulations: Energy, exergy and exergoeconomic analyses, more realistic results can be obtained by using dynamic simulations. Such simulations allow to analyze variable parameters in the system (temperature, pressure, flow rate, etc.) over time.

2.6. Energy Efficiency Calculator

Energy efficiency (η) is calculated as follows (5):

$$\eta = \frac{W_{\text{exit}}}{Q_{\text{input}}} \quad (5)$$

- W_{exit}: The net work produced by the system, i.e. the difference between turbine and compressor.
- Q_{input}: The total energy transferred to the solar receiver.

Accepted assumptions:

- The isentropic efficiencies of turbines, compressors, and other components have been accepted as constant.
- The CO_2 fluid is constantly operating under supercritical conditions (above critical temperature and pressure).
- The input energy comes from a constant heat source obtained from solar radiation.

2.7. Exergy Loss Calculator

Exerge loss (Ex_{loss}) evaluates energy losses and irreversibility in the system. The calculation is made by the formula (6):

$$Ex_{\text{loss}} = Q_{\text{input}} \text{ x } (1 - \frac{T_{\text{enviroment}}}{T_{source}}) \quad (6)$$

Here:

- $T_{\text{enviroment}}$: Ambient temperature.
- T_{source}: Source temperature, that is, the temperature reached in the solar receiver.
- Q_{input}: The total energy transferred to the solar receiver.

Accepted assumptions:

- System irreversibility (such as friction, heat transfer losses) was taken into account.
- The exergy loss of each component in the cycle is calculated individually based on their isentropic efficiency.
- The ambient temperature is considered constant, that is, no changes in the external environment are taken into account.

2.8. ANN (Artificial Neural Networks) Methodology

Artificial Neural Networks (ANNs) are a powerful artificial intelligence (AI) methodology used to model complex and nonlinear relationships by mimicking the functioning of biological neural networks. These networks use various algorithms to learn the relationships between input data and output, and direct the training data and optimization processes. Below is a detailed explanation of the ANN algorithm used, input/output parameters, and learning processes.

2.8.1 Artificial Neural Network Algorithm

Artificial neural networks are generally used with multi-layer (MLP - Multi-Layer Perceptron) structures. These structures contain multiple layers (input layer, hidden layers, and output layer). The

neurons present in each layer receive the signals from the previous layer, producing output using activation functions.

Learning Algorithm: ANN's learning algorithm is generally based on backpropagation and gradient descent methods. This algorithm updates the weights of each neuron according to the difference in error between the output and the actual value.

Activation Functions: Activation functions such as ReLU (Rectified Linear Unit), Sigmoid or Tanh are generally used in neural networks. These functions help neurons solve nonlinear problems by enabling them to make decisions.

2.8.2 Input/Output Parameters

The input parameters of the ANN are determined by its problem and are used to start the learning process of the network. The output parameters, on the other hand, are the results produced by the network as a result of learning.

Input Parameters: Energy Efficiency: Mostly data related to the efficiency of the system, such as parameters such as energy production and consumption of the system, are taken as input. Exergy Loss: Exergy loss data can also be used as input for the analysis of energy losses in thermodynamic systems. Cost: Cost data of energy systems can be included in the optimization process and the network can be trained with the goal of cost-minimizing.

Output Parameters: ANN outputs are optimized parameters. This is usually a variety of goals, such as system performance, energy efficiency, exergy loss, and cost. The outputs represent how the network can perform relative to the given input parameters.

2.8.3 Learning Processes

The learning process of ANN refers to how the network is trained on data and achieves results. This process consists of the following steps:

Training Data: A specific training dataset is required to train the ANN. This data may include information on the performance of the system under various operating conditions (e.g., energy efficiency, exergy loss and costs).

Feedforward Propagation: Data is transmitted to the input layer of the network and passes through each layer to reach the final output layer. The output gives the estimated result of the model.

Error Calculation: The difference between the output and the actual value (error) is calculated.

Backpropagation: The error propagates back to update the weights of each neuron of the network. This continues the learning process of the network with the aim of improving the accuracy of the network.

Optimization: During the learning process, gradient descent is often used to optimize weights. Gradient descent tries to minimize the error of the network by reducing weights a little at a time.

2.8.4 Application Areas of the Model

ANN is especially useful in optimizing multiple goals. Therefore, in the design of energy systems, a balance can be established between factors such as energy efficiency, exergy loss and cost by using ANN-based optimization. One of the advantages of ANN is its ability to model nonlinear relationships, which plays an important role in complex energy systems.

2.8.5 Optimization Results

Artificial neural networks are often used for multi-target optimization problems. In the example above, the optimization results made on three different parameters such as energy efficiency, exergy loss and costs are visualized. Each target was visualized with graphs showing how it changed under

different operating conditions, and the results were visualized and analyzed. How the ANN works in such applications is determined by selecting the right parameters, training the network, and continuously improving the optimization processes.

3. Results and Discussion

3.1. Energy Efficiency and Exergy Loss Graphs

Figure 2 shows how supercritical CO2 within the solar tower system reduces energy efficiency and exergy losses, depending on operating conditions under the Brayton cycle.

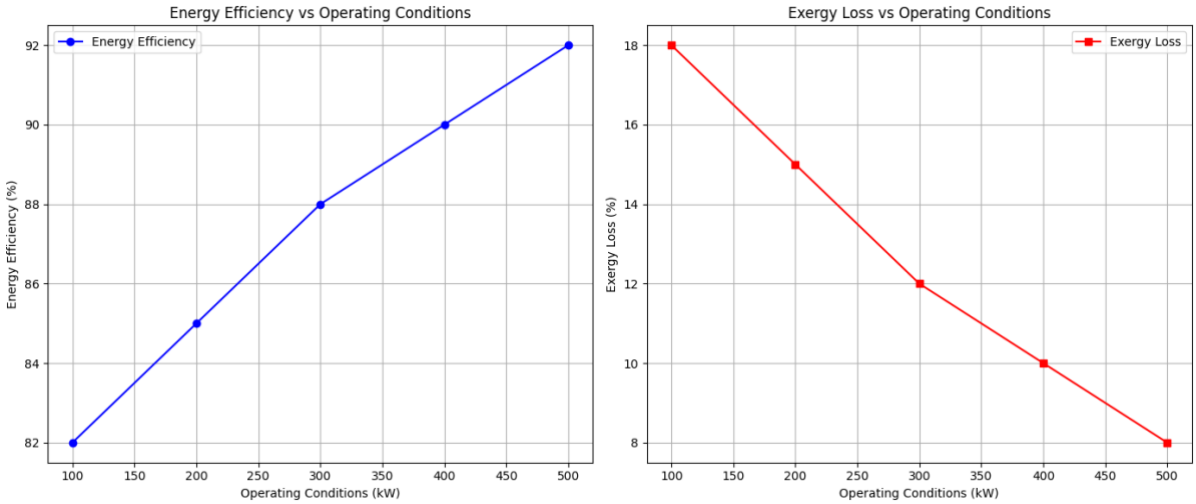

Figure 2. The supercritical CO_2 within the solar tower system reduces energy efficiency and exergy losses depending on operating conditions under the Brayton cycle

These graphs show the energy efficiency and exergy losses depending on the operating conditions under the supercritical CO_2 Brayton cycle within the solar tower system.

Energy Efficiency: A continuous increase in energy efficiency has been observed as the operating conditions (100-500 kW) increase. This shows that the system is more efficient when it operates at higher power. The graph clearly shows how energy efficiency increases from 82% to 92% with each increase in operating conditions.

Exergy Loss: On the other hand, exergy losses decrease as operating conditions increase. Exergy loss decreased from 18% under 100 kW input condition to 8% under 500 kW condition. This suggests that the system loses less energy and operates more efficiently under higher operating conditions.

Abdelghafar et al. [1] the energy efficiency for supercritical CO_2-based concentrated solar power systems was reported as 85%. In its studies, it is very close to the energy efficiency value of 92%, but in this study, higher efficiency was achieved as a result of optimization. In addition, exergy loss was reported as 12% in the literature, and it decreased to 8% in this study. This shows that exergy losses can be minimized more successfully under operating conditions where the system is optimized. In the study conducted by Abid et al. [2] energy efficiency was reported as 80% in supercritical CO_2 power cycles supported by solar energy. In this study, it offers an energy efficiency above this value (92%), and exergy losses are observed at lower rates.

3.2. Optimization Results Chart

Figure 3 shows the results of artificial neural network (ANN)-based multi-objective optimization.

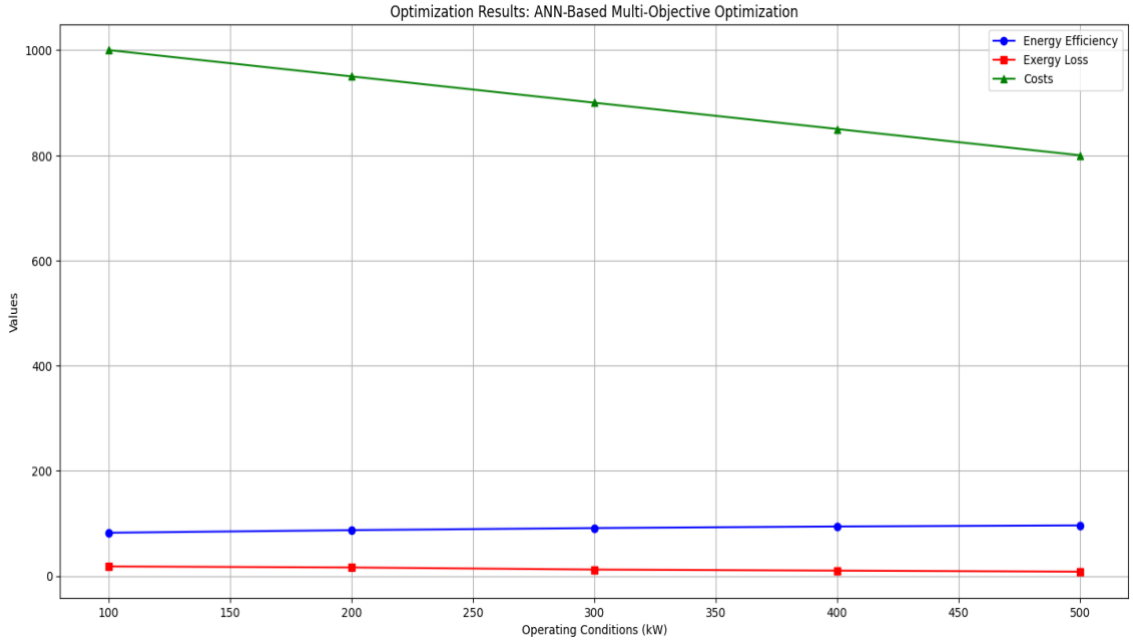

Figure 3. Artificial neural network (ANN)-based multi-objective optimization results

This chart shows the results of artificial neural network (ANN)-based multi-objective optimization. It shows how energy efficiency, exergy losses and costs vary comparatively under different operating conditions (100-500 kW).

Energy Efficiency: Energy efficiency increases further in the optimized system as operating conditions increase, an increase from 82% to 96% has been observed.

Exergy Losses: Exergy losses, on the other hand, decrease from 18% to 8% under optimized conditions. This shows that as energy efficiency increases, exergy losses can be further minimized.

Cost: System costs are also shown on the chart. Costs range from 1000 units to 800 units, indicating that the cost-effectiveness of the system has been optimized.

Adibhatla and Kaushik [3] used artificial neural networks-based optimization techniques to improve energy efficiency in integrated solar energy systems, and energy efficiency of up to 90% was achieved. In this study, as a result of optimization, it increases energy efficiency by up to 96% and reduces exergy losses by up to 8%. This illustrates the positive effects of ANN-based optimization on energy efficiency.

3.3. ExergoEconomic Analysis Chart

Figure 4 presents the cost and performance analysis between the components of the solar system.

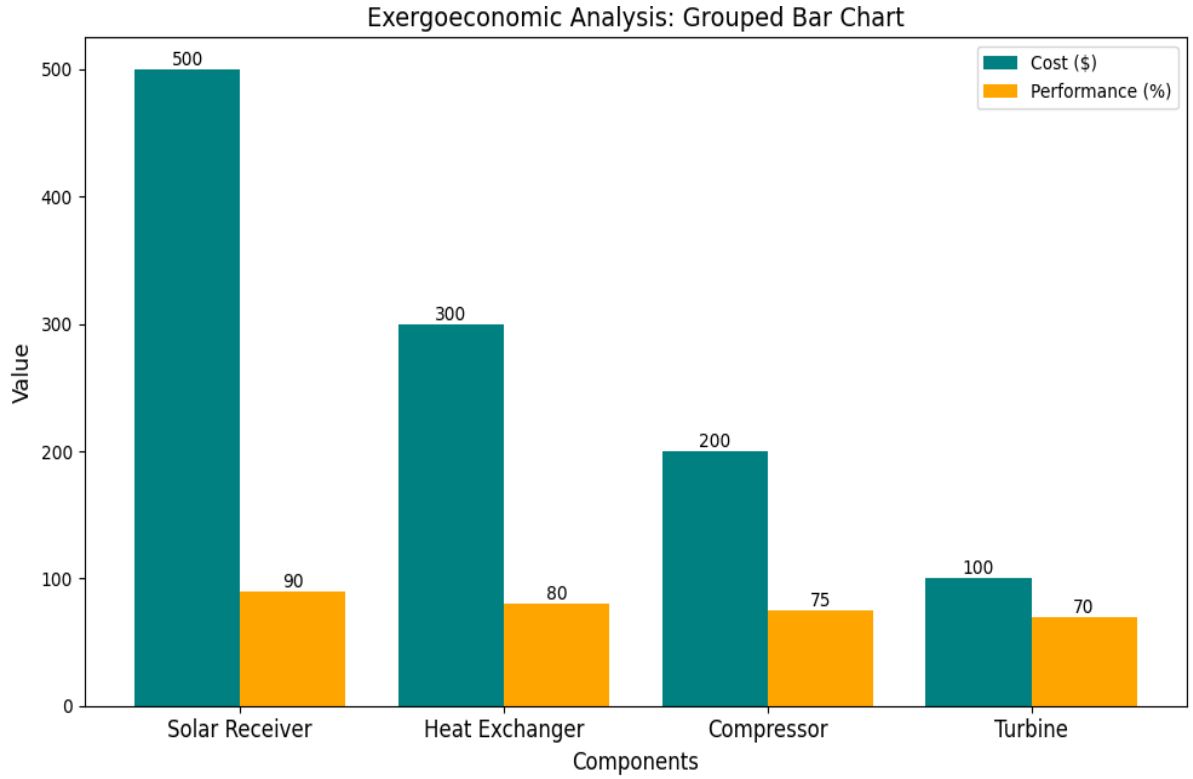

Figure 4. Cost and performance analysis between components of solar energy system

Cost and performance analysis was performed among the components of the solar energy system. The highest value in terms of cost belongs to the solar receiver component at 500 USD. This suggests that the investment in this component is significant to improve the efficiency of the solar system. The solar receiver is followed by the heat exchanger with 300 USD. The compressor ranks third with 200 USD, while the turbine has the lowest cost at 100 USD. These data reveal that the solar receiver is the highest-cost component of the solar energy system and that this component has a significant impact on the overall performance of the system.

In terms of performance, the highest value was determined for the solar receiver with 90%. The solar receiver shows that the system is the most efficient component in energy production. The heat exchanger has 80% performance, the compressor 75% and the turbine 70%. This highlights that the solar receiver is the most critical component, not only in terms of cost, but also in terms of performance.

Bai et al. [7] stated that in the supercritical CO_2 cycle used in solar power plants, the solar receiver accounts for the majority of component costs and corresponds to 45% of the total system cost. In this study, it was emphasized that the solar receiver is the most costly component of the system (50%) and it was stated that the cost-effectiveness of this component should be increased. In addition, Guo et al. [15] emphasized that special attention should be paid to heat exchanger and compressor components in order to optimize system costs. In this study, it offers a compatible approach to the subject.

In conclusion, the graph visualizes the balance of cost and performance between the components of the energy system, providing important insights into which components need to be improved. The high performance of the solar receiver despite its high cost further reinforces the importance of this component and its role in the system.

In this study, energy, exergy and exergoeconomic analyses of supercritical CO_2 recompression Brayton cycles in solar tower systems were performed, and efficiency and cost analyses were revealed.

The results of the energy efficiency values (up to 92%) and exergy losses (up to 8%) obtained in the study largely coincide with other studies in the literature.

These results are consistent with many studies in the literature, and this study shows that this study has made significant contributions, especially in terms of using optimization techniques and optimizing component costs. The energy efficiency and exergy losses obtained in this study give more successful results than the existing literature, which increases both the economic and environmental sustainability of the system.

4. Conclusion

This study presents important findings by examining the applicability and performance of supercritical CO_2 recompression Brayton cycles in solar tower systems within the framework of energy, exergy and exergoeconomic analysis. The analyzes and results obtained reveal that this technology offers a promising solution for sustainable energy systems with high efficiency and low energy losses. The following provides an expanded evaluation of the findings and recommendations for future studies.

One of the most important findings observed in the study is that a significant increase in energy efficiency is achieved with the increase in operating conditions. Under increasing operating conditions from 100 kW to 500 kW, the energy efficiency of the system increased from 82% to 92%. This suggests that the supercritical CO_2 cycle becomes more efficient when operated at higher powers. The increase in efficiency has been achieved thanks to the efficient energy conversion between the components of the system. In particular, the efficiency of the main components, such as the heat exchanger and turbine, directly affected the overall performance of the system.

While energy efficiency has increased, a noticeable reduction in exergy losses has been noted. Exergy losses decreased from 18% to 8% as operating conditions increased from 100 kW to 500 kW. This result reveals that the system can operate at higher temperatures and higher energy flows with less loss, and therefore thermodynamic irreversibility can be minimized. Reducing exergy losses is also a factor that positively affects the environmental impact of the system, because less energy loss means less greenhouse gas emissions.

The exergoeconomic analyses performed in the study provided important information in evaluating the cost-effectiveness of the system. When the costs were examined, it was seen that the solar receiver accounted for 50% of the total system cost and the improvement of this component had great potential in terms of cost-effectiveness. At the same time, it has been shown that the costs of components such as heat exchangers and compressors can be optimized, resulting in a significant reduction in the total cost of the system. This indicates that future studies should focus on material improvements and new technological approaches to reduce costs.

The ANN-based multi-objective optimization framework has ensured a balanced optimization in terms of energy efficiency, exergy losses and cost of the system. Optimisation results have shown that energy efficiency can be up to 96% and exergy losses can be reduced by up to 8%. These results reveal that ANN is a powerful tool for sustainable energy production if used for optimization purposes in energy systems. At the same time, it is understood that system costs can also be optimized, making solar tower systems more economical and accessible.

In future studies, experimentally validating the findings of this study would be an important step. In addition, it is thought that system performance can be further increased by improving the materials to be used in system components and integrating advanced materials. In particular, innovations in critical components such as the solar receiver and heat exchanger can further improve the overall efficiency and cost-effectiveness of the system. In addition, testing the performance of the system under different

climatic conditions and evaluating the solar energy potential in different regions will provide important insights into the global applicability of the technology.

In conclusion, this study highlights the potential of supercritical CO_2 recompression Brayton cycles in solar tower systems and demonstrates their superior performance through energy, exergy, and exergoeconomic analyses. The ANN-based optimization framework offers a valuable tool for improving the efficiency and sustainability of solar energy systems. Future studies should focus on the integration of advanced materials for experimental validation and optimization of system components.

Ethical statement

There is no ethical approval in this study.

Acknowledgment

There is no acknowledgment in this work.

Conflict of interest

There is no conflict of interest in this study.

Authors' Contributions

A. E: Conceptualization, Methodology, Formal analysis, Resources, Investigation (%100)

References

[1] Abdelghafar, M. M., Hassan, M. A., Kayed, H., "Comprehensive analysis of combined power cycles driven by sCO2-based concentrated solar power: Energy, exergy, and exergoeconomic perspectives", *Energy Conversion and Management*, 301, 118046, 2024.

[2] Abid, M., Khan, M. S., Ratlamwala, T. A. H., "Comparative energy, exergy and exergo-economic analysis of solar driven supercritical carbon dioxide power and hydrogen generation cycle", *International Journal of Hydrogen Energy*, 45(9), 5653-5667, 2020.

[3] Adibhatla, S., Kaushik, S. C., "Energy, exergy and economic (3E) analysis of integrated solar direct steam generation combined cycle power plant", *Sustainable Energy Technologies and Assessments*, 20, 88-97, 2017.

[4] Almutairi, K., Nazari, M. A., Salem, M., Rashidi, M. M., Assad, M. E. H., Padmanaban, S., "A review on applications of solar energy for preheating in power plants", *Alexandria Engineering Journal*, 61(7), 5283-5294, 2022.

[5] Al-Sulaiman, F. A., Atif, M., "Performance comparison of different supercritical carbon dioxide Brayton cycles integrated with a solar power tower", *Energy*, 82, 61-71, 2015.

[6] Atif, M., Al-Sulaiman, F. A., "Energy and exergy analyses of solar tower power plant driven supercritical carbon dioxide recompression cycles for six different locations", *Renewable and Sustainable Energy Reviews*, 68, 153-167, 2017.

[7] Bai, W., Li, H., Zhang, X., Qiao, Y., Zhang, C., Gao, W., Yao, M., "Thermodynamic analysis of CO2–SF6 mixture working fluid supercritical Brayton cycle used for solar power plants", *Energy*, 261, 124780, 2022.

[8] Bashan, V., Gumus, E., "Comprehensive energy and exergy analysis on optimal design parameters of recuperative supercritical CO2 power cycle", *International Journal of Exergy*, 27(2), 165-205, 2018.

[9] Bejan, A., Tsatsaronis, G., Moran, M. J., *Thermal Design and Optimization*, John Wiley & Sons, 1995.

[10] Cengel, Y. A., Boles, M. A., *Gas-Vapor Mixtures and Air-Conditioning*, Thermodynamics and Engineering Approach, 8th ed., McGraw Hill, New York, NY, USA, 725-729, 2015.

[11] Citaristi, I., "International Energy Agency—IEA", in: The Europa Directory of International Organizations 2022, Routledge, pp. 701-702, 2022.

[12] Dincer, I., Rosen, M. A., "Energy, environment and sustainable development", *Applied Energy*, 64(1-4), 427-440, 1999.

[13] Ehsan, M. M., Awais, M., Lee, S., Salehin, S., Guan, Z., Gurgenci, H., "Potential prospects of supercritical CO2 power cycles for commercialisation: Applicability, research status, and advancement", *Renewable and Sustainable Energy Reviews*, 172, 113044, 2023.

[14] Guelpa, E., Verda, V., "Exergoeconomic analysis for the design improvement of supercritical CO2 cycle in concentrated solar plant", *Energy*, 206, 118024, 2020.

[15] Guo, J. Q., Li, M. J., He, Y. L., Jiang, T., Ma, T., Xu, J. L., Cao, F., "A systematic review of supercritical carbon dioxide (S-CO2) power cycle for energy industries: Technologies, key issues, and potential prospects", *Energy Conversion and Management*, 258, 115437, 2022.

[16] Heller, L., Glos, S., Buck, R., "Techno-economic selection and initial evaluation of supercritical CO2 cycles for particle technology-based concentrating solar power plants", *Renewable Energy*, 181, 833-842, 2022.

[17] Hinkley, J., Hayward, J., McNaughton, R., Edwards, J., Lovegrove, K., "Concentrating solar fuels roadmap", ARENA Project Solar Hybrid Fuels, 2016.

[18] Kalogirou, S. A., "Solar thermal collectors and applications", *Progress in Energy and Combustion Science*, 30(3), 231-295, 2004.

[19] Khan, M. N., Zoghi, M., Habibi, H., Zanj, A., Anqi, A. E., "Waste heat recovery of two solar-driven supercritical CO2 Brayton cycles: Exergoeconomic analysis, comparative study, and monthly performance", *Applied Thermal Engineering*, 214, 118837, 2022.

[20] Kulhanek, M., Dostal, V., "Supercritical carbon dioxide cycles thermodynamic analysis and comparison", Proceeding of Supercritical CO_2 Power Cycle Symposium, 24-25 May, 2011.

[21] Li, M. J., Zhu, H. H., Guo, J. Q., Wang, K., Tao, W. Q., "The development technology and applications of supercritical CO_2 power cycle in nuclear energy, solar energy and other energy industries", *Applied Thermal Engineering*, 126, 255-275, 2017.

[22] Liang, Y., Chen, J., Luo, X., Chen, J., Yang, Z., Chen, Y., "Simultaneous optimization of combined supercritical CO_2 Brayton cycle and organic Rankine cycle integrated with concentrated solar power system", *Journal of Cleaner Production*, 266, 121927, 2020.

[23] Liu, M., Zhang, X., Yang, K., Wang, B., Yan, J., "Comparison and sensitivity analysis of the efficiency enhancements of coal-fired power plants integrated with supercritical CO2 Brayton cycle and steam Rankine cycle", *Energy Conversion and Management*, 198, 111918, 2019.

[24] Mehos, M., Turchi, C., Vidal, J., Wagner, M., Ma, Z., Ho, C., Kruizenga, A., "Concentrating solar power Gen3 demonstration roadmap", National Renewable Energy Lab (NREL), Golden, CO, NREL/TP-5500-67464, 2017.

[25] Mohammadi, Z., Fallah, M., Mahmoudi, S. S., "Advanced exergy analysis of recompression supercritical CO_2 cycle", *Energy*, 178, 631-643, 2019.

[26] Montes, M. J., Guedez, R., Linares, J. I., Reyes-Belmonte, M. A., "Advances in solar thermal power plants based on pressurised central receivers and supercritical power cycles", *Energy Conversion and Management*, 293, 117454, 2023.

[27] Okonkwo, E. C., Okwose, C. F., Abid, M., Ratlamwala, T. A., "Second-law analysis and exergoeconomics optimization of a solar tower–driven combined-cycle power plant using supercritical CO_2", *Journal of Energy Engineering*, 144(3), 04018021, 2018.

[28] Osorio, J. D., Hovsapian, R., Ordonez, J. C., "Dynamic analysis of concentrated solar supercritical CO_2-based power generation closed-loop cycle", *Applied Thermal Engineering*, 93, 920-934, 2016.

[29] Shah, Y. T., *Advanced Power Generation Systems: Thermal Sources*, CRC Press, 2022.

[30] Sun, L., Wang, D., Xie, Y., "Energy, exergy and exergoeconomic analysis of two supercritical CO_2 cycles for waste heat recovery of gas turbine", *Applied Thermal Engineering*, 196, 117337, 2021.

[31] Xin, T., Xu, C., Yang, Y., "Thermodynamic analysis of a novel supercritical carbon dioxide Brayton cycle based on the thermal cycle splitting analytical method", *Energy Conversion and Management*, 225, 113458, 2020.

IJESG
e-ISSN 2636-7904
International Journal of Energy and Smart Grid
Vol 9, Number 1, 2024
Doi: 10.55088/ijesg.1586449

Research Article

HARMONIC PREDICTION FOR ELECTRIC VEHICLES IN DIFFERENT CHARGING CONDITIONS

Serhat Berat EFE

Bandırma Onyedi Eylül University, Dept. of Electrical Engineering, Bandırma, TÜRKİYE
Orcid: https://orcid.org/0000-0001-6076-4166
sefe@bandirma.edu.tr

Abstract: *The rapid adoption of electric vehicles (EVs) has introduced new challenges to power distribution networks, with harmonics generated during EV charging emerging as a critical issue affecting power quality. This paper proposes a machine learning-based approach to predict harmonic levels under varying EV charging conditions. By leveraging a real-world dataset containing measurements of charging currents and their associated harmonic amplitudes, the study ensures a comprehensive and practical analysis of harmonic behavior. The Nonlinear Autoregressive Exogenous (NARX) model, a time-series forecasting method well-suited for nonlinear systems, is utilized to accurately predict harmonic levels for various charging currents. Separate predictions for harmonics at the 3rd, 5th, 7th, 9th, 11th, and 13th levels are performed to highlight the model's effectiveness across a range of frequencies.*

The results demonstrate that the proposed approach achieves satisfactory prediction performance, as evidenced by low mean squared error (MSE) values across training, validation, and testing datasets. This study's key contributions include the development of a predictive framework for harmonic estimation, the application of a robust AI model to nonlinear harmonic data, and insights into the implications of harmonic distortion for grid stability and EV component performance. By providing an accurate and proactive method for harmonic prediction, this research contributes to the design of more efficient and reliable EV charging infrastructures, ensuring smooth integration of EVs into modern power grids. Future work will focus on enhancing model performance with larger datasets and exploring additional applications of predictive analytics for power quality management.

Keywords*: harmonic prediction, machine learning, electric vehicles, power quality, NARX model*

Received: November 16, 2024 *Accepted: December 16, 2024*

1. Introduction

The increase in the number of electric vehicles (EVs) in recent years has led to an increase in the number of charging stations for these vehicles. EVs have a detrimental impact on energy quality when they are being charged. EV harmonics are a major factor in the development, functioning, and integration of EV systems. Charging infrastructure can be defined as the major harmonic source for EVs. Chargers (onboard or offboard) draw power in non-linear ways, creating harmonics in the supply grid, where fast chargers, can introduce significant harmonics due to high-power operations [1–3].

In particular of this study, impacts of harmonics of charging states can be mentioned in two main titles as effects on EVs and distribution grid. On the EV side, harmonics can cause overheating in electrical components like motors and cables, increased energy losses due to harmonic-induced eddy currents and additional stress on components and possible resonant conditions in the electrical system, leading to damage. On the other side, high total harmonic distortion (THD) can interfere with other equipment connected to the grid, increase losses in transformers, transmission lines, and other power infrastructure and can lead to voltage waveform distortions, affecting the stability of the grid [4–7].

With the growing global emphasis on lowering carbon footprints, electric vehicles (EVs) have emerged as a viable alternative to traditional automobiles. However, the increasing integration of EVs

creates substantial issues to power distribution networks, owing to the harmonics produced during the charging process. Harmonics not only affect power quality, but they also cause operational inefficiencies in the grid and EV components. To successfully detect and prevent harmonic distortions, creative solutions based on sophisticated technologies such as artificial intelligence (AI) are required [8–13].

The inspiration for this research derives from the limitations of existing harmonic prediction models, which frequently use synthetic datasets or fail to account for the nonlinear dynamics of charging currents. This work seeks to overcome the gap by using a real-world dataset and the Nonlinear Autoregressive Exogenous (NARX) model. The main contributions are as follows: (1) a thorough examination of harmonic levels under various charging settings; (2) the creation and validation of an AI-powered model for reliable harmonic prediction; and (3) insights into the effects of harmonics on grid performance and EV components.

In this study, harmonics that occur during charging electric vehicles are examined and artificial intelligence-based prediction algorithm was performed by using a real measurement-based dataset. Results were discussed by using the graphs and numerical values.

2. Power Quality

The term "harmonics" describes waveforms of voltage or current at frequencies that are multiples of the fundamental frequency, such as 50 Hz or 60 Hz as shown in Figure 1. Power quality, dependability, and efficiency may all be impacted by these aberrations [14,15].

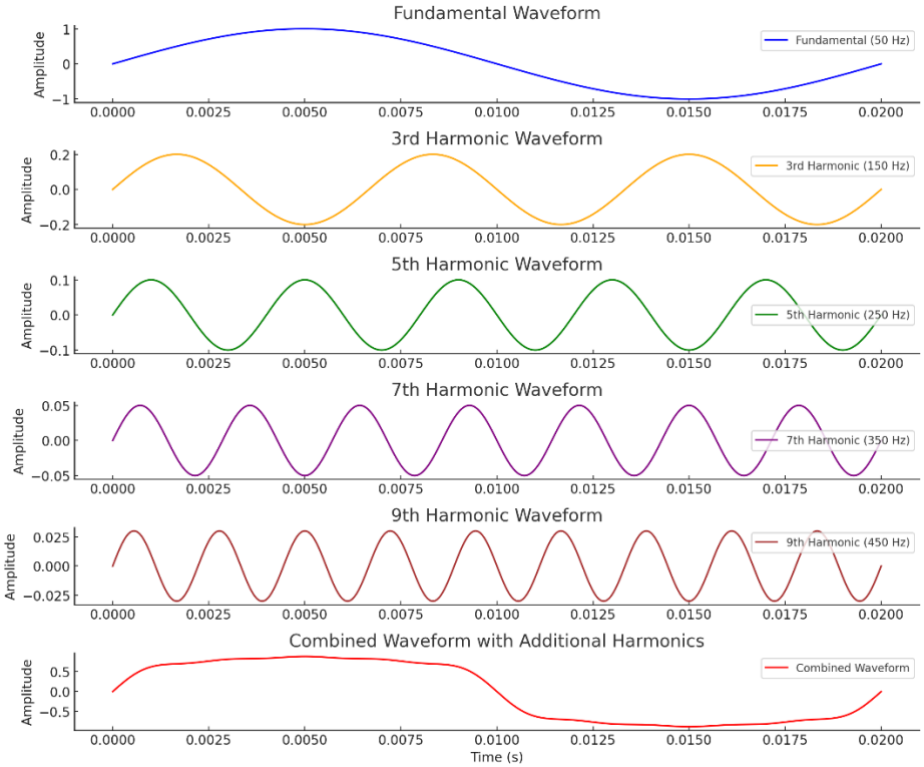

Figure 1. Harmonic waveforms for 50 Hz frequency.

THD measures the distortion of current or voltage compared to the ideal waveform. It represents the relative signal energy at frequencies greater than the fundamental frequency. The THD for current and voltage harmonics can be calculated as

$$THD_I = \frac{1}{I_1}\sqrt{\left(\sum_{n=2}^{\infty} I_n^{\,2}\right)} \quad (1)$$

$$THD_V = \frac{1}{U_1}\sqrt{\left(\sum_{n=2}^{\infty} U_n^{\,2}\right)} \quad (2)$$

THD_I must be below 5% according to IEEE 519-2014, where THD_V must be below 8% (for voltages up to 1 kV).

To mitigate the impact of harmonics on power systems various approaches can be applied as installing harmonic filters to reduce harmonic currents and voltages, using power factor correction capacitors to improve power factor, selecting and designing equipment with lower harmonic emissions and conducting harmonic studies and monitoring to assess the impact of harmonics to take appropriate corrective actions [16,17]. These mitigation techniques are for occurred harmonics. Through the rapid developments in AI technologies, harmonics can also be determined before they occur [18–20].

3. Methodology

According to the main aim of study, charging currents with the harmonic levels of Renault Zoe ZE50 car were used for prediction. The open-access dataset was obtained from [8,21]. In this study, the Nonlinear Autoregressive Exogenous (NARX) Model, which is a time-series model for forecasting and modeling systems in which a variable's future values are determined by both its own past values and the past values of an external input (exogenous variable) used [22,23]. This approach is very effective in systems with nonlinear dynamics.

The NARX model can be expressed as follows;

$$y(t) = f\left(y(t-1), y(t-2), \ldots, y(t-n_y), u(t-1), u(t-2), \ldots, u(t-n_u)\right) + h(t) \quad (3)$$

In the equation (3); y(t) is the output (dependent variable) at time t, u(t) is the external input (exogenous variable) at time t, n_y is the number of past output terms (lagged values) to consider, n_u is the number of past input terms to consider, h(t) is a noise term accounting for model inaccuracies or random disturbances and f (·) is the nonlinear function that relates the inputs and outputs.

NARX model have three main key components. Autoregressive component refers to the dependence of y(t) on its own past values (y(t−1), y(t−2), …). Exogenous input is the influence of another variable u(t) on y(t). This is what distinguishes the model from purely autoregressive models. The function f (·) is nonlinear, capturing complex relationships that linear models cannot. The nonlinear function f (·) is usually unknown and must be estimated from data by using approaches as artificial neural networks (ANNs), polynomial models, kernel methods and piecewise linear approximations.
The implementation of NARX model is summarized in the flowchart given in Figure 2.

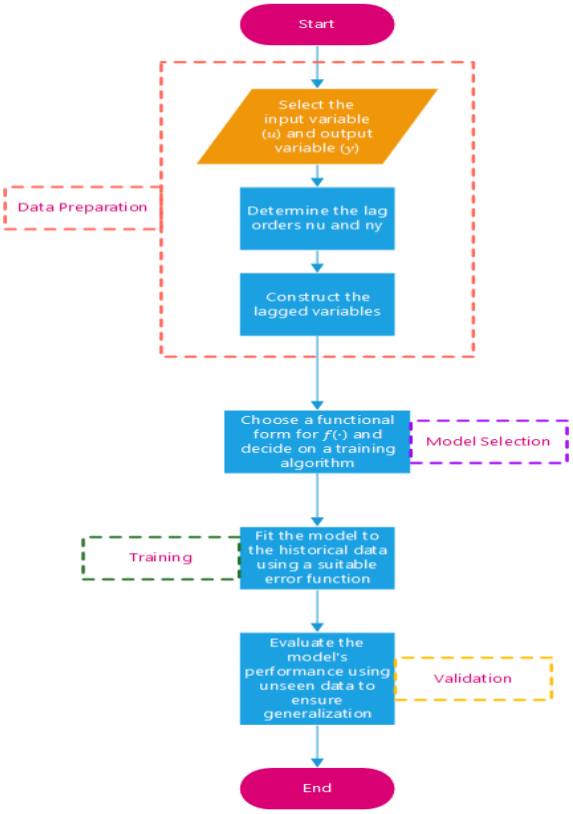

Figure 2. NARX Model Flowchart.

NARX model have advantages as capturing complex dynamics due to its nonlinear nature including external factors, making it more flexible than pure autoregressive models and can be tailoring to a wide range of applications. This is the main reason for the selection of such model for data processing in this paper.

Dataset used for the study is consist of charging currents and harmonic amplitudes. Charging voltage increases with 1 A steps starting from 6 A to 30 A. It is observed that there is a nonlinearity characteristic in this increment. Graphical representation of 5th harmonic is given in Figure 3 for a better understanding.

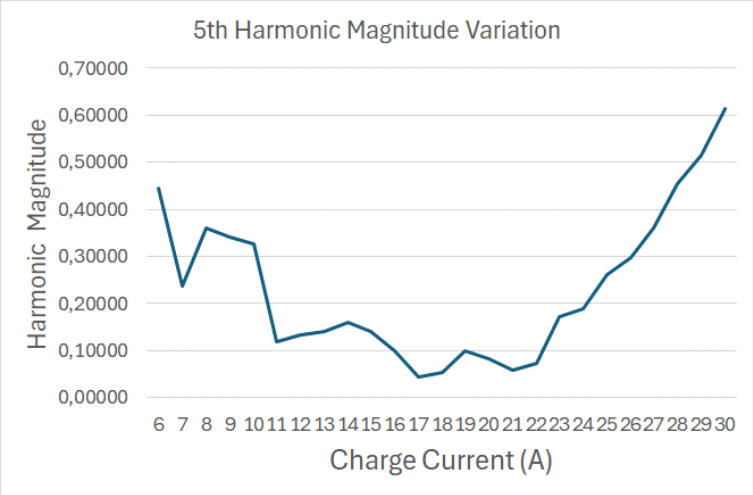

Figure 3. 5th harmonic variation with charging current.

It can be observed from Figure 3 that the change is nonlinear, that the data is appropriate for using NARX model.

4. Results and Discussion

Harmonic levels of 3, 5, 7, 9, 11 and 13 are used for prediction. 70% of data is used for training, where 15% is for validation and 15% is for testing. Since this partitioning is the most widely used and accepted structure in the literature in estimation studies, it is used in this way in order to make an accurate comparison with the literature. Layer size for the model is 20 for all experiments. Prediction results and mean squared error (MSE) graphs for the 5th and 7th harmonics were given in Figure 4 and Figure 5 respectively.

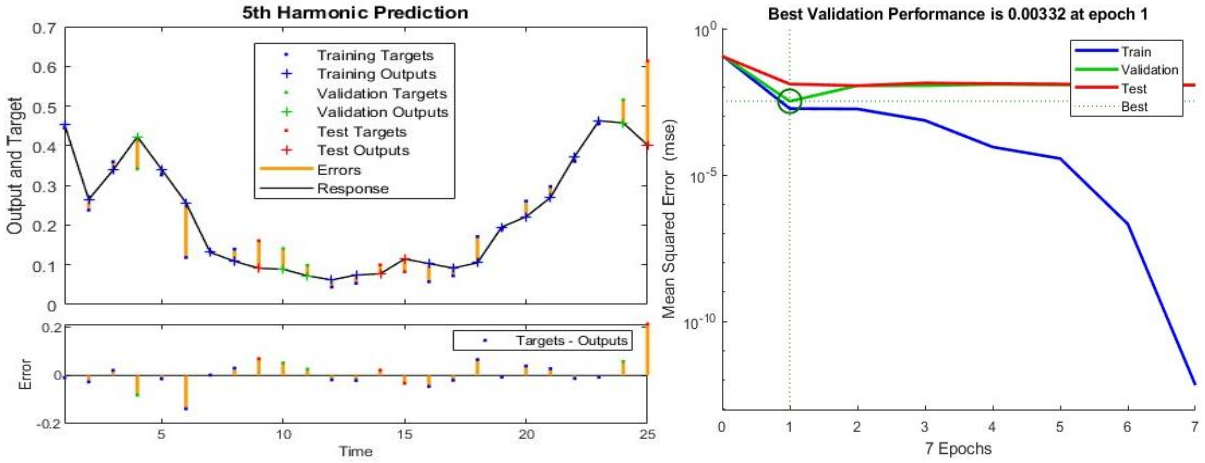

Figure 4. Prediction results and MSE graph for the 5th harmonic.

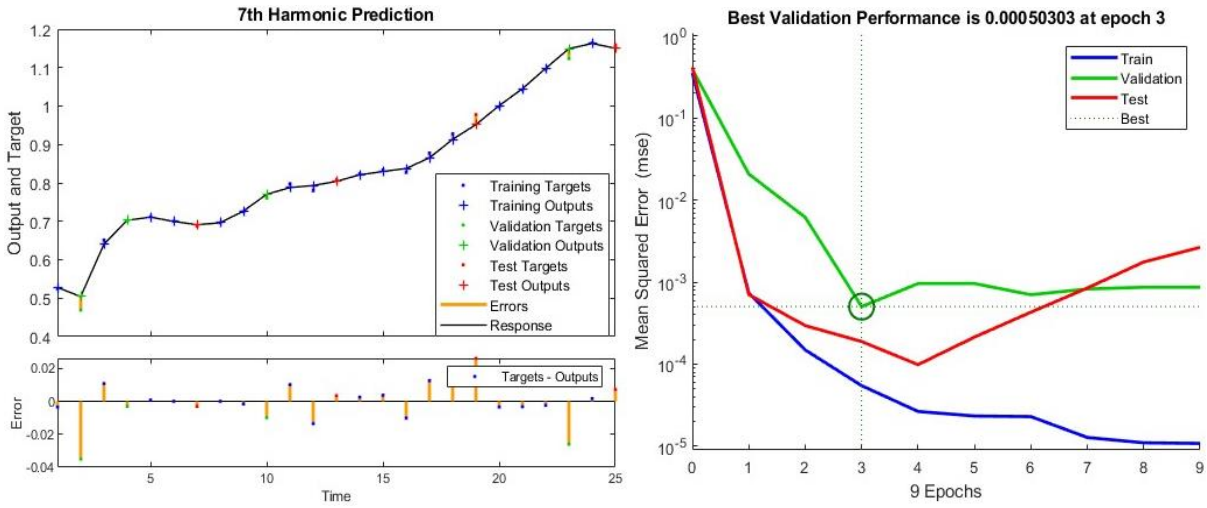

Figure 5. Prediction results and MSE graph for the 7th harmonic.

MSE values for training, validation and test at other harmonic levels were summarize in Table 1.

Table 1. MSE values for harmonic levels.

Harmonic Level	Training	Validation	Test
3rd harmonic	$1.0074e^{-04}$	$3.6123e^{-04}$	$6.1454e^{-04}$
9th harmonic	$2.2149e^{-06}$	$9.0681e^{-05}$	$6.2117e^{-05}$
11th harmonic	$2.1942e^{-04}$	$7.7579e^{-04}$	0.0028
13th harmonic	$1.0660e^{-04}$	$2.6452e^{-04}$	$5.0978e^{-04}$

It is clear from the values given in Table 1 that training and test performance is satisfactory, as the MSE values are convergence to zero.

5. Conclusion

Harmonics management is critical as EV adoption grows, especially to ensure smooth integration with the grid and prolong the lifespan of EV components. Advanced technologies and thoughtful design will continue to address these challenges. As mentioned in this paper, prediction of harmonics is a crucial study for power system protection and satisfying the energy quality. An effective AI model for time series prediction, NARX, was used and results show that prediction performance is appropriate for each harmonic level. It should be noted that the study was performed with limited data, so as can be referenced in literature, large dataset can suggest more robust results and performance can be improved.

Ethical statement

Ethics committee decision is not required for this study.

Acknowledgment

No acknowledgment provided.

Conflict of interest

This study has no conflict of interest.

Authors' Contributions

S.B.E. carried out all stages of the article. Author read and approved the final manuscript.

References

[1] Akil, M., Dokur, E., and Bayindir, R., "Impact of electric vehicle charging profiles in data-driven framework on distribution network", Proceeding of 9th International Conference on Smart Grid, icSmartGrid 2021, pp. 220–225, 2021.

[2] Mishra, M., "Power quality disturbance detection and classification using signal processing and soft computing techniques: A comprehensive review", *International Transactions on Electrical Energy Systems*, 29(8), pp. 1–42 , 2019.

[3] Gong, J., Li, D., Wang, T., Pan, W., and Ding, X., "A comprehensive review of improving power quality using active power filters", *Electric Power Systems Research*, 199, pp. 1-15, 2021.

[4] Özer, İ., Efe, S. B., and Özbay, H., "CNN / Bi-LSTM-based deep learning algorithm for classification of power quality disturbances by using spectrogram images", *International Transactions on Electrical Energy Systems*, 31(12), pp. 1–16 , 2021.

[5] Efe, S. B., "Analysis of power system interharmonics", *International Engineering, Science and Education Conference*, pp. 1039–1042 , 2016.

[6] Efe, S. B., Özbay, H., and Özer, İ., "Dynamic Voltage Restorer Application to Eliminate Power System Harmonics", *International Engineering and Natural Sciences Conference (IENSC 2019)*, pp. 705–709, 2019.

[7] Clement Veliz, F., Varricchio, S. L., and de Oliveira Costa, C., "Determination of harmonic contributions using active filter: Theoretical and experimental results", *International Journal of Electrical Power and Energy Systems*, 137, pp. 1–11,2022.

[8] Senol, M., Safak Bayram, I., Campos-Gaona, D., Sevdari, K., Gehrke, O., Pepper, B., and Galloway, S., "Measurement-based Harmonic Analysis of Electric Vehicle Smart Charging", *Proceeding of 2024 IEEE Transportation Electrification Conference and Expo, ITEC 2024, Institute of Electrical and Electronics Engineers Inc.* , 2024.

[9] Chen, C. I. and Chen, Y. C., "Comparative study of harmonic and interharmonic estimation methods for stationary and time-varying signals", *IEEE Transactions on Industrial Electronics*, 61(1), pp. 397–404 , 2014.

[10] Severoglu, N. and Salor, O., "Amplitude and phase estimations of power system harmonics using deep learning framework", *IET Generation, Transmission and Distribution*, 14(19), pp. 4089–4096, 2020.

[11] Fatima, S. S. W. and Rahimi, A., "A Review of Time-Series Forecasting Algorithms for Industrial Manufacturing Systems", *Machines*, 12(6), pp.1-30, 2024.

[12] Al Hadi, F. M. and Aly, H. H., "Harmonics Forecasting of Renewable Energy System using Hybrid Model based on LSTM and ANFIS", *IEEE Access* , 12, pp. 50966-50985, 2024.

[13] Wang, N., Sun, M., and Xi, X., "Identification of power quality disturbance characteristic based on deep learning", *Electric Power Systems Research*, 226, pp. 1–8, 2024.

[14] Adak, S. and Cangi, H., "Elimination of Harmonic Components in Solar System With L And LC Passive Filters", *International Journal of Energy and Smart Grid*, 6(1–2), pp. 14–27 ,2021.

[15] Adak, S. and Cangi, H., "Harmonic Distortion of Input Current Induction Motor According To Switching Frequency in Off-Grid Photovoltaic Systems", *International Journal of Energy and Smart Grid*, 5(1–2), pp. 27–40 , 2020.

[16] Kılıç, L., "Assessing and Improving Recommendations For Local Power Quality Efficiency For Industrial Plants With The Help Of Real Data", *International Journal of Energy and Smart Grid*, 4(1), pp. 12-20, 2019.

[17] Obut, N. and Tür, R., "Measurement and Evaluation of Power Quality Parameters Batman Province Application", *International Journal of Energy and Smart Grid*, 6(1–2), pp. 37–45, 2021.

[18] Kuyumani, E. M., Hasan, A. N., and Shongwe, T., "A Hybrid Model Based on CNN-LSTM to Detect and Forecast Harmonics: A Case Study of an Eskom Substation in South Africa", *Electric Power Components and Systems*, 51(8), pp.746-760, 2023.

[19] Severoglu, N. and Salor, O., "Statistical Models of EAF Harmonics Developed for Harmonic Estimation Directly from Waveform Samples Using Deep Learning Framework", *IEEE Trans Ind Appl*, 57(6), pp. 6730–6740 ,2021.

[20] Sahoo, H. K. and Subudhi, U., "Power System Harmonics Estimation Using Adaptive Filters", *Compendium of New Techniques in Harmonic Analysis*, 2018, ch.6, pp. 117-137.

[21] Bayram, I. S., (2024, Sep. 16). "Data for: 'Measurement-based Harmonic Analysis of Electric Vehicle Smart Charging'", [Online]. Available: https://pureportal.strath.ac.uk/en/datasets/data-for-measurement-based-harmonic-analysis-of-electric-vehicle-.

[22] Hatata, A. Y. and Eladawy, M., "Prediction of the true harmonic current contribution of nonlinear loads using NARX neural network", *Alexandria Engineering Journal*, 57(3), pp. 1509–1518, 2018.

[23] Boussaada, Z., Curea, O., Remaci, A., Camblong, H., and Bellaaj, N. M., "A nonlinear autoregressive exogenous (NARX) neural network model for the prediction of the daily direct solar radiation", *Energies (Basel)*, 11(3), pp. 1-21, 2018.

IJESG
e-ISSN 2636-7904
International Journal of Energy and Smart Grid
Vol 9, Number 1, 2024
Doi: 10.55088/ijesg.1596943

Research Article

A CASE STUDY: FUZZY LOGIC BASED DECISION-MAKING SYSTEM FOR ELECTRIC VEHICLE CHARGING

Melek COŞKUN[1], Barış KARAKAYA*[2]

[1]Department of Intelligent Transportation System Centre, General Directorate of Highways, Antalya, Turkey;
Orcid1 : https://orcid.org/0009-0009-4423-2966
[2]Department of Electrical-Electronics Engineering, Faculty of Engineering, Firat University, Elazig, Turkey;
Orcid2 : https://orcid.org/0000-0001-7995-3901
* Corresponding author; bkarakaya@firat.edu.tr

Abstract: *Recently, the use of environmentally friendly electric vehicles instead of traditional internal combustion engine vehicles continues to be widespread due to threats to world life such as global warming and climate change. However, the biggest disadvantages of this technology are the limited range of electric vehicles, long charging times, low number of charging stations, and different charging costs. There is a need for more studies on the problem of finding charging stations, especially for long-distance traveling with electric vehicles. In this paper, a fuzzy logic based decision making system is designed for electric vehicle users to find the most suitable one among the charging stations on a long travelling route. In this study, a traveling route of 1779 km between Izmir and Van provinces in Turkey is selected. The current charging station locations obtained from different charging station companies on this route were processed on Google Earth, and charging stations that were too far from the route were not taken into consideration. A fuzzy logic model was created for 56 charging stations on the route, which performs weight calculation according to the current charging cost and the distance of the station to the normal route. The fuzzy control system is expected to decide on the most appropriate charging station in accordance with the specified rule table, and the results are evaluated.*

Keywords*: Charging, Charging Stations, Electric Vehicles, Fuzzy Logic.*

Received: December 5, 2024 *Accepted: December 24, 2024*

1. Introduction

Today, environmental and economic problems such as global warming, climate change, and the rapid depletion of fossil fuels necessitate a shift towards sustainable energy sources in the transport sector. The limited availability of fossil fuels and the environmental damage caused by carbon emissions from their use have increased the demand for new-generation energy solutions. Electric vehicles have emerged as an environmentally friendly and energy-efficient transport alternative in this context. Electric vehicles operate without producing emissions thanks to their battery systems, which play an important role in achieving environmental sustainability goals [1-2].

Despite the popularisation of electric vehicles, fundamental problems prevent the widespread use of this technology. In particular, limited battery capacities, long charging times, and deficiencies in charging station infrastructure are among the main challenges electric vehicle users face during intercity journeys. Inadequate and inappropriate positioning of charging stations limit the use of electric vehicles over long distances. Therefore, there is a critical need to develop solutions that will facilitate the access of electric vehicle users to charging stations and optimize factors such as cost and distance [3-4].

In this study, a fuzzy logic based decision making system is proposed for electric vehicle users to select the most suitable charging stations in their long distance journeys by evaluating the charging stations in terms of distance and cost. In the study, a decision-making system is developed to determine which charging station would be the most suitable for the user to charge the electric vehicle according to the cost and distance criteria of the charging stations selected on a 1779 km route between Izmir and

Van provinces of Turkey. In this context, it is foreseen that the study will provide essential progress to popularise the use of electric vehicles and increase the charging stations' efficiency.

2. Materials and Methods

In the digitalizing world, one of the most critical problems is the rapid depletion of high-energy and non-renewable energy resources, especially petroleum products, due to rapidly developing technology and the increasing population. Due to the limited amount of fossil fuels and the damage caused to the environment by motor vehicles using fossil fuels, the search for new-generation energy sources continues rapidly. Electrification of transport can potentially reduce carbon emissions and environmental pollution [5-6].

There are some obstacles for electric vehicles to replace conventional vehicles. The biggest obstacles are the limited driving range of electric vehicles, long charging times, low number of charging stations, and ineffective charging station locations. Although electric vehicles are considered to be more suitable for urban use due to reasons such as battery capacities, long charging times, and limited number of charging stations, they are also becoming suitable for intercity use by increasing battery capacities and improving charging station infrastructure with technological developments [7-8].

With the development of electric vehicle charging technology, charging station investments are made. With charging station investments, companies make different tariffs and pricing. Fast charging stations save time but increase the cost of charging. This paper aims to make the traveling of electric vehicles less costly with their current battery capacities between current charging stations. For this purpose, electric vehicle users will be able to have information about the charging stations on their routes. The problem of finding the most suitable charging station among the charging stations on the route with the current charging status of the electric vehicle is tried to be solved. For this purpose, a fuzzy logic control-based charging station algorithm was created by evaluating the multiple requirements of electric vehicles at the same time. Charging stations of different brands with different tariffs on the determined route were detected and processed on Google Earth. It is aimed to determine the most suitable charging station by calculating the current charging status of the electric vehicle and the distances and charging costs to these charging stations while traveling on its route. For this case, a route between Izmir and Van in Turkey was determined, and 56 charging stations on this route were evaluated according to these criteria. A weight value was calculated for each charging station using fuzzy logic. The fuzzy logic system designed in MATLAB environment for 56 stations in total is simulated to determine the accuracy of the system. Figure 1 shows the travel route between Izmir and Van and the charging stations of different companies whose locations are marked on the route.

2.1. Battery Electric Vehicles

Battery electric vehicles operate with a completely different energy generation system than internal combustion engine vehicles. Instead of fossil fuels, they realize vehicle movement by storing energy through rechargeable batteries and transmitting it to electric motors. These batteries convert the stored electrical energy into mechanical energy and enable the vehicle to move. This design simplifies the structure of the vehicle and makes energy conversion more efficient by not requiring components such as fuel tanks and exhaust systems found in internal combustion engine vehicles [9-10].

This operating principle makes electric vehicles an environmentally friendly transport option. Unlike internal combustion engine vehicles, electric vehicles do not cause emissions during use. This feature helps to reduce air pollution and contributes to the fight against global warming and sustainable environmental goals. The fact that they run on electrical energy makes it possible to utilize renewable energy sources, creating the potential further to reduce the carbon footprint [11-12].

Despite these advantages, there are some significant challenges to the widespread adoption of battery electric vehicles. In particular, the lack of charging station infrastructure is still a major disadvantage for electric vehicle users on long-distance journeys. The low number of charging stations and their lack of availability in suitable locations increase users' concerns about being stranded on the road, making it difficult to adopt this technology. This problem is one of the main factors limiting the use of electric vehicles, especially in intercity journeys [13].

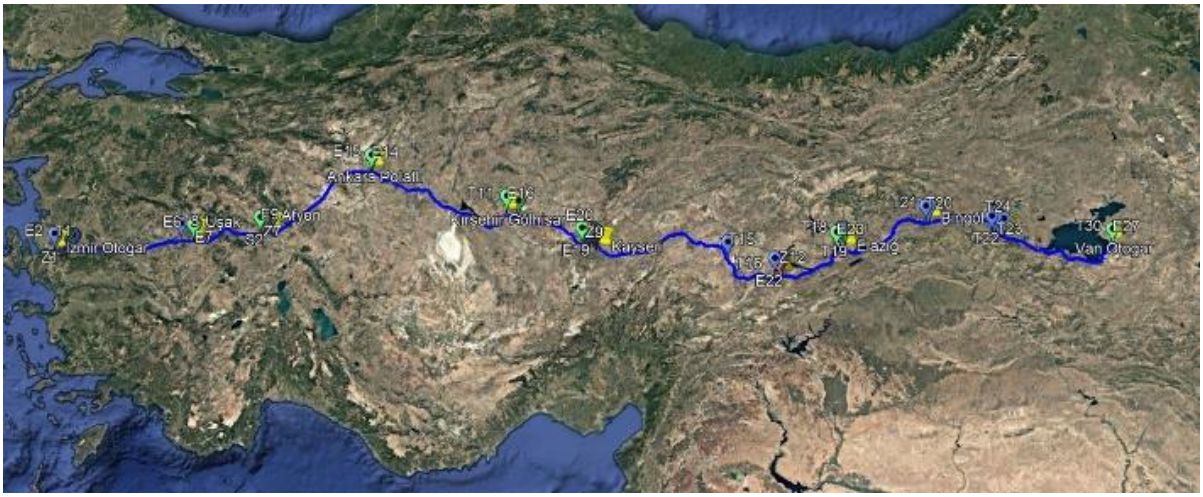

Figure 1. Selected travel routes between Izmir and Van and different brands of charging stations

2.2. Charging Stations

Electric vehicle charging stations are critical infrastructure elements used to meet the energy needs of battery electric vehicles. These stations perform the charging process by transmitting electrical energy to the batteries of the vehicles. Effective positioning and increasing the number of charging stations play an important role in the wider use of electric vehicles [14-15].

Since the study focuses on charging optimization in long-distance journeys, DC fast charging stations are taken into consideration. DC fast charging stations provide faster energy transfer, allowing electric vehicle users to charge more efficiently on long-distance journeys [16].

Reliable and accessible charging infrastructure for electric vehicle users directly affects the adoption rate of these vehicles. SAE (Society of Automotive Engineers), IEC (International Electromechanical Commission), and CHAdeMO standards are used worldwide [17]. Various specific charging standards, such as SAE J1772, IEC 61851, IEC 62196, and CHAdeMO, are widely used. However, IEC standards are widely accepted and applied in charging infrastructure in Turkey. Since this study focuses on the charging infrastructure in Turkey, the proposed fuzzy logic controller design is based on IEC standards. Accordingly, the technical specifications of IEC standards are presented in Table 1, and it is emphasized that the study is designed in accordance with the charging infrastructure of Turkey. This approach strengthens the suitability of the study for both local context and technical compatibility.

The IEC 61851 standard, widely used in Europe, includes both AC and DC charging modes. Table 1 presents the electrical parameters and technical specifications of each mode. For example, Mode 1 is a low-current charging method and requires a longer charging time, while Mode 4 provides ultra-fast DC charging, allowing users to cover a long range in a short time.

Table 1. Technical parameters of the IEC 61851 standard [18]

Source	Mode	Phase	Max. Voltage (V)	Max. Current (A)
AC	Mode 1	1	≤250	≤16
AC	Mode 1	3	≤480	≤16
AC	Mode 2	1	≤250	≤32
AC	Mode 2	3	≤480	≤32
AC	Mode 3	1	≤250	≤32
AC	Mode 3	3	≤480	≤32
DC	Mode 4	-	≤1000	≤400

Since the paper aims to optimize charging stations for long-distance journeys, it is important to provide details on charging station standards to implement the proposed solution and help select the most suitable charging method for different electric vehicle usage scenarios.

2.3. Fuzzy Logic Controller

Fuzzy logic is used in the development of non-linear systems, complex systems that lack clarity in their inputs or definitions. A fuzzy logic algorithm is a control approach that shows how the system will respond to multiple inputs according to predetermined rules [19].

In this study, the Fuzzy Logic Toolbox library in MATLAB was used to create the fuzzy logic controller selected as the decision-making algorithm. After the data from the variables are collected, it passes through the fuzzy logic controller and decides which charging station will be more logical to choose at what rate at the output.

The most suitable charging station is determined by calculating the charging cost of the charging stations on the travel route for the electric vehicle and the distance to the travel route. From this point of view, a fuzzy logic control based electric vehicle charging algorithm is proposed by reflecting multiple requirements of electric vehicles at the same time. The multiple requirements include the distance between the electric vehicle and the charging station and the charging cost of the charging station. The proposed scheduling algorithm focuses on finding the charging station preference priority for the electric vehicle. Considering the whole distance and total traveling cost, the fuzzy logic control generates a weight value as output, which is the concept of EV charging priority. Given the weight values, the proposed scheduling algorithm recommends the closest and most convenient scheduled charging stations to the EVs for charging [20].

Distance is the distance from the location of all charging stations on the route of the electric vehicle to its own location. The cost is found by calculating the charging tariffs of the charging stations of different brands on its route. As a result, distance and cost are used as inputs to the fuzzy logic control. Based on these inputs, the management system produces a weight matrix which is the output of the fuzzy logic control. The weight matrix is used in the charge scheduling algorithm operated by the management system. The management system focuses on recommending the closest and most cost-effective charging station for the electric vehicle to its route. In this study, fuzzy logic control is used in the management system to handle multiple parameters simultaneously. Fuzzy logic control inputs are distance and cost. Equation 1 is used to normalize these two factors in the range (0,1).

$$0 \leq x = \frac{x - x_{min}}{x_{max} - x_{min}} \leq 1 \quad (1)$$

This formula is used to normalize distance and cost. Here, x indicates distance or cost. While creating the scenarios to be given to the fuzzy system inputs, the average values are battery capacity 70

kwh, E brand charging station unit price 9,48 tl/kwh, T and Z brand charging stations 7,99 tl/kWh, and S brand charging stations 7,50 tl/kWh. It is assumed that 18 kWh of energy is spent per 100 km.

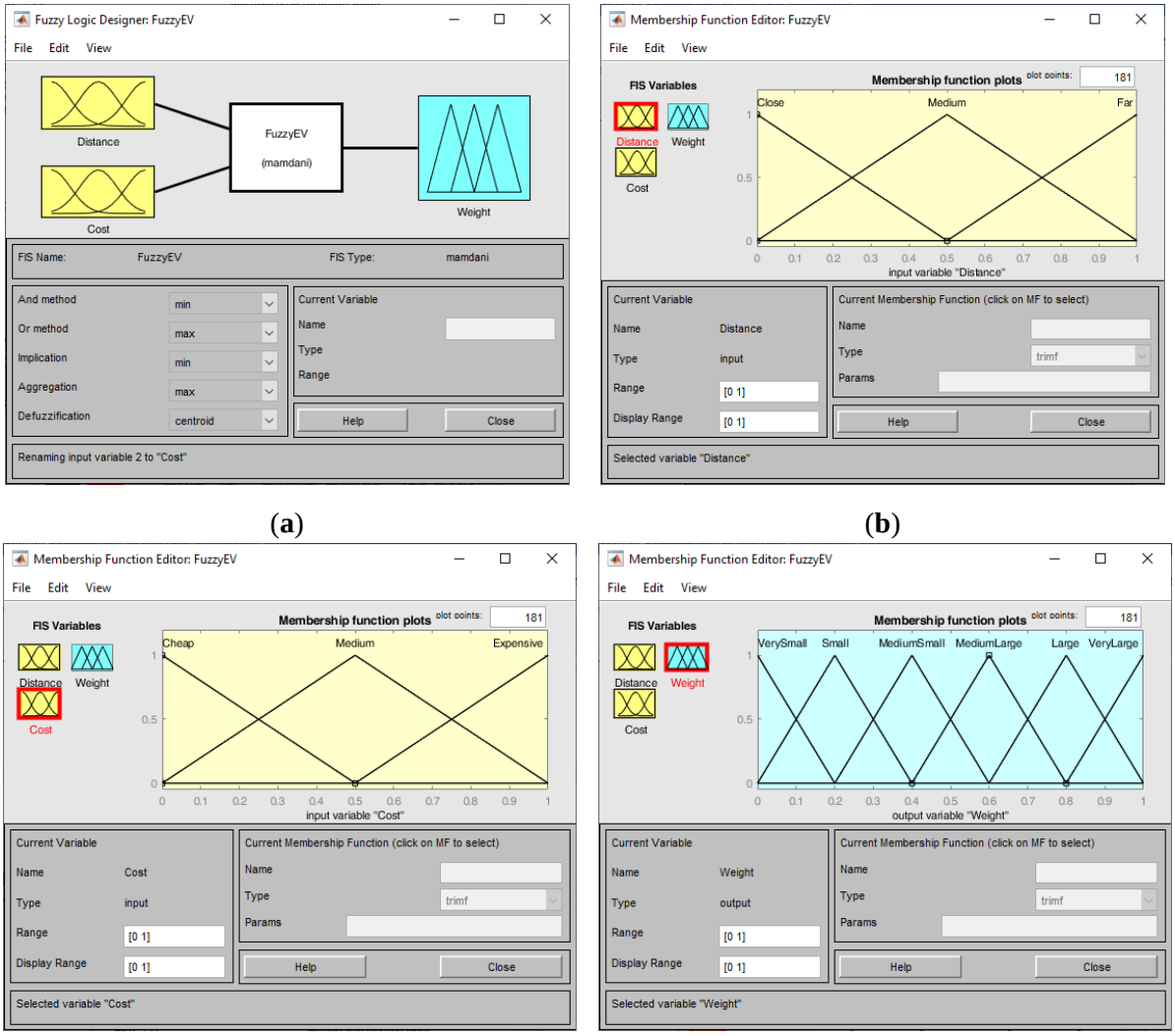

Figure 2. a) General representation of the designed model, b) Membership functions for Distance input, c) Membership functions for Cost input, d) Membership functions for Weight output

MATLAB/Simulink interface was used to design the controller and algorithm of the system. The general representation of the model designed with the Fuzzy Logic Designer Toolbox in MATLAB environment is given in Figure 2. a, the visualizations for the selection of membership functions are given in Figure 2. b for distance, Figure 2. c for cost and Figure 2.d for weight as output. The rule table of the fuzzy control system is shown in Table 2. The fuzzy logic controller operates according to the rules specified in the table, and all mappings and combinations of if/then rules are presented to calculate the weight value at the output. The weight value linguistic variables are defined as "Very Small, Small, Medium Small, Medium Large, Large, Very Large". Finally, the weight value is calculated by the fuzzification method. The charging station with the larger weight value calculated by this method has higher priority in terms of selection.

Table 2. Mapping and combination of if/then rules

Rules	Distance	Cost	Weight
Rule 1	Close	Cheap	Very Large
Rule 2	Close	Medium	Large
Rule 3	Close	Expensive	Medium Large
Rule 4	Medium	Cheap	Large
Rule 5	Medium	Medium	Medium Large
Rule 6	Medium	Expensive	Medium Small
Rule 7	Far	Cheap	Medium Small
Rule 8	Far	Medium	Small
Rule 9	Far	Expensive	Very Small

In accordance with this rule table, 56 charging stations on the route were analyzed, and the fuel cost to be spent as a result of selecting these charging stations in terms of total travel cost was calculated. During this calculation, both the calculated total fuel cost, the distance of the charging station to the normal travel route, and the charging station tariff were normalized. The total fuel cost is calculated for a TOGG brand short-range electric vehicle manufactured in Turkey, where the vehicle user will be fully charged only once on the specified route, and the electric vehicle has a standard energy cost for each kilometer distance outside the route and is selected the same for all possibilities.

Table 3. Projected weight versus distance and charging costs of some sample charging stations on the route

Charge Station	Distance	Cost	Normalized Total Cost	Expected Weight
S1	0.55	0.01	0.94	Very Large
T15	0.17	0.25	0.78	Large
Z9	0.39	0.25	0.74	Medium Large
T2	0.56	0.25	0.71	Medium Large
Z11	0.56	0.25	0.71	Medium Large
T14	0.56	0.25	0.71	medium large
E3	0.14	1.00	0.11	Small
E4	0.24	1.00	0.09	Very Small

Here, S1 represents the 1st numbered charging station on the route of brand S. Similarly, charging stations belonging to E, Z, and T brands are numbered.

3. Results and Discussion

The designed Mamdani fuzzy logic decision making system with two inputs and one output is intended to be tested for 100 different scenarios generated randomly in MATLAB environment. For this reason, randomly generated distance and cost values are applied as input to the fuzzy logic controller as shown in Figure 3.

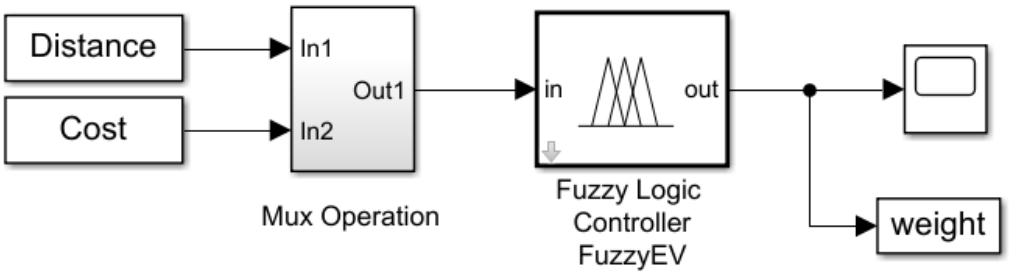

Figure 3. Simulation model of the designed fuzzy logic decision making system

The designed fuzzy logic decision making system generated output weight values according to the distance and cost values in the range of 0-1 randomly applied to its input. The change of weight values obtained from 100 different scenarios generated in the MATLAB environment is given in Figure 4.

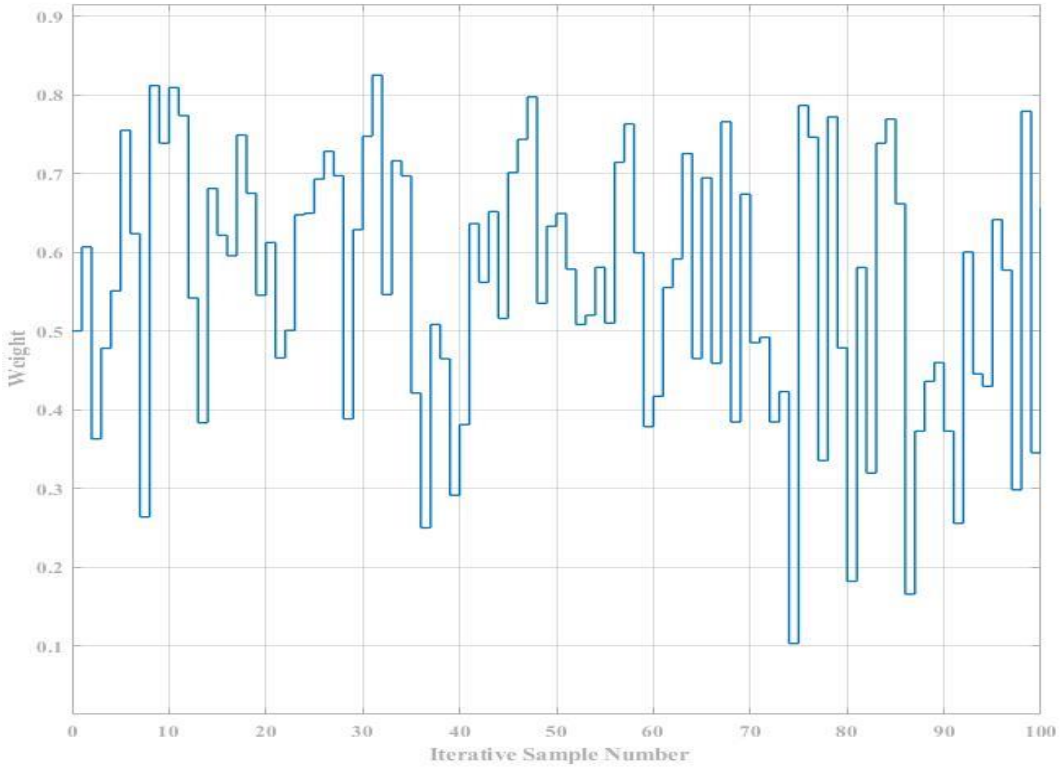

Figure 4. Variation of weight values calculated by the fuzzy logic decision making system for 100 different scenarios

As can be seen from the change, within the framework of the rules and inputs entered into the model, the scenario with the highest weight is the 32nd scenario, with a weight value of 0.8248. The input values are 0.2587 for Distance and 0.0909 for Cost. The lowest weight is obtained as 0.1030 in the 75th Scenario, and the input values are 0.0729 for Distance and 0.2229 for Cost.

4. Conclusion

In this paper, a fuzzy logic based decision making system is designed for electric vehicle users to select the most suitable charging station from the charging stations on their routes while travelling.

In order to demonstrate the real-time applicability of the study, an electric vehicle traveling between Izmir and Van in Turkey and 56 charging stations belonging to four different companies with known locations on the travel route are selected. While on the travel route, the distance between the electric vehicle and the charging station and the charging costs of the relevant charging station are normalized and given as fuzzy logic inputs. As a result of this sample data, a weight value was calculated for each charging station and a priority ranking was determined for electric vehicle drivers according to this value. The charging station with the highest weight value is the most suitable charging station. With this designed system, it is expected to solve the confusion in the charging station selection of electric vehicle users during their travels. In future studies, we will focus on the queuing problem at charging stations on any route determined by using current data from the charging station in Turkey.

Ethical statement

This study does not involve the use of human or animal subjects, nor does it involve hazardous chemicals, and therefore no ethical approval is required.

Acknowledgement

This study was derived from Melek Coşkun's Master's Thesis, titled "Determining the Optimal Charging Station for Electric Vehicles."

Conflict of interest

The authors declare no conflicts of interest.

Authors' Contributions

M.C: Conceptualization, Methodology, Formal analysis, Writing-Original draft preparation (%50)

B.K: Conceptualization, Methodology, Resources, Investigation, Writing-Original draft preparation (%50).

All authors read and approved the final manuscript.

References

[1] Yoro, K.O., Daramola, M.O., "CO2 emission sources, greenhouse gases, and the global warming effect", *Advances in carbon capture*, Woodhead Publishing, 3-28, 2020.

[2] Dobrzycki, A., Kasprzyk, L., Çetin, M.S., Gençoğlu, M.T., "Analysis of the influence of the charging process of an electrical vehicle on voltage distortions in the electrical installation", *Applied Sciences*, 14(17), 7691, 2024.

[3] Sanguesa, J.A., Torres-Sanz, V., Garrido, P., Martinez, F. J., Marquez-Barja, J. M., "A review on electric vehicles: Technologies and challenges", *Smart Cities*, 4(1), 372–404, 2021.

[4] Hannan, M.A., Azidin, F.A., Mohamed, A., "Hybrid electric vehicles and their challenges: A review", *Renewable and Sustainable Energy Reviews*, 29, 135–150, 2014.

[5] Özbay, H., Közkurt, C., Dalcalı, A., Tektaş, M., "Geleceğin ulaşım tercihi: Elektrikli araçlar" *Akıllı Ulaşım Sistemleri ve Uygulamaları Dergisi,* 3(1), 34–50, 2020.

[6] Dobrzycki, A., Çetin, M.S., Gençoğlu, M.T., "Harmonics generated during the electric vehicle charging process", Proceeding of 2nd International Conference on Advances and Innovations in Engineering (ICAIE), 173–178, 2023.

[7] Alanazi, F., "Electric vehicles: Benefits, challenges, and potential solutions for widespread adaptation" *Applied Sciences*, 13(10), 6016, 2023.

[8] Lebrouhi, B.E., Khattari, Y., Lamrani, B., Maaroufi, M., Zeraouli, Y., Kousksou, T., "Key challenges for a large-scale development of battery electric vehicles: A comprehensive review", *Journal of Energy Storage*, 44, 103273, 2021.

[9] Çetin, M.S., Güler, H., Gençoğlu, M.T., "Fuzzy logic based battery control system design for electric vehicles", Proceeding of 2021 IEEE Innovations in Intelligent Systems and Applications Conference (ASYU), 1–4, 2021.

[10] Liu, W., Placke, T., Chau, K.T., "Overview of batteries and battery management for electric vehicles", *Energy Reports*, 8, 4058–4084, 2022.

[11] Sanguesa, J. A., Torres-Sanz, V., Garrido, P., Martinez, F. J., Marquez-Barja, J.M., "A review on electric vehicles: Technologies and challenges", *Smart Cities*, 4(1), 372–404, 2021.

[12] Sun, X., Li, Z., Wang, X., Li, C., "Technology development of electric vehicles: A review", *Energies*, 13(1), 90, 2019.

[13] Ghasemi-Marzbali, A., "Fast-charging station for electric vehicles, challenges and issues: A comprehensive review", *Journal of Energy Storage*, 49, 104136, 2022.

[14] Al-Hanahi, B., Ahmad, I., Habibi, D., Masoum, M.A., "Charging infrastructure for commercial electric vehicles: Challenges and future works", *IEEE Access*, 9, 121476–121492, 2021.

[15] Narasipuram, R.P., Mopidevi, S., "A technological overview & design considerations for developing electric vehicle charging stations", *Journal of Energy Storage*, 43, 103225, 2021.

[16] Sadeghian, O., Oshnoei, A., Mohammadi-Ivatloo, B., Vahidinasab, V., Anvari-Moghaddam, A., "A comprehensive review on electric vehicles smart charging: Solutions, strategies, technologies, and challenges", *Journal of Energy Storage*, 54, 105241, 2022.

[17] Çetin, M.S., Gençoğlu, M.T., Dobrzycki, A., "Investigation of charging technologies for electric vehicles", *Turkish Journal of Science and Technology*, 19(1), 97–106, 2024.

[18] Zoroğlu, B., Yapıcı, A.T., Kurt, Ü.G., "Electric vehicle status of standards and electric vehicle charging stations in Turkey", Proceeding of International Marmara Sciences Congress (IMASCON), Kocaeli, Türkiye, 299-308, 2020.

[19] Zadeh, L.A., "Fuzzy logic", *Granular, Fuzzy, and Soft Computing*, New York, NY: Springer US, 19-49, 2023.

[20] Park, J., Sim, Y., Lee, G., Cho, D.H., "A fuzzy logic based electric vehicle scheduling in smart charging network", Proceeding of 2019 16th IEEE Annual Consumer Communications & Networking Conference (CCNC), 1–6, 2019.

IJESG
e-ISSN 2636-7904
International Journal of Energy and Smart Grid
Vol 9, Number 1, 2024
Doi: 10.55088/ijesg.1598117

Review Article

A REVIEW OF ELECTRIC VEHICLES: THEIR IMPACT ON THE ELECTRICITY GRID AND ARTIFICIAL INTELLIGENCE-BASED APPROACHES FOR CHARGING LOAD MANAGEMENT

Muhammed Sefa CETIN*[1], Muhsin Tunay GENCOGLU[2], Habip SAHIN[3]

[1] Fırat University, Faculty of Engineering, Department of Electrical-Electronics Engineering, Elazığ, Türkiye
Orcid1: https://orcid.org/0000-0001-5587-0001
[2] Fırat University, Faculty of Engineering, Department of Electrical-Electronics Engineering, Elazığ, Türkiye
Orcid2: https://orcid.org/0000-0002-1774-1986
[3]Fırat University, Vocational School of Technical Sciences, Department of Electricity and Energy, Elazığ, Türkiye Orcid3: https://orcid.org/ 0000-0002-0907-2022
* Corresponding author; mscetin@firat.edu.tr

Abstract: *The widespread use of electric vehicles contributes significantly to environmental sustainability by reducing the use of fossil fuels. However, the increasing number of electric vehicles and the charging demand may cause negative impacts such as overloading, voltage fluctuations and energy supply-demand imbalances in electricity grids. In this article, artificial intelligence-based methods applied for the management of the negative impacts of electric vehicles on the grid are discussed comprehensively and artificial intelligence approaches in the literature used to manage electric vehicle charging load are analyzed. Among these approaches, energy management strategies based on charging demand forecasting, dynamic pricing, routing, charging scheduling and smart grid integration are analyzed in detail. This article summarizes the latest innovative artificial intelligence-based solutions developed to manage the charging load of electric vehicles, improve grid stability, increase charging service price prediction accuracies, maximize grid and user satisfaction, ensure load balance, reduce charging and operating costs, reduce energy consumption and optimize power flow. This article also presents comprehensive information about the bilateral (grid and user perspective) management algorithms of the charging load of electric vehicles.*

Keywords*: Electric vehicles, charging load management, electricity grid, artificial intelligence.*

Received: December 8, 2024 *Accepted: December 25, 2024*

1. Introduction

Today, global problems such as increasing carbon emissions, climate change and environmental degradation are caused by the intensive use of fossil fuels and the transportation sector accounts for a significant portion of these emissions. Internal combustion engine vehicles increase greenhouse gas emissions through road transportation, leading to global warming, decreased air quality and energy security problems. In this context, electric vehicles stand out as a powerful solution to reduce carbon emissions from transportation by operating with zero emissions, being compatible with renewable energy sources and reducing dependence on fossil fuels. The rapid development of electric vehicle technology plays an important role in achieving sustainable transportation goals [1,2].

However, with the widespread deployment of electric vehicles, some challenges also arise, especially the impacts of charging infrastructure on the electricity grid. Intensive charging demand may lead to negative impacts on the grid. Innovative approaches are currently being used to manage these issues. Electric vehicles offer an important solution to combat climate change by both reducing environmental impacts and encouraging the development of energy infrastructure [3,4]. In this article; electric vehicles are analyzed, the negative impacts of charging of electric vehicles on the grid and artificial intelligence-based methods applied to eliminate these impacts are discussed. This article

contributes to the literature by offering valuable insights and important information on the use of artificial intelligence in managing the charging load of electric vehicles, providing a significant reference for researchers and readers in this field.

2. Electric Vehicles and Their Impacts

Electric vehicles stand out as an important solution for reducing carbon emissions from transportation. Unlike internal combustion engine vehicles based on fossil fuels, electric vehicles operate directly with zero emissions and reduce the amount of carbon emitted to the environment. Especially when charged with renewable energy sources, the carbon footprint of electric vehicles becomes even smaller and contributes to a sustainable transportation infrastructure. These vehicles not only improve air quality, but also increase energy security by reducing dependence on fossil fuels. The rapid development of electric vehicle technology, supported by battery efficiency, charging infrastructure and cost advantages, offers a powerful solution for mitigating the negative environmental impacts of the transportation sector [5,6].

Unlike internal combustion engines, electric vehicles use electrical energy instead of fossil fuels and therefore do not cause carbon emissions. Electric vehicles offer significant advantages such as their environmentally friendly structure, low emission rates and energy efficiency. Their utilization of electrical energy instead of fossil fuels has the potential to significantly reduce carbon emissions and air pollution. Moreover, thanks to advances in battery technologies, they also contribute to sustainable energy by preventing environmental degradation when integrated with renewable energy sources. The widespread adoption of electric vehicles will have a positive environmental impact on conserving natural resources and mitigating the effects of global warming [7]. Electric vehicles provide long-term savings for individual users with low operating and maintenance costs, while contributing to local economies by encouraging the development of charging infrastructure with innovative technologies. The widespread adoption of electric vehicles will have positive economic impacts for the vehicle sector, the energy sector and users [8].

In addition to the positive effects of the widespread use of electric vehicles, there will also be negative effects. With the widespread use of electric vehicles, problems such as overloading, voltage fluctuations and energy demand increases may occur in electricity grids, especially during peak charging demand. This situation may cause the existing grid infrastructure to be insufficient and the energy supply-demand balance to deteriorate. However, approaches such as smart grid technologies, artificial intelligence-supported energy management algorithms, energy storage systems, integration of renewable energy sources, dynamic pricing and vehicle-to-grid energy transfer (V2G) are used as solutions to manage these negative impacts on the grid [9,10].

3. Impacts of Electric Vehicle Charging on the Grid

Power quality refers to the capability of an electrical system to provide constant voltage, frequency and waveform to energy consuming devices. In cases where power quality is poor, the performance of electrical devices may be reduced and even damaged. Power quality problems in networks are usually caused by voltage fluctuations, harmonic distortions and sudden load changes. These problems both cause disruption in the energy consumption of end users and adversely affect the overall efficiency of energy systems [11].

Power quality problems are among the main technical challenges that affect the stability of energy systems and cause problems for both individual and industrial users. Among these problems, voltage fluctuations, harmonic distortions, phase shifts and deviations in the grid frequency stand out. Voltage

fluctuations occur as a result of sudden addition or removal of load to the grid and may prevent the proper operation of electronic devices. Harmonic distortions are caused by nonlinear loads and cause serious distortions in the energy waveform and reduce energy efficiency. Phase shifts are imbalances between phases during energy transmission and cause synchronization problems in energy systems. In addition, the imbalance between increasing demand and supply in the grid may trigger frequency deviations and create instability in energy systems. Power quality problems may cause disruptions in energy distribution and high costs while shortening the life of devices [12-14].

The proliferation of electric vehicles may create new problems affecting power quality due to the increase in energy demand and variable load profiles. In particular, charging multiple electric vehicles at the same time may lead to voltage drops and imbalances in the grid. This causes overloading on power distribution lines, pushing the limits of the existing infrastructure. Furthermore, the non-linear nature of electric vehicle chargers increases harmonic distortion, which causes distortion of the energy waveform. Sudden energy withdrawals during the charging process may create deviations in the grid frequency and disturb the energy supply-demand balance. These effects not only undermine the stability of energy systems, but may also lead to longer charging times and increased costs for electric vehicle users. The intensive charging requirements of electric vehicles challenge the capacity of the existing grid infrastructure to manage power quality issues. Smart grid technologies and innovative energy management systems are of great importance to solve these problems effectively [15,16].

4. Managing the Impact of Electric Vehicle Charging Load on the Grid with Artificial Intelligence Based Algorithms

The proliferation of electric vehicles creates various challenges in terms of energy demand and grid stability. In order to overcome these challenges and manage the grid effectively, artificial intelligence-based algorithms have become an important solution tool in recent years. These algorithms are used in various fields such as optimizing energy consumption, ensuring load balance of charging stations, managing dynamic pricing strategies and maintaining the energy supply-demand balance effectively [17,18].

There are several advantages of performing electric vehicle charging management with artificial intelligence algorithms. These algorithms play a critical role in understanding energy consumption algorithms and impacts on the grid by analyzing large amounts of data. Variables such as charging times of electric vehicles, load density on the grid, energy prices and production levels of renewable energy sources may be analyzed in real time with artificial intelligence algorithms. These analyses enable the implementation of optimized energy management strategies to minimize imbalances on the grid [19,20].

There are many artificial intelligence-based management algorithms used to manage the effects of electric vehicle charging on the grid. Demand forecasting and load balancing forecasts energy demand and balances the load between charging stations. Charging timing optimization directs users to charge during low demand hours. Charging management based on battery status (SoC) priorities vehicles with low battery levels. V2G integration feeds energy from vehicle batteries back to the grid. Charging station layout optimization ensures stations are strategically located. Renewable energy integration plans the charging of vehicles with renewable energy sources. Multi-agent decision-making optimizes energy management by enabling cooperation between charging stations. Real-time traffic and charging status monitoring directs vehicles to the most appropriate charging stations. All of these methods are actively used. However, some of these methods are prominent in the literature. In this paper, studies on managing electric vehicle charging load with dynamic pricing, charging demand forecasting, routing, charging scheduling and smart grid strategies are analyzed.

In [21], a machine learning-based approach is developed to predict the charging behavior of electric vehicles and manage charging loads. Charging data, weather, traffic and local event information are combined to predict charging time and energy consumption. The algorithms used included Random Forest (RF), Support Vector Machine (SVM), XGBoost and Artificial Neural Networks (ANN). This article specifically aimed to improve the accuracy of charging time and energy consumption prediction and optimize the charging load. This study also aims to reduce the impacts on the grid by balancing the charging loads according to the predicted data.

In [22], an energy management system is developed to predict the charging demand of hybrid electric vehicles (HEVs) in microgrids based on renewable energy sources and to reduce the impact of this demand on the grid. HEV charging demand is estimated using Support Vector Regression (SVR) and charging scheduling is optimized based on these estimates. Charging strategies are divided into two as "coordinated charging" and "smart charging". Dragonfly Algorithm is used for optimization and the method is tested on IEEE microgrid test system. The results showed a 2.5% reduction in grid operating costs.

In [23], a two-layer deep learning model is developed to manage the charging load of electric vehicles and reduce fluctuations on the grid. The model aims to optimize pricing and charging strategies of electric vehicle users. In the first layer, charging decisions are solved by Deep Reinforcement Learning (DRL) and in the second layer, charging station selection is solved by Deep Q-Learning (DQL). The model also aims to both reduce charging costs and increase grid stability by directing charging tariffs to electric vehicle users.

In [24], a charging navigation strategy is developed to manage the charging load of electric vehicles. The strategy aims to optimize the routing of electric vehicles to charging stations taking into account empty load rates and dynamic electricity prices. With the "four networks and four flows" model, an integration between the energy network, traffic network and information network are achieved. By analyzing dynamic electricity pricing and empty load rates, the optimal charging time and station for vehicles is proposed. This method reduces the peak and trough difference on the network by providing an even distribution of charging loads.

In [25], an energy consumption model is developed to minimize the energy consumption of electric vehicles and a DRL and Transformer based network is used to optimize this model. The model takes into account vehicle dynamics, path information and charging losses when optimizing the routes of electric vehicles to reduce energy consumption. This method provides more effective results by focusing on minimizing energy consumption instead of traditional distance minimization. This article presents a solution to balance the load on the grid and manage energy consumption through the integration of charging stations and the planning of electric vehicle routes.

In [26], a Safe Reinforcement Learning (SRL) method is developed to solve the dynamic and stochastic routing problem for electric commercial vehicles. In this article, routing strategies are developed considering the uncertainties in energy consumption and customer demands. The model is formulated as a Markov Decision Process and aims to minimize energy consumption while reducing the risk of battery depletion. Through Monte Carlo simulations, dynamic customer demands and energy consumption probability distributions are estimated to plan routing and charging stops.

In [27], a deep learning framework is developed to optimize the charging times of electric vehicles and manage their load on the grid. The behavior of CopulaGAN electric vehicle charging sessions is modelled. An AutoRegressive eXogenous Neural Network (ARXNN) is used for price prediction. Grey Wolf Optimization is used for the optimization of charging and discharging times. This method aims to meet the needs of both electric vehicle users and grid operators in order to reduce charging costs and balance charging loads.

In [28], a charging scheduling method based on the Soft Actor-Critic (SAC) algorithm is developed to efficiently manage electric vehicle charging demands in a distribution network. This method aims to minimize costs and improve grid stability by effectively managing electric vehicle charging loads while considering the randomness in renewable energy generation, electricity prices, and electric vehicle charging demands.

In [29], a Twin-Delayed Deep Deterministic Policy Gradient (TDDPG) based reinforcement learning controller is developed to optimize active and reactive power control in three-phase grid-connected in-vehicle chargers to manage the impact of electric vehicle charging load on the grid. The system aims to manage grid-to-vehicle (G2V) and V2G bidirectional power flows. This improves the stability of the grid while ensuring precise tracking of active and reactive power references. This article presents a smart energy management platform to manage the charging loads of electric vehicles and mitigate their impact on the grid.

In [30], a Multi-Agent Reinforcement Learning (MARL) method is developed to manage the charging load of electric vehicles and balance their energy demands on the grid. The proposed method is based on a centralized training and decentralized execution framework to simultaneously optimize energy purchasing strategies and energy distribution strategies. Electric vehicle flow is predicted by a Long Short-Term Memory (LSTM)-based neural network, while energy purchasing strategies are determined by the Multi-Agent Deep Deterministic Policy Gradient (MADDPG) method. Furthermore, an online heuristic routing (OHD) method is proposed for energy distribution.

In [31], a machine learning-based system is proposed to manage the charging load of electric vehicles while considering the impacts on the distribution grid. The system integrates conventional charging, fast charging, and V2G technologies to optimize grid performance. Charging station routing and speed selection are performed using LSTM networks, which successfully minimize load variance, power losses, and voltage fluctuations. Additionally, user charging costs are reduced by leveraging V2G technology, allowing energy feedback to the grid during peak hours. Various machine learning algorithms, including Decision Trees (DT), RF, SVM, K-Nearest Neighbors (KNN) and Deep Neural Networks (DNN) are evaluated with LSTM emerging as the most accurate and robust method. The proposed system provides a reliable, data-driven solution for grid stability and user satisfaction by optimizing energy distribution and reducing overload risks.

Artificial intelligence-based approaches are becoming increasingly important in energy management to mitigate the adverse effects of electric vehicles on electricity grid. As demonstrated in various studies [21-31], these methods offer innovative solutions in fields such as balancing charging loads, optimizing pricing strategies and enhancing grid integration. In addressing issues like load intensity and grid instability during electric vehicle charging processes, artificial intelligence-supported algorithms facilitate decision-making processes and deliver valuable outcomes for both users and grid operators. This article emphasizes the opportunities presented by artificial intelligence in the development of charging load management strategies, providing a significant contribution to the creation of more flexible and sustainable solutions in the future.

Table 1. Studies in the literature.

Reference	Management Strategy	AI Method	Aims	Application Field
[21]	Charging demand	RF, SVM, XGBoost, ANN	Balancing charging loads, improve forecasting accuracy	Charging stations
[22]	Charging demand	SVR	Ensure grid load balance, reduce operating costs	Microgrid (Renewable energy and HEV integration)
[23]	Pricing and routing	DRL, DQL	Enhance grid stability, lower charging costs	Charging stations and users
[24]	Pricing and routing	Dynamic pricing, Graph theory	Balancing charging loads, reduce traffic congestion	Traffic and grid integration
[25]	Routing	Transformer based DRL	Enhance grid stability, reduce energy consumption	Vehicle routing
[26]	Routing	SRL	Enhance grid reliability, reduce energy consumption	Vehicle routing
[27]	Scheduling	CopulaGAN, ARXNN	Ensure grid balance, lower charging costs	Parking lots
[28]	Scheduling	SAC	Enhance grid stability, reduce costs	Distribution network
[29]	Smart Grid	Twin-Delayed DDPG	Improve grid stability, optimise power flow	Smart grid (V2G and G2V integration)
[30]	Smart Grid	MARL (MADDPG, LSTM)	Ensure grid balance, enhance user satisfaction	Smart grid (Charging station network)
[31]	V2G	LSTM, DT, RF, SVM, KNN, DNN	Flattening the load curve, reducing power losses, minimizing voltage fluctuations	Charging stations and distribution grids

5. Conclusions

The widespread adoption of electric vehicles is recognized as an important step towards reducing carbon emissions in the transportation sector and eliminating fossil fuel dependency. However, the intense charging demand created by this transformation on the energy infrastructure may lead to problems that threaten grid stability. To mitigate the negative impacts of electric vehicles on the grid and to optimize energy management, artificial intelligence-based solutions are becoming prominent. This paper provides a comprehensive review of artificial intelligence approaches for electric vehicle charging management. Methods such as charging demand forecasting, dynamic pricing, charging scheduling and smart grid integration stand out as effective algorithms to balance charging loads, optimize costs and increase grid stability. Artificial intelligence-based solutions have demonstrated significant success in effectively managing the charging load of electric vehicles, enhancing grid stability, and optimizing energy costs.

In the future, integrating these methods with renewable energy sources and supporting them with energy storage technologies will provide higher efficiency and flexibility in energy management. In addition, multiple systems and hybrid artificial intelligence models that enable real-time management of all components on the grid stand out as promising areas for both academic research and industrial applications. In conclusion, the adaptation of artificial intelligence-based methods is a critical strategy to manage the impacts of electric vehicles on energy infrastructure and the grid and to create a more sustainable transportation system. Future studies should focus on the broader applications and applicability of these methods.

Ethical statement

Ethics Committee approval is not required.

Conflict of interest

The authors declare no conflict of interest.

Authors' Contributions

M. S. C: Conceptualization, Writing - Original draft preparation, Formal analysis (%40).
M. T. G: Methodology, Resources, Investigation (%30).
H. S: Conceptualization, Methodology, Writing - Original draft preparation, Investigation (%30).
All authors read and approved the final manuscript.

References

[1] Tian, X., Zha, H., Tian, Z., Lang, G., Li, L., "Carbon emission reduction capability assessment based on synergistic optimization control of electric vehicle V2G and multiple types power supply", *Energy Reports*, 11, 1191-1198, 2024.

[2] Qadir, S. A., Ahmad, F., Al-Wahedi, A. M. A., Iqbal, A., Ali, A., "Navigating the complex realities of electric vehicle adoption: A comprehensive study of government strategies, policies, and incentives", *Energy Strategy Reviews*, 53, 101379, 2024.

[3] Çetin, M. S., Gençoğlu, M. T., Dobrzycki, A., "Investigation of Charging Technologies for Electric Vehicles", *Turkish Journal of Science and Technology*, 19(1), 97-106, 2024.

[4] Williams, B., Bishop, D., Hooper, G., Chase, J. G., "Driving change: Electric vehicle charging behavior and peak loading", *Renewable and Sustainable Energy Reviews*, 189, 113953, 2024.

[5] Zhao, X., Hu, H., Yuan, H., Chu, X., "How does adoption of electric vehicles reduce carbon emissions? Evidence from China", *Heliyon*, 9(9), 2023.

[6] Guo, X., Sun, Y., Ren, D., "Life cycle carbon emission and cost-effectiveness analysis of electric vehicles in China", *Energy for Sustainable Development*, 72, 1-10, 2023.

[7] Albrechtowicz, P., "Electric vehicle impact on the environment in terms of the electric energy source—Case study", *Energy Reports*, 9, 3813-3821, 2023.

[8] Rapson, D. S., Muehlegger, E., "The economics of electric vehicles", *Review of Environmental Economics and Policy*, 17(2), 274-294, 2023.

[9] Khalid, M. R., Khan, I. A., Hameed, S., Asghar, M. S. J., Ro, J., "A comprehensive review on structural topologies, power levels, energy storage systems, and standards for electric vehicle charging stations and their impacts on grid", *IEEE Access*, 9, 128069-128094, 2021.

[10] Şengör, İ., Çiçek, A., Erenoğlu, A. K., Erdinç, O., Catalão, J. P., "User-comfort oriented optimal bidding strategy of an electric vehicle aggregator in day-ahead and reserve markets", *International Journal of Electrical Power & Energy Systems*, 122, 106194, 2020.

[11] Dobrzycki, A., Kasprzyk, L., Çetin, M. S., Gençoğlu, M. T., "Analysis of the Influence of the Charging Process of an Electrical Vehicle on Voltage Distortions in the Electrical Installation", *Applied Sciences*, 14(17), 7691, 2024.

[12] Nour, M., Chaves-Ávila, J. P., Magdy, G., Sánchez-Miralles, Á., "Review of positive and negative impacts of electric vehicles charging on electric power systems", *Energies*, 13(18), 4675, 2020.

[13] Rahman, S., Khan, I. A., Khan, A. A., Mallik, A., Nadeem, M. F., "Comprehensive review & impact analysis of integrating projected electric vehicle charging load to the existing low voltage distribution system", *Renewable and Sustainable Energy Reviews*, 153, 111756, 2022.

[14] Dobrzycki, A., Çetin, M. S., Gençoğlu, M. T., "Harmonics generated during the electric vehicle charging process", 2. International Conference on Advances and Innovations in Engineering (ICAIE), Elazığ, Türkiye, pp. 173-178, 2023.

[15] Tavakoli, A., Saha, S., Arif, M. T., Haque, M. E., Mendis, N., Oo, A. M., "Impacts of grid integration of solar PV and electric vehicle on grid stability, power quality and energy economics: A review", *IET Energy Systems Integration*, 2(3), 243-260, 2020.

[16] Wang, L., Qin, Z., Slangen, T., Bauer, P., Van Wijk, T., "Grid impact of electric vehicle fast charging stations: Trends, standards, issues and mitigation measures—An overview", *IEEE Open Journal of Power Electronics*, 2, 56-74, 2021.

[17] Abdullah, H. M., Gastli, A., Ben-Brahim, L., "Reinforcement learning based EV charging management systems–a review", *IEEE Access*, 9, 41506-41531, 2021.

[18] Zhang, X., Chan, K. W., Li, H., Wang, H., Qiu, J., Wang, G., "Deep-learning-based probabilistic forecasting of electric vehicle charging load with a novel queuing model", *IEEE Transactions on Cybernetics*, 51(6), 3157-3170, 2020.

[19] Dabbaghjamanesh, M., Moeini, A., Kavousi-Fard, A., "Reinforcement learning-based load forecasting of electric vehicle charging station using Q-learning technique", *IEEE Transactions on Industrial Informatics*, 17(6), 4229-4237, 2020.

[20] Shern, S. J., Sarker, M. T., Ramasamy, G., Thiagarajah, S. P., Al Farid, F., Suganthi, S. T., "Artificial Intelligence-Based Electric Vehicle Smart Charging System in Malaysia", *World Electric Vehicle Journal*, 15(10), 440, 2024.

[21] Shahriar, S., Al-Ali, A. R., Osman, A. H., Dhou, S., Nijim, M., "Prediction of EV charging behavior using machine learning", *IEEE Access*, 9, 111576-111586, 2021.

[22] Lan, T., Jermsittiparsert, K., Alrashood, S. T., Rezaei, M., Al-Ghussain, L., Mohamed, M. A., "An advanced machine learning based energy management of renewable microgrids considering hybrid electric vehicles' charging demand", *Energies*, 14(3), 569, 2021.

[23] Lin, H., Zhou, Y., Li, Y., Zheng, H., "Aggregator pricing and electric vehicles charging strategy based on a two-layer deep learning model", *Electric Power Systems Research*, 227, 109971, 2024.

[24] Zhong, J., Liu, J., Zhang, X., "Charging navigation strategy for electric vehicles considering empty-loading ratio and dynamic electricity price", *Sustainable Energy, Grids and Networks*, 34, 100987, 2023.

[25] Tang, M., Zhuang, W., Li, B., Liu, H., Song, Z., Yin, G., "Energy-optimal routing for electric vehicles using deep reinforcement learning with transformer", *Applied Energy*, 350, 121711, 2023.

[26] Basso, R., Kulcsár, B., Sanchez-Diaz, I., Qu, X., "Dynamic stochastic electric vehicle routing with safe reinforcement learning", *Transportation Research Part E: Logistics and Transportation Review*, 157, 102496, 2022.

[27] Gharibi, M. A., Nafisi, H., Askarian-Abyaneh, H., Hajizadeh, A., "Deep learning framework for day-ahead optimal charging scheduling of electric vehicles in parking lot", *Applied Energy*, 349, 121614, 2023.

[28] Jin, J., Xu, Y., "Optimal policy characterization enhanced actor-critic approach for electric vehicle charging scheduling in a power distribution network", *IEEE Transactions on Smart Grid*, 12(2), 1416-1428, 2020.

[29] Ahmadian, A., Sedghisigarchi, K., Gadh, R., "Empowering dynamic active and reactive power control: A deep reinforcement learning controller for three-phase grid-connected electric vehicles", *IEEE Access*, 2024.

[30] Zhang, Y., Yang, Q., An, D., Li, D., Wu, Z., "Multistep multiagent reinforcement learning for optimal energy schedule strategy of charging stations in smart grid", *IEEE Transactions on Cybernetics*, 53(7), 4292-4305, 2022.

[31] Shibl, M., Ismail, L., Massoud, A., "Electric vehicles charging management using machine learning considering fast charging and vehicle-to-grid operation", *Energies*, 14(19), 6199, 2021.

IJESG
e-ISSN 2636-7904
International Journal of Energy and Smart Grid
Vol 9, Number 1, 2024
Doi: 10.55088/ijesg.1596043

Review Article

TRANSMISSION LINE INSPECTION WITH UAVS: A REVIEW OF TECHNOLOGIES, APPLICATIONS, AND CHALLENGES

Esra INCE

Fırat University, Faculty of Engineering, Dep. of Electrical and Electronics Engineering, Elazıg, Türkiye
Orcid: https://orcid.org/0000-0001-9258-4178
* Corresponding author; esraozdemir@firat.edu.tr

Abstract: *Regular inspection of energy transmission lines plays a critical role to ensure the safety of energy infrastructures and minimise failure risks. While traditional inspection methods have limitations such as high cost, long duration and hazardous working conditions, unmanned aerial vehicles (UAVs) are emerging as an innovative alternative in this field. This paper provides a comprehensive review of the use of UAVs in the inspection of power transmission lines, focusing on the sensor technologies, artificial intelligence (AI) algorithms and field applications. The integration of LiDAR, thermal camera and multispectral sensors into UAVs offers many advantages such as three-dimensional modelling of power lines, detection of thermal anomalies and assessment of environmental risks. In addition, deep learning and reinforcement learning algorithms have been observed to improve the performance of UAVs by accelerating data processing and improving autonomous navigation. In this study, different approaches and case studies in the literature are analysed in detail, and the strengths and limitations of UAV-based inspection systems are comparatively evaluated. Accordingly, environmental challenges, sensor integration and legal regulations stand out as the main obstacles faced by these technologies in field applications. However, it is emphasised that significant improvements in data processing processes can be achieved with the integration of 5G technology and edge computing systems. This study not only evaluates the current status of UAVs in the inspection of energy infrastructures, but also provides recommendations for future research. More widespread adoption of UAV-based inspection systems will contribute to a more reliable, efficient and sustainable management of the energy sector.*

Keywords*: Energy transmission line inspection, Unmanned aerial vehicles, Artificial intelligence assisted systems, Lidar and Sensor Technologies*

Received: December 4, 2024 *Accepted: December 25, 2024*

1. Introduction

Regular maintenance and inspection of power transmission lines is critical to meet the growing energy demand of modern societies. Traditional inspection methods are often carried out by ground crews or helicopter-assisted inspections, which can be both costly and dangerous. Challenges such as mountainous regions, dense vegetation and extreme weather conditions limit the effectiveness of these methods and make reliable monitoring of energy transmission lines difficult. In this context, UAVs have emerged as an innovative and effective solution for the inspection of power transmission lines [1,2].

UAVs, especially multi-rotor models, provide detailed monitoring of transmission lines at close range, thanks to their ability to move around power transmission towers with high precision and to perform stationary inspections. These vehicles are equipped with optical and thermal cameras capable of providing high resolution data. In Aydın et al.'s study, it was shown that the optical cameras of UAVs can detect minor damages on power transmission towers and this makes significant contributions to preventive maintenance processes [3]. In addition, thermal cameras are often used as an effective tool for detecting invisible overheating or deterioration of insulators [2,4].

Rapid advances in UAV technology, combined with AI algorithms, have enabled these systems to become more autonomous and efficient. In Chen and Lee's study, it was shown that deep learning-

based algorithms are used for UAVs to adapt to environmental conditions and these algorithms can classify structural anomalies in real time [5]. In particular, algorithms such as YOLO and R-CNN are used to automatically detect anomalies such as insulator damages, line sagging and structural deterioration, which are commonly encountered in power transmission lines [1,4].

In Zhang et al.'s study, it was reported that new route planning algorithms developed for UAVs optimise the inspection processes of power transmission lines and enable these processes to be completed in a shorter time [6]. These algorithms make it easier for UAVs to cope with challenges such as dense vegetation or complex environmental conditions. In addition, Rezwan et al. integrated UAVs with multispectral sensors to analyse environmental risk factors. Multispectral sensors allow a detailed assessment of environmental conditions and have been used to analyse the impact of vegetation on power transmission lines [7].

Finally, Lekidis et al. detailed how UAVs can be integrated with different sensor systems and the contributions of these integrations to the inspection processes of energy transmission lines. In the study, it was shown that the combined use of LiDAR, thermal cameras and optical sensors provides a more comprehensive assessment of the condition of power lines [8]. These technologies make it possible to manage energy infrastructure more reliably and reduce operational costs.

This review aims to comprehensively evaluate the innovative solutions, existing methods and challenges that UAVs offer in the inspection of energy transmission lines. Commonalities, differences and future research opportunities in the existing literature will be discussed, and how UAV-based inspections can contribute to more efficient and safe management of energy infrastructures. In this paper, technological developments and applications for the inspection of energy transmission lines with UAVs are discussed in detail.

In this paper, technological developments and applications for the inspection of energy transmission lines with UAVs are discussed in detail. Section 2 covers the technological infrastructure of UAV-based inspections, sensor systems and AI algorithms. Chapter 3 analyses the practical applications and case studies of UAVs on power transmission lines and evaluates the success stories and shortcomings in this field. Section 4 discusses the challenges faced by these technologies and provides recommendations for future research. The final section summarises the overall conclusions of the study and highlights future research directions.

2. Technological Landscape of UAV-Based Inspections

Regular maintenance and inspection of energy transmission lines is critical to ensure the continuity of energy supply and prevent failures. Traditional methods have serious limitations such as high cost, long inspection times and hazardous working conditions. Therefore, UAVs have emerged as an important alternative for the inspection of energy transmission lines. With their advanced sensor systems, AI-supported analysis tools and autonomous flight capabilities, UAVs provide reliable inspection of power lines. The integration of technologies such as LiDAR, thermal imaging and multispectral sensors into UAVs allows precise assessment of the condition of the lines [1,9].

LiDAR sensors create three-dimensional models of power transmission lines and analyse their geometric structure in detail. This technology is used as an effective tool for detecting mechanical deformations in the lines as well as environmental threats, especially risks caused by vegetation. The study by Lekidis et al. demonstrated how LiDAR-based sensors and AI algorithms can be combined in the inspection of power lines. In the study, the data collected by the UAVs were processed in real time via edge computing nodes and a significant speed and accuracy in fault detection was achieved. Figure 1 details the data collection, analysis and fault reporting stages of UAVs and clearly shows the applications of these processes on power transmission lines [4].

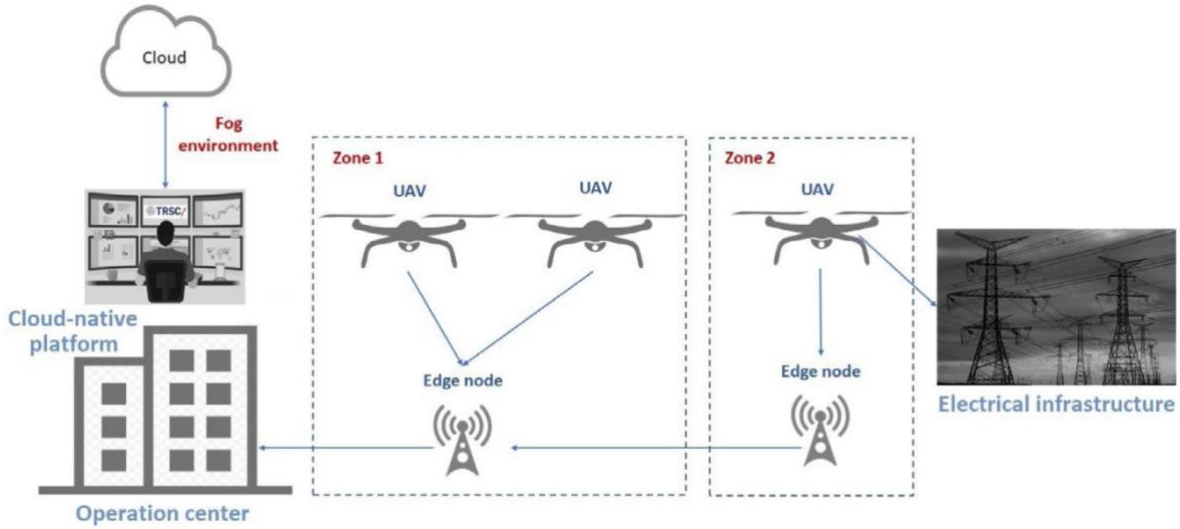

Figure 1. Methodology architecture

Artificial intelligence plays a central role in analysing the data collected in the inspection processes of power transmission lines and in the development of autonomous control systems. Deep learning algorithms such as YOLO and R-CNN can automatically detect damage to insulators, line sagging and other structural anomalies, minimising human intervention in the process. By integrating AI algorithms with 5G technology, Lekidis et al.'s study enabled the data collected by UAVs to be analysed with low latency and transmitted instantly to maintenance teams. Such systems have not only accelerated inspection processes, but also increased reliability [4].

Besides, other sensor technologies such as thermal cameras and multispectral sensors are widely used to detect different problems in power lines. Thermal cameras are an effective tool for detecting thermal anomalies such as overheating, while multispectral sensors are used to analyse environmental conditions and assess potential threats from vegetation [2,9]. The use of these sensors in combination with LiDAR enables more comprehensive monitoring of power lines. For example, the proximity of vegetation to power lines and whether it poses a potential threat can be easily analysed with multispectral data.

Autonomous control systems also offer an important innovation in the inspection of power lines. Rezwan et al. used deep reinforcement learning algorithms to enable UAVs to move reliably in complex environmental conditions. These systems have increased the effectiveness of UAVs in processes such as obstacle avoidance, route optimisation and mission planning [2]. Especially in large-scale energy infrastructures, faster and more efficient inspection processes have been realised thanks to such autonomous systems.

These technological developments are important tools that increase the effectiveness of UAVs in the inspection of energy transmission lines. Figure 1 visualises the overall operation of UAV-based energy inspection systems, detailing how these processes are integrated, how the collected data is processed and how the results are analysed. This figure clarifies the central role that UAVs play in both the collection and processing processes and can be used as a visual support for the explanations in this section [4].

3. Practical Applications and Case Studies

Regular inspection of energy transmission lines plays a vital role in ensuring the safety of energy infrastructure and preventing outages. The costly, time-consuming and dangerous nature of traditional inspection methods has made the use of UAVs more attractive in this field. Equipping UAVs with different sensor systems and AI-supported analysis tools provides a more precise and effective inspection of energy transmission lines. Several studies evaluating the practical applications of these vehicles detail the operational benefits and technical contributions of UAVs [10–12].

Wang et al. demonstrated the successful inspection of power transmission lines with UAVs equipped with optical cameras. In this study, deep learning based image processing algorithms were used to detect structural deformations and insulator damages in power towers. This method eliminated manual analysis processes and provided faster and more reliable results [13,14]. Similarly, the integration of thermal cameras with UAVs has been effective in detecting failures due to overheating. Thermal cameras have made significant contributions to preventive maintenance processes by detecting thermal anomalies that cannot be detected by the human eye [15,16].

The use of LiDAR sensors in the inspection of power transmission lines has made it possible to create three-dimensional models of the lines and to analyse environmental impacts in detail. In the study by Azevedo et al. it was reported that LiDAR-based systems detail the geometric structure of power lines and predict the risks arising from vegetation. This study reveals that LiDAR sensors offer a more comprehensive analysis when integrated with other sensors [17,18]. Studies using multispectral sensors in conjunction with LiDAR have also enabled a broader analysis of environmental factors and the condition of power lines [19,20].

The use of multiple UAV systems in energy inspection allows large areas to be inspected simultaneously. Rezwan et al. developed a system in which multiple UAVs inspect power transmission lines simultaneously and task assignment processes are optimised with Ant Colony Optimisation (ACO) algorithm. This approach significantly reduced inspection times and increased operational efficiency in large-scale energy infrastructures [21,22].

In Lekidis et al.'s study, a system was designed to analyse power lines in real time with the integration of AI-supported algorithms and 5G technology. In the study, the data collected by UAVs were processed by edge computing nodes and fault detection processes were accelerated [4].

These studies of practical applications demonstrate the multifaceted benefits of UAVs in the inspection of energy transmission lines. Both the integration of sensor technologies and the use of multiple UAV systems play a critical role in improving the security of energy infrastructures and reducing operational costs.

4. Challenges and Future Research Opportunities

Although the use of UAVs in the inspection of energy transmission lines offers significant advantages, these technologies face various operational and technical challenges. Environmental conditions, data processing limitations and legal regulations are among the main factors limiting the effectiveness of UAV-based systems in field applications. To overcome these challenges and make these systems more efficient, future research should focus on developing AI algorithms, improving sensor integration and data security.

One of the biggest challenges in field applications of UAVs is the harsh environmental conditions. Dense vegetation, complex terrain and adverse weather conditions can directly affect the flight safety and data collection efficiency of UAVs. Rezwan et al. analysed the effects of wind and other weather conditions on UAV performance and developed reinforcement learning-based algorithms to deal with

such environmental factors. These algorithms have improved the reliability of UAVs in obstacle avoidance, route optimisation and autonomous navigation processes [21,22]. However, the coordination of multiple UAV systems in complex geographical areas poses a significant challenge. It is emphasised that task assignment algorithms should be further developed for the simultaneous operation of multiple UAVs [11,20].

One of the most striking technical challenges is the integration of sensor technologies and data processing. The combination of LiDAR, thermal camera and multispectral sensors provides a powerful infrastructure for detailed analysis of power transmission lines. However, real-time processing of the data collected from these sensors requires improvements in data fusion and analysis algorithms. In Azevedo et al. highlighted the limitations of integrating LiDAR and thermal sensors to make sense of the data and developed algorithms to optimise these processes. Such improvements can enable faster and more reliable processing of large data sets [17,18].

Another important obstacle to the widespread adoption of UAV-based energy control systems is the legal regulations. Lekidis et al. pointed out that flight restrictions in different countries limit the field applications of UAV-based systems. The study suggested that the development of autonomous control systems compatible with legal regulations could be an effective method to overcome these limitations [4]. In addition, data security and privacy are among the important issues that need to be resolved for the use of UAVs in energy infrastructures. Protecting the collected data and providing access only to authorised persons is a critical requirement for the wide-scale applicability of these systems [14,19].

To overcome these challenges, future research should focus on sensor and AI integration of UAVs. In particular, the use of edge computing and 5G technologies can make real-time analysis processes more efficient by reducing data processing times. The development of autonomous control systems that can operate reliably in different geographical conditions will improve the operational performance of UAVs, as proposed by Rezwan et al [21,22]. In addition, modelling environmental factors with simulations and incorporating these models into route planning processes can provide significant improvements in field applications [11,20].

In conclusion, although the challenges faced by UAV-based energy control systems limit the potential of these technologies in field applications, innovative research in areas such as AI, sensor integration and data security show promise to overcome these problems. Future studies will contribute to the wider adoption of these technologies and more efficient and secure management of energy infrastructures.

5. Conclusions and Recommendations

This study comprehensively analyzed the advancements and challenges of UAVs in inspecting power transmission lines. The review highlighted key technological innovations, practical implementations, and areas requiring further research. The following conclusions synthesize the findings and emphasize actionable insights for improving UAV-based systems while addressing the suggestions provided by the reviewers.

The integration of advanced sensor technologies such as LiDAR, thermal cameras, and multispectral sensors has significantly enhanced the capabilities of UAVs in detecting structural anomalies, environmental risks, and thermal irregularities. As summarized in Table 1, LiDAR enables the creation of detailed three-dimensional models of power lines and surrounding vegetation, which is essential for precise risk assessments. Similarly, thermal and multispectral sensors complement these capabilities by improving fault detection and environmental monitoring. These sensor technologies provide a robust foundation for addressing the diverse requirements of power line inspections.

Table 1. Comparison o f Publications on UAV-Based Transmission Line Inspection by Features

Publications	Year	Sensor Technologies	Algorithms	Challenges	Innovations and Contributions
[1]	2021	LiDAR	Deep Learning-based PointNet	Dataset scarcity	Workflow efficiency
[2]	2022	-	-A*, PSO, ACO	Energy, obstacles	Federated learning
[3]	2017	Binocular Cameras	Ratio Detection, Hough Transform	Noise in edge detection	Real-time power line distance measurement
[4]	2022	LiDAR, multispectral sensors, thermal cameras	R-CNN, Fast R-CNN	GPS instability, data latency, high accident rate	5G network slicing, edge computing, AI-assisted fault detection
[5]	2019	Laser rangefinder, cameras	PID controllers	High wind speeds, vegetation interference	Autonomous inspection workflow for energy assets
[6]	2024	Multispectral cameras, thermal imaging	A* Algorithm, R-CNN	Signal loss, data processing speed	Real-time data transmission, remote control efficiency
[7]	2024	-	BACOHBA, HBA	Multi-wind field task assignment	Multi-UAV optimization
[8]	2024	-	FGATS	Multi-depot task assignment, UAV recharging, grouping optimization	İmproved large-scale UAV assignment efficiency
[9]	2019	LiDAR	PL2DM	Real-time processing with large data volume	Developed PL2DM for real-time segmentation and modeling of power lines
[10]	2020	Cameras	Feature Extraction, Clustering	Noise in detection	Automatic power pylon detection
[11]	2020	Cameras, 4G communication	AdaBoost, K-Means Clustering	Noise interference, real-time image processing	High-accuracy defect detection, automated image analysis
[12]	2020	Optical Camera	Multi-source Information Fusion	GPS and Directional Data Limitation	Accurate Tower Detection
[13]	2022	LiDAR, Ultraviolet Imagers, HD Cameras	Improved Median Filtering	Image Quality Issues	Enhanced Fault Detection in Power Lines

Table 1 Continued.

Publications	Year	Sensor Technologies	Algorithms	Challenges	Innovations and Contributions
[14]	2023	Cameras, LiDAR	Image Recognition, Path Planning	Manual operation reliance	Autonomous UAV inspection system
[15]	2022	LiDAR	Deep Separation Convolution, YOLOv3	Visual positioning lag	Improved UAV spatial positioning accuracy
[16]	2023	Satellite Internet, FANET	Multi-agent Reinforcement Learning, Q-Learning	Communication stability, battery energy consumption	Spatiotemporal routing strategy for UAVs
[17]	2019	Thermal infrared camera, LiDAR	Path planning algorithms	Navigation precision issues	Autonomous powerline inspection system with multiple sensor integration
[18]	2024	LiDAR	Monte Carlo simulation	Wind conditions	Semi-autonomous landing
[19]	2023	Electromagnetic Field Sensors	-	Electromagnetic interference, collision risks	Insights into safe UAV operation distances
[20]	2024	BeiDou RTK, UAV cameras	YOLOv4, LSD algorithm	EM interference, weather impact	Accurate tilt detection, real-time monitoring
[21]	2023	Ultrasonic sensors, monocular cameras	Deep Deterministic Policy Gradient	Long training times, slow convergence	Integrated artificial potential field to speed training
[22]	2024	Cameras, LiDAR, GPS	Multi-source data fusion	Complex environments	Improved obstacle detection accuracy

Artificial intelligence-driven algorithms, including YOLO, R-CNN, and reinforcement learning methods, have transformed UAV-based inspections. These algorithms automate fault detection, optimize flight paths, and accelerate data analysis processes, reducing reliance on human intervention. The integration of edge computing and 5G technologies, as highlighted in Table 1, has further enhanced real-time data processing, enabling faster and more accurate fault identification. These advancements underscore the potential for UAV systems to achieve greater autonomy and efficiency in operational settings.

Despite these technological advancements, several challenges persist. Environmental conditions, such as adverse weather and complex terrains, continue to hinder UAV performance. As noted in Table 1, studies addressing these challenges often propose reinforcement learning algorithms and robust UAV designs to improve reliability. Additionally, legal and regulatory barriers pose significant obstacles to widespread UAV deployment. Variations in regulations across regions create uncertainty, while data security and privacy concerns further complicate the adoption of UAV-based systems for energy infrastructure inspections.

A comparative analysis of existing approaches reveals both the strengths and limitations of current systems. Multi-sensor setups that combine LiDAR, thermal cameras, and multispectral sensors, as described in several studies within Table 1, offer superior fault detection capabilities but also highlight the need for improved data fusion algorithms. Similarly, multi-UAV systems optimized with swarm

intelligence methods such as Ant Colony Optimization (ACO) demonstrate potential in reducing inspection times, though their scalability in large-scale operations remains a challenge. These findings indicate that while progress has been made, further research is necessary to overcome the identified technical and operational limitations.

Building on these insights, future research should focus on enhancing the efficiency and applicability of UAV-based systems. Artificial intelligence algorithms such as YOLO and R-CNN should be further refined to handle complex environmental conditions and process larger datasets in real time. Advances in sensor integration are also critical, with efforts directed toward developing more precise and reliable systems that combine LiDAR, thermal imaging, and multispectral data streams. Moreover, designing UAV systems capable of operating across diverse geographical conditions would significantly enhance their versatility, especially in regions with challenging terrains or extreme weather conditions.

Expanding the application scope of UAV technologies to other industries, such as agriculture and disaster management, represents another promising research avenue. Lessons learned from energy infrastructure inspections can inform the development of UAV-based solutions for monitoring crop health, assessing post-disaster damage, and managing other critical infrastructures. The comparative data presented in Table 1 can serve as a reference point for identifying transferable technologies and methods.

Additionally, recommendations for future research should include exploring the potential of multi-UAV systems in large-scale operations. Algorithms like ACO and Particle Swarm Optimization (PSO), as detailed in Table 1, should be further developed to optimize task allocation, route planning, and resource management. These efforts could significantly reduce operational costs and inspection times while increasing the scalability of UAV-based solutions.

In conclusion, UAV-based inspection systems offer significant advantages over traditional methods, including improved precision, cost efficiency, and operational flexibility. However, realizing their full potential will require addressing the existing challenges through continued innovation. By integrating advanced sensor technologies, refining AI algorithms, and expanding the application scope of UAV systems, researchers and practitioners can unlock new possibilities for energy infrastructure management and beyond. This study provides a comprehensive roadmap for advancing UAV technologies, supported by the comparative insights detailed in Table 1, and emphasizes the importance of interdisciplinary collaboration in achieving these goals.

Ethical statement

Ethics Committee approval is not required.

Conflict of interest

The author declare no conflict of interest.

Authors' Contributions

E.İ: Conceptualization, Methodology, İnvestigation, Formal analysis, Writing - Original draft preparation (%100)

References

[1] Guan, H., Sun, X., Su, Y., Hu, T., Wang, H., Wang, H., Peng, C., Guo, Q., "UAV-lidar aids automatic intelligent powerline inspection", *International Journal of Electrical Power & Energy Systems*, 130, 106987, 2021.

[2] Rezwan, S., Choi, W., "Artificial Intelligence Approaches for UAV Navigation: Recent Advances and Future Challenges", *IEEE Access*, 10, 26320–26339, 2022.

[3] Shuai, C., Wang, H., Zhang, G., Kou, Z., Zhang, W., "Power lines extraction and distance measurement from binocular aerial images for power lines inspection using UAV", *Proceedings of the 9th International Conference on Intelligent Human-Machine Systems and Cybernetics (IHMSC)*, Vol. 2, pp. 69–74, 2017.

[4] Lekidis, A., Anastasiadis, A.G., Vokas, G.A., "Electricity infrastructure inspection using AI and edge platform-based UAVs", *Energy Reports*, 8, 1394–1411, 2022.

[5] Takaya, K., Ohta, H., Kroumov, V., Shibayama, K., Nakamura, M., "Development of UAV system for autonomous power line inspection", *Proceedings of the 23rd International Conference on System Theory, Control, and Computing (ICSTCC)*, pp. 762–767, 2019.

[6] Bin Ou, Z., Huang, Z.H., Qiu, S., "Application of Computer Remote Control UAV in Transmission Line Inspection", *Proceedings of the 2024 IEEE 7th International Electrical Energy Conference (CIEEC)*, pp. 1–6, 2024.

[7] Li, K., Yan, X., Han, Y., "Multi-mechanism swarm optimization for multi-UAV task assignment and path planning in transmission line inspection under multi-wind field", *Applied Soft Computing*, 150, 111033, 2024.

[8] Chen, X.L., Jia, Y.H., Liao, X.C., Chen, W.N., "A fuzzy grouping-based memetic algorithm for multi-depot multi-UAV power pole inspection", *Applied Soft Computing*, 168, 112472, 2025.

[9] Azevedo, F., Dias, A., Almeida, J., Oliveira, A., Ferreira, A., Santos, T., Martins, A., Silva, E., "LiDAR-based real-time detection and modeling of power lines for unmanned aerial vehicles", *Sensors (Switzerland)*, 19, 1–28, 2019.

[10] Fang, S., Haiyang, C., Sheng, L., Xiaoyu, W., "A Framework of Power Pylon Detection for UAV-based Power Line Inspection", *Proceedings of the 2020 IEEE 5th Information Technology and Mechatronics Engineering Conference (ITOEC)*, pp. 350–357, 2020.

[11] Yu, C., Qu, B., Zhu, Y., Ji, Y., Zhao, H., Xing, Z., "Design of the Transmission Line Inspection System Based on UAV", *Proceedings of the 2020 10th International Conference on Power and Energy Systems (ICPES)*, pp. 543–548, 2020.

[12] Chen, D.-Q., Guo, X.-H., Huang, P., Li, F.-H., "Safety Distance Analysis of 500kV Transmission Line Tower UAV Patrol Inspection", *IEEE Letters on Electromagnetic Compatibility Practice and Applications*, 2, 124–128, 2022.

[13] Du, Q., Dong, W., Su, W., Wang, Q., "UAV Inspection Technology and Application of Transmission Line", Proceedings of the 2022 IEEE 5th International Conference on Information Systems and Computer-Aided Education (ICISCAE), pp. 594–597, 2022.

[14] Hao, Z., Yu, H., Yu, W., Binbin, L., Yi, C., Cong, W., Ning, Z., "Design and implementation of UAV inspection and control platform for transmission lines", *Proceedings of the 2023 8th International Conference on Information Systems Engineering (ICISE)*, pp. 620–624, 2023.

[15] Zhang, Y., Dong, L., Luo, J., Lu, L., Jiang, T., Yuan, X., Kang, T., Jiang, L., "Intelligent Inspection Method of Transmission Line Multi Rotor UAV Based on Lidar Technology", Proceedings of the 2022 8th Annual International Conference on Networking, Information and Systems Computing (ICNISC), pp. 232–236, 2022.

[16] He, K., Zhou, Q., Shen, Y., Gao, J., Shuai, Z., "Spatiotemporal Precise Routing Strategy for Multi-UAV-Based Power Line Inspection Using Hybrid Network of FANET and Satellite Internet", Proceedings of the 2023 IEEE IAS Industrial and Commercial Power Systems Asia (ICPS Asia), pp. 1013–1018, 2023.

[17] He, T., Zeng, Y., Hu, Z., "Research of multi-rotor UAVs detailed autonomous inspection technology of transmission lines based on route planning", *IEEE Access*, 7, 114955–114965, 2019.

[18] Gendron, É., Leclerc, M.A., Hovington, S., Perron, É., Rancourt, D., Lussier-Desbiens, A., Hamelin, P., Girard, A., "Assessing wind impact on semi-autonomous drone landings for in-contact power-line inspection", *Drone Systems and Applications*, 12, 1–16, 2024.

[19] Dianovský, R., Pecho, P., Veĺký, P., Hrúz, M., "Electromagnetic Radiation from High-Voltage Transmission Lines: Impact on UAV Flight Safety and Performance", *Transportation Research Procedia*, 75, 209–218, 2023.

[20] Zhang, X., Yang, M., Wang, D., Chen, B., Song, K., "A transmission line tower tilt detection method based on BeiDou positioning signals and UAV inspection images", *Journal of Radiation Research and Applied Sciences*, 17, 101192, 2024.

[21] Zheng, X., Ding, Z., Zhang, X., Mu, C., "Path planning of power line inspection based on DDPG for obstacle avoidance with UAV", *Proceedings of the 2023 IEEE 6th International Electrical Energy Conference (CIEEC)*, pp. 2919–2923, 2023.

[22] Xi, Y., Chen, J., Tao, X., "Obstacle Detection and Avoidance Algorithm in UAV Patrol Inspection of Transmission Lines Based on Multi-Source Data Fusion and Computer Vision", *Proceedings of the 2024 International Conference on Telecommunications and Power Electronics (TELEPE)*, pp. 614–619, 2024.